Post-transcriptional regulation of neuronal identity and plasticity

A Dissertation

Presented to

The Faculty of the Graduate School of Arts and Sciences
Brandeis University

Neuroscience

Sacha B. Nelson, M.D., Ph.D., Advisor

In Partial Fulfillment
of the Requirements for the Degree
Doctor of Philosophy

by

Sean O'Toole

August 2017

The signed version of this form is on file in the Graduate School of Arts and Sciences.

This dissertation, directed and approved by Sean O'Toole's Committee, has been accepted and approved by the Faculty of Brandeis University in partial fulfillment of the requirements for the degree of:

DOCTOR OF PHILOSOPHY

Eric Chasalow, Dean
Graduate School of Arts and Sciences

Dissertation Committee:

Sacha B. Nelson, M.D., Ph.D.
Gina Turrigiano, Ph.D., Dept. of Biology
Michael Rosbash, Ph.D., Dept of Biology
Leon Reijmers, Ph.D., Sackler School of Graduate Biomedical Sciences, Tufts University

ABSTRACT

Post-transcriptional regulation of neuronal identity and plasticity

A dissertation presented to the Faculty of the
Graduate School of Arts and Sciences of Brandeis University
Waltham, Massachusetts

By Sean O'Toole

Neurons have the difficult task of persisting throughout the life of the animal. This requires a rigid adherence to their highly specialized identity. Paradoxically, they must be flexible, able to modulate their properties in the face of a constantly shifting activity landscape. The work presented here suggests that these two critical processes depend (at least partially) on regulation through microRNAs. I have shown that proprioceptive sensory neurons display a decline in cell-type specific gene expression as well as a loss of their specialized muscle afferents upon conditional ablation of the microRNA biogenesis enzyme Dicer. Also, demonstrated here is the fact that parvalbumin-positive fast-spiking cells employ mir-7 to modulate their intrinsic excitability during activity deprivation in culture, as well as sensory deprivation *in vivo*. These studies support a role for microRNAs in the maintenance of neuronal identity and the regulation of plasticity.

Table of Contents

Chapter 1:

Introduction:

Mammalian nervous systems are composed of a vast array of diverse cell types whose properties and functions vary to an enormous degree. The breadth of this diversity is apparent upon juxtaposition of the highly specialized, cylindrical, outer segment of the photoreceptor to the semi two-dimensional, fractal-like, dendritic branch patterns of the purkinje cell. Neurons vary in their morphology, plasticity and functional properties. How does such exquisite diversity arise and how is it maintained? Arguably, the modern conceptual framework for understanding the development of differentiated cell types was introduced by C. H. Waddington (WADDINGTON, 1942). Waddington proposed that "developmental reactions" are canalized, that they are tuned through natural selection to bring about a definite end result regardless of relatively minor environmental perturbations. Waddington referred to the differentiation of cells from the embryonic state as epigenesis (the modern version of this term now holds a more genomic context). He would later illustrate the cellular differentiation process as a large number of marbles falling down a hill patterned with various grooves that produced a predictable pattern of landing points. The landing point of each marble would represent one of many different yet stereotyped cell fates. The analogy remains relevant; it still elegantly conveys cellular differentiation and body pattern formation without betraying the complex processes lying underneath.

While Waddington's marble analogy addresses the differentiation process behind neuronal development it does not account for how neuronal identity is retained post-differentiation. This retention and maintenance of neuronal identity serves as the bedrock of adult nervous system function. The importance of retaining identity is critically apparent considering that neurogenesis in adults, although present in some areas such as the striatum and hippocampus (Ernst et al., 2014; Spalding et al., 2013), is virtually absent in other areas such as the neocortex (Bhardwaj et al., 2006). So, for structures like the neocortex, the mechanisms governing the persistence of identity and function are especially important. However, this rigidity has to be balanced, paradoxically, against numerous forms of global plasticity that are necessary for the proper transmission of information and the stability of the network (Schaefer et al., 2007). This balancing of plasticity and the maintenance of identity is further complicated by the vast array of neuronal types whose differing molecular identities likely impose differing regulatory requirements.

The mechanisms dictating the maintenance of cell identity and global plasticity have been partially defined. For example, we know that epigenetic regulation through chromatin modification and transcription factors are essential to both of these processes (Alberini, 2009; Deneris and Hobert, 2014; Tognini et al., 2015; Turrigiano, 2008). It is established that microRNAs have an important developmental role in cell fate decisions and contribute to numerous forms of plasticity (McNeill and Van Vactor, 2012). Less appreciated are the roles of microRNAs in the maintenance of cell identity, as well as in global plasticity mechanisms. Conditional knockouts of microRNA pathway members and perturbations of specific microRNAs have broached these subjects (Davis et al., 2008; Hou et al., 2015; Schaefer et al., 2007; Zehir et al., 2010), however, there remains much to learn. This thesis aims to further our

understanding of how microRNAs operate in the adult animal, with a focus on the maintenance of cell identity and modulation of global plasticity. This chapter begins with an overview of the microRNA system, followed by a more specialized treatment of how microRNAs operate in the nervous system, contrasting the developmental roles of microRNAs to their less characterized roles in the maintenance of cell identity. Finally, we touch on the already established role of microRNAs in local (synaptic) plasticity, as well as on evidence for their involvement in global plasticity.

MicroRNAs, from cradle to grave:

MicroRNAs are small, approximately 22 base pair in length, RNAs that regulate translation through complimentary base pairing (Bartel, 2009; Krol et al., 2010b). They were initially discovered in C. Elegans some 20 years ago when it was found that a small non-coding RNA product, lin-4, was able to repress production of lin-14, a heterochronic regulator of development that is down-regulated as the animal matures (Lee et al., 1993). Since then, small RNAs have been discovered in a variety of metazoan organisms, including fruit flies, mice, humans and many others (Berezikov, 2011). The cloning and sequencing of these molecules has revealed hundreds of microRNA variants in the genome (Griffiths-Jones et al., 2008; Lagos-Quintana et al., 2001; Lau et al., 2001; Lee and Ambros, 2001). What is remarkable about the microRNA field is the staggering pace at which the field has advanced; possibly afforded by the fact that many tools already developed to study mRNAs were easily refined or co-opted for the study of small RNAs.

For the most part, microRNAs are transcribed by RNA polymerase II (Lee et al., 2004), although in some cases they are generated by RNA polymerase III (Borchert et al., 2006). There are two broad classes of microRNAs;intergenic and intronic (Krol et al., 2010b), as well as a

small group that lie directly within exons (Ha and Kim, 2014). Intergenic microRNAs constitute their own distinct expression unit and a lot of their regulation is similar to that regulating mRNA transcription (Bracht et al., 2004; Fukao et al., 2007; Liu et al., 2007). The product of a microRNA gene is referred to as a primary-microRNA, typically several hundred base pairs in length; this transcript has a 5' cap and a poly-A tail. This primary-transcript is further processed by two enzymes: Drosha and DGCR8 (named Pasha in *D. melanogaster*, Pash-1 in *C. elegans*) (Ha and Kim, 2014), jointly named the Microprocessor complex. These enzymes recognize the beginning of a hairpin structure characteristic of microRNAs. After processing, 5' and 3' cuts are made at the beginning of the hairpin structure, removing unstructured RNA tails, and leaving behind a double stranded piece of RNAs joined by a loop (Denli et al., 2004; Gregory et al., 2004; Lee et al., 2004). Afterwards, the pre-miRNA is then transported, via exportin5, from the nucleus into the cytoplasm (Lee et al., 2003; Lund et al., 2004). After nuclear export, Dicer, along with its cofactor Trbp, binds to the hairpin and makes two additional cuts, removing the loop region, leaving behind two separate ~22 base paired RNAs (Bernstein et al., 2001; Bernstein et al., 2003; Grishok et al., 2001). The enzymatic reactions performed by the Microprocessor and Dicer complexes demand precision (Ha and Kim, 2014). Slight variations of a base pair or two, in the location of the cut site, can alter the seed sequence, likely leading to aberrant repressive behavior. At this point it should be mentioned that intronic microRNAs, that are generated through splicing, are often (though not always) subject to the regulatory regimes of their host genes, do not require the Drosha/Dgcr8 complex for processing, and after nuclear export are processed by Dicer (Ha and Kim, 2014). Although, the majority of microRNAs are Dicer-dependent, one exception, mir-482, bypasses Dicer and instead relies on Argonaute-2 (Ago2) for its final processing step; the mechanism governing mir-482 processing is thought to

rely on its hairpin structure (Cheloufi et al., 2010; Cifuentes et al., 2010; Yang et al., 2010). After nucleolytic cleavage by Dicer, the enzyme complex is left with two separate complimentary RNA strands. Before handing the mature microRNA off to the Argonaute complex, one of these strands is selected while the other is discarded and degraded. Typically, one strand of the microRNA is rarer than the other, presumably as a result of how this selection process occurs. At this point the mature microRNA is ready to regulate its targets (Krol et al., 2010b).

The methods and software used to predict microRNA targets from genomic data have been continuously refined. As a result, the field seems to be focusing on more stringent and accurate means of selection. The employed algorithms rely on several core features of microRNA target selection. First, the business end of the microRNA is at the 5' proximal region of the molecule. This region contains an 8 to 6 bp stretch referred to as the seed sequence that is responsible for recognizing the mRNA target (Friedman et al., 2009). How strongly a seed matches it mRNA target typically informs how repressive the relationship will be. For example, 6 base pair matches are typically weaker than 8 bp matches (Agarwal et al., 2015). Additionally, the precise location of the match within the seed sequence as well as the presence or absence of a mismatch is also thought to be important. However, base pair recognition is not the only determining factor. The thermodynamic stability of the match is also thought to be important (delta G of the base-pair interaction) (Garcia et al., 2011). Context also plays a role. The three-dimensional structure of the mRNA surrounding the binding site is also important, as it seems to dictate the accessibility of the binding site (Agarwal et al., 2015). Typically, the 3' untranslated region is the most likely source of microRNA recognition. Finally, evolutionary conservation of the binding site is also suggestive of a bona fide interaction (Agarwal et al., 2015).

Aside from the direct structural determinants of local mRNA structure and the thermodynamic stability of the interaction, there are other factors affecting the relationship between microRNAs and their targets. The UTR landscape, which can vary from one cell type to another, will affect the function of the microRNA (Nam et al., 2014). It is estimated that each gene in the human genome has, on average, 7 splice variants (Pan et al., 2008);and many of these variants differ in the number or type of microRNA binding sites. These differing microRNA recognition sites between isoforms can have important regulatory consequences. For example, alternative isoforms of TRK-C differ in their mir-9 and mir-125 binding sites (Laneve et al., 2007). As a result during a gradual increase in mir-9/125 expression, that occurs normally during neuronal maturation, there is a down-regulation of a truncated/catalytically inactive version of the neurotrophin receptor. Additionally, stoichiometry is a key determinant of mRNA-microRNA interactions. The availability or concentration of the mRNA will affect the degree of post-transcriptional repression. The repressive action of microRNAs can be higher for mRNAs expressed at lower levels (Mukherji et al., 2011). The concentration of the microRNA also matters (Mullokandov et al., 2012). Every sequenced cell population contains hundreds of different microRNA species. However, many of these microRNAs are of low abundance. One study suggests that microRNAs below 1,000 reads per million can effectively be ignored in terms of their functional impact on translation (Mullokandov et al., 2012). However, the possibility that these low abundance microRNAs serve some unknown function unrelated to translation rates/transcript levels cannot be excluded. Finally, and perhaps most controversially, is the competitive RNA hypothesis (Salmena et al., 2011). This theory postulates that mRNAs compete for microRNA binding sites and that increasing the level of one mRNA can relieve the repression of another mRNA containing similar microRNA binding sites. This concept is

intriguing in that it portrays microRNAs and mRNAs as a part of an interconnected dynamic regulatory network. Additionally, other mRNA species, such as circular RNAs, are thought to play a role in this regulatory landscape, serving as endogenous microRNA sponges. However, the competitive endogenous RNA hypothesis, despite its intellectual appeal, may not apply to physiological levels of expression (Denzler et al., 2016).

Our understanding of microRNA-mediated repression has evolved considerably over the last several decades. Our initial understanding of microRNA repression comes from *C. elegans* where microRNAs were initially thought to suppress translation while leaving transcript levels unaffected (Olsen and Ambros, 1999). This created the idea that an observed disconnect between transcript level and translation was suggestive of post-transcriptional regulation through microRNAs. However, since earlier studies in *C. elegans,* the picture has become more complicated (Krol et al., 2010b). Our updated view still includes an effect of microRNAs on translation efficiency, while incorporating other avenues of repression through de-adenylation of the poly-A trail or directly degrading the transcript. In fact, several studies revealed that in mammallian cell lines, microRNAs almost always lowered the levels of their target mRNAs (Guo et al., 2010; Lim et al., 2005). Therefore, when looking for particularly potent post-transcriptional regulators, it is now important to not only look for a change in protein, but also a change in transcript levels. This point, that levels of transcripts are controlled by microRNA expression, will become important in both chapters 2 and 3, where deep sequencing of mRNAs is used to look for signs of microRNA regulation, in systems where massively parallel observation of protein expression levels is simply not possible.

A long-standing question in the field is that of microRNA stability. Only a decade ago, the assumption was that microRNAs had long half-lives (on the order of hours to days)

(Bhattacharyya et al., 2006; Gatfield et al., 2009; Hwang et al., 2007). Although, deletion of Dicer can completely deplete microRNA levels (Murchison et al., 2005), few studies have carefully examined microRNA half-lives in post-mitotic cells (such as neurons). In fact, some neuronal microRNAs turnover rapidly and the rate of this turnover is governed by activity (Krol et al., 2010a). A further complication is that the number of binding partners present in the cell is itself a regulator of stability (Ruegger and Grosshans, 2012). If an Argonaute bound microRNA is not actively suppressing some transcript it may be discarded from the Argonaute binding pocket and subsequently degraded. The physical mechanisms mediating microRNA turnover/degradation are not entirely known. Exonucleases Xrn1 and Xrn2 are suspected to be involved in microRNA degradation, and uridylation of the 3' end may be important for decreasing microRNA stability (Ruegger and Grosshans, 2012). Finally, the turnover kinetics of microRNAs may be differentially regulated between cell types. One study demonstrated that hippocampal interneurons regulate proteins thought to govern microRNA turnover differentially in comparison to pyramidal cells, during pilocarpine-induced seizures (Kinjo et al., 2016). Additionally, as chapter 3 will suggest, neuronal activity may differentially regulate microRNA levels between cell types. However, to a large degree, the turnover, biogenesis and repressive function of microRNAs across cell-types tend to be conserved.

Higher order functions of miRNAs:

Although it is useful to understand the synthesis, repressive action and stability of microRNAs, these subjects alone fail to fully encompass their function. How do we move from complimentary base pairing to higher order processes? The 6 to 8 base pair seed sequence enables the recognition of hundreds of other mRNA molecules and each target may be regulated by a number of different microRNAs (Selbach et al., 2008). This endows allows any microRNA

to regulate entire systems as opposed to only affecting a single gene. Also, microRNAs have been positioned in a number of feedforward and feedback loops, further complicating their regulatory roles within the cell (Tsang et al., 2007). Therefore, although the physical function of a microRNA is simple: the negative modulation of translation, the coordinate impact of performing this function on a number of transcripts simultaneously can have a number of highly unique and coordinated effects. Individual microRNAs can coordinate the transition of the epigenetic landscape within neurons (Yoo et al., 2009). They can encourage cell motility (Ma et al., 2007) or tip the scales of cellular differentiation within a set of neuronal progenitors (Kim et al., 2007). Alternatively, they can serve as buffers of physiological noise by repressing the translation of inappropriately expressed transcripts (Herranz and Cohen, 2010). Given these examples we can appreciate that understanding microRNA function requires not only understanding its Watson-Crick base-pairing, but also appreciating the often less understood mechanisms of coordinated cellular action in which it participates.

Neuronal microRNAs in Development and Maintenance:

Although, microRNAs are present throughout the organism their expression is highest and most diverse within the nervous system (McNeill and Van Vactor, 2012). Also, differences in microRNA expression pattern between species tend to be most striking in the head and sensory epithelium (Berezikov, 2011). Furthermore, the size distribution of expressed 3'UTRs within the nervous system is shifted towards longer sequences, relative to in non-neural tissue (Miura et al., 2013), implying an important role of regulatory elements within the nervous system. Lastly, even if highly conserved, prominently expressed microRNAs do not change between species, the evolution of the UTR landscape is changing quite dynamically (Mayr, 2016). In other words, the sequence of highly expressed microRNAs can remain constant while

their underlying targets shift through evolution altering the function of the microRNA. All of this supports a strong role for microRNAs in the nervous system.

The most striking examples of neuronal microRNA function are found in development, where small RNAs act as tipping point molecules, pushing the cell towards one fate or another. Knockout of dicer disrupts the transition between neurogenesis and gliogenesis (Kawase-Koga et al., 2009). mir-9 is critical for switching the expression of opposing chromatin remodeling complexes in neural progenitors and triggering their migration from the neural tube (Yoo et al., 2009). Mir-7a controls the spatial patterning of dopaminergic neurons through control of pax6 expression (de Chevigny et al., 2012). The theme here is that if the cell is a boulder (or even a marble) precariously sitting on top of a hill above two opposing valleys, microRNAs are the transient gust of wind or tremor that pushes the boulder towards one path or another.

Alternatively, microRNAs can suppress transcriptional noise or sharpen cell identify. Mir-124 inhibits non-neuronal transcripts and when overexpressed shifts the expression profile of a non-neuronal cell type towards a more brain like expression pattern (Lim et al., 2005). Mir-218 is necessary for the development of motor neurons, and is thought to suppress genes normally present in surround interneuron types within the spinal cord (Amin et al., 2015; Thiebes et al., 2015). Both of these examples occur in early development, however, the idea that microRNAs enhance cellular function by repressing transcripts normally expressed in other cell types, hints at a broader role for microRNAs in the maintenance of cell-type identity during adult life.

Evidence for microRNAs as guardians of cell identity comes from several lines of evidence, including a number of conditional pathway mutant knockouts. Dgcr8 knockout leads to a loss of cone specific gene expression and a decline in the size and function of the outer

segment (Busskamp et al., 2014). Cortical excitatory neurons, dopaminergic neurons, purkinje cells, cerebellar granular cells and a number of other cell-types, all decline in function and eventually die when Dicer is conditionally ablated (Davis et al., 2008; Fiorenza and Barco, 2016; Kim et al., 2007; Liu et al., 2007; Schaefer et al., 2007). However, in many of these cases, the full effect of the knockout is not fully realized for weeks or even months. One interpretation is that the stability of previously transcribed/translated Dicer or Dgcr8 (before condition knockout) or the long lasting stability of microRNAs, lengthens the time course over which neurodegeneration occurs. Also, even after some critical microRNA(s) has been depleted it may take additional time for the cell's expression profile to drift outside of a tolerable range. The interpretation of pathway mutants is further complicated by evidence for non-microRNA related functions of these enzymes (Yang and Lai, 2011). There is evidence, found in the retinal pigment epithelium, that Dicer is needed to inhibit active Alu elements by digesting their transcription products (Kaneko et al., 2011). Also, there is an unexplained binding activity against numerous mRNAs, tRNAs other RNA species, by Dicer, that may have a positive impact on their stabilities (Rybak-Wolf et al., 2014). Drosha-mediated cleavage of stem loop structures within mRNAs is also a complicating factor. Finally, there has been some observation of phenotypic mismatch between Dicer and DGCR8 knockouts in the same cell type (Burger and Gullerova, 2015). Since all of these studies do not look directly at cell-identify, the cause of neuronal decline in response to knocking out pathway mutants is difficult to determine. However, one study did observe a loss of cone enriched gene expression in photoreceptors after loss of DGCR8. Furthermore, the decline in this cell type could be partially rescued by the reintroduction of mir-182, the most highly abundant microRNA in these cells (Busskamp et al., 2014).

It is tempting to believe that the reason for the eventual cell loss in pathway mutants is the deregulation of the apoptotic machinery. In this view, the expression of a caspase or some other positive regulator of apoptosis reaches a critical expression level and initiates apoptosis. In chapter two I will suggest an alternative explanation: that the microRNA system helps to retain cellular identity by repressing the transcripts of surrounding cell-types that share a common progenitor and therefore may still aberrantly express some of the mRNAs associated with a differentiation path not taken. Additionally, in keeping with a role in cellular identity, the most specialized portions of the neuron may be most sensitive to conditional ablation of Dicer.

microRNAs as mediators of local and global plasticity:

We also know that a number of brain-expressed and -enriched microRNAs are heavily regulated by neuronal activity. The most striking examples come from studies of photoreceptors demonstrating that light exposure rapidly regulates a number of microRNAs (Krol et al., 2010a). Surprisingly, these microRNAs are destabilized by increased or decreased activity through modulation of their turnover kinetics. Also, differential expression, as opposed to a change in turnover, is seen during the application of drugs that block activity (TTX) or raise it (picrotoxin) during long (days) and short time scales (hours or less) in dissociated cultures (van Spronsen et al., 2013). *In vivo*, microRNAs are regulated by drugs of abuse, including cocaine and alcohol (Im et al., 2010; Li et al., 2013), as well as by memory tasks (Bredy et al., 2011; Griggs et al., 2013; Lin et al., 2011). MicroRNAs can also be differentially regulated by disease states such as epilepsy, autism and schizophrenia (Beveridge et al., 2010; Hu et al., 2011; Olde Loohuis et al., 2015). Finally, microRNAs are even reported to be processed locally within dendritic spines (Huang et al., 2012; Lugli et al., 2005). These forms of regulation are consistent with roles in various forms of neuronal plasticity.

In fact, the literature has several examples of small RNAs being directly involved in plasticity. Mir-132/212, an activity-regulated microRNA, is implicated in numerous learning and memory associated processes (Edbauer et al., 2010; Remenyi et al., 2013). Mir-26a and mir-384-5p are reported to be necessary for LTP in hippocampal neurons (Gu et al., 2015). Mir-34c loss facilitates fear conditioning (Gao et al., 2010). MicroRNAs are also integral to neurotrophin-mediated modulation of synaptic translation, in which pre-synaptic BDNF secretion triggers the processing of let-7 and other microRNAs, facilitating the exchange of mRNAs between the spine and dendritic p-bodies (Huang et al., 2012). In each of these examples, and many others, microRNAs in mature neurons either directly or indirectly affect synaptic plasticity.

Less explored, is the role of microRNAs in global, as opposed to synapse-specific, forms of plasticity. Here, global plasticity refers to changes in response to the net level of firing or synaptic activity that ultimately alters the neurons response to all inputs (lacks specificity). Although, recently it was found that mir-124 is necessary for synaptic scaling while mir-132 is involved in monocular deprivation (Hou et al., 2015; Mellios et al., 2011). Aside from these two examples very little is known about the role of microRNAs in global plasticity. Conceptually, microRNAs are attractive candidates by which to fine tune global neuronal properties, such as occur in synaptic scaling or intrinsic excitability. Their ability to make minor adjustment to translation across multiple different transcripts lends itself well to the regulation of properties crucial to balancing the transfer of information and network excitability. In chapter three we will add to this literature, where I describe the cell-type specific regulation of mir-7 in fast-spiking cells and its control of membrane excitability. In addition to helping us better understand the regulation of excitability, this discovery offers the possibility of selectively altering excitability in Fast-spiking (FS), parvalbumin-positive interneurons, whose function is tightly linked with

diseases such as schizophrenia, autism and epilepsy. One use of this knowledge might be altering the excitability of FS cells in patients with epilepsy using viral therapy. The end result of this treatment could be to enhance inhibition in the network, possibly counteracting epileptic episodes.

Concluding Remarks:

During early development, microRNAs trigger abrupt changes while also silencing genes specifically expressed in other related cell-types, so as to pave the way for cellular differentiation and maturation. Also, subsets of microRNAs are necessary for several types of plasticity in the cell. However, as alluded to in the beginning of this chapter, the roles of neuronal microRNAs in the adult animal are not simply relegated to controlling local or synaptic plasticity, but, they can play a more global role as well. In this thesis I expand the neuronal microRNA literature by examining two other important, but, less studied aspect of microRNA function in adult neurons. In chapter two the role of microRNAs in the long-term maintenance of cellular identity and specialization is explored. While, in chapter 3 I describe a new role for the brain enriched microRNA mir-7b involving the regulation of FS cell excitability in an activity and experience dependent manner.

References:

Agarwal, V., Bell, G.W., Nam, J.W., and Bartel, D.P. (2015). Predicting effective microRNA target sites in mammalian mRNAs. Elife *4*.
Alberini, C.M. (2009). Transcription factors in long-term memory and synaptic plasticity. Physiol Rev *89*, 121-145.
Amin, N.D., Bai, G., Klug, J.R., Bonanomi, D., Pankratz, M.T., Gifford, W.D., Hinckley, C.A., Sternfeld, M.J., Driscoll, S.P., Dominguez, B.*, et al.* (2015). Loss of motoneuron-specific microRNA-218 causes systemic neuromuscular failure. Science *350*, 1525-1529.
Bartel, D.P. (2009). MicroRNAs: target recognition and regulatory functions. Cell *136*, 215-233.
Berezikov, E. (2011). Evolution of microRNA diversity and regulation in animals. Nature reviews Genetics *12*, 846-860.
Bernstein, E., Caudy, A.A., Hammond, S.M., and Hannon, G.J. (2001). Role for a bidentate ribonuclease in the initiation step of RNA interference. Nature *409*, 363-366.

Bernstein, E., Kim, S.Y., Carmell, M.A., Murchison, E.P., Alcorn, H., Li, M.Z., Mills, A.A., Elledge, S.J., Anderson, K.V., and Hannon, G.J. (2003). Dicer is essential for mouse development. Nat Genet *35*, 215-217.
Beveridge, N.J., Gardiner, E., Carroll, A.P., Tooney, P.A., and Cairns, M.J. (2010). Schizophrenia is associated with an increase in cortical microRNA biogenesis. Mol Psychiatry *15*, 1176-1189.
Bhardwaj, R.D., Curtis, M.A., Spalding, K.L., Buchholz, B.A., Fink, D., Bjork-Eriksson, T., Nordborg, C., Gage, F.H., Druid, H., Eriksson, P.S.*, et al.* (2006). Neocortical neurogenesis in humans is restricted to development. Proceedings of the National Academy of Sciences of the United States of America *103*, 12564-12568.
Bhattacharyya, S.N., Habermacher, R., Martine, U., Closs, E.I., and Filipowicz, W. (2006). Relief of microRNA-mediated translational repression in human cells subjected to stress. Cell *125*, 1111-1124.
Borchert, G.M., Lanier, W., and Davidson, B.L. (2006). RNA polymerase III transcribes human microRNAs. Nature structural & molecular biology *13*, 1097-1101.
Bracht, J., Hunter, S., Eachus, R., Weeks, P., and Pasquinelli, A.E. (2004). Trans-splicing and polyadenylation of let-7 microRNA primary transcripts. RNA *10*, 1586-1594.
Bredy, T.W., Lin, Q., Wei, W., Baker-Andresen, D., and Mattick, J.S. (2011). MicroRNA regulation of neural plasticity and memory. Neurobiol Learn Mem *96*, 89-94.
Burger, K., and Gullerova, M. (2015). Swiss army knives: non-canonical functions of nuclear Drosha and Dicer. Nat Rev Mol Cell Biol *16*, 417-430.
Busskamp, V., Krol, J., Nelidova, D., Daum, J., Szikra, T., Tsuda, B., Juttner, J., Farrow, K., Scherf, B.G., Alvarez, C.P.*, et al.* (2014). miRNAs 182 and 183 are necessary to maintain adult cone photoreceptor outer segments and visual function. Neuron *83*, 586-600.
Cheloufi, S., Dos Santos, C.O., Chong, M.M., and Hannon, G.J. (2010). A dicer-independent miRNA biogenesis pathway that requires Ago catalysis. Nature *465*, 584-589.
Cifuentes, D., Xue, H., Taylor, D.W., Patnode, H., Mishima, Y., Cheloufi, S., Ma, E., Mane, S., Hannon, G.J., Lawson, N.D.*, et al.* (2010). A novel miRNA processing pathway independent of Dicer requires Argonaute2 catalytic activity. Science *328*, 1694-1698.
Davis, T.H., Cuellar, T.L., Koch, S.M., Barker, A.J., Harfe, B.D., McManus, M.T., and Ullian, E.M. (2008). Conditional loss of Dicer disrupts cellular and tissue morphogenesis in the cortex and hippocampus. The Journal of neuroscience : the official journal of the Society for Neuroscience *28*, 4322-4330.
de Chevigny, A., Core, N., Follert, P., Gaudin, M., Barbry, P., Beclin, C., and Cremer, H. (2012). miR-7a regulation of Pax6 controls spatial origin of forebrain dopaminergic neurons. Nature neuroscience *15*, 1120-1126.
Deneris, E.S., and Hobert, O. (2014). Maintenance of postmitotic neuronal cell identity. Nature neuroscience *17*, 899-907.
Denli, A.M., Tops, B.B., Plasterk, R.H., Ketting, R.F., and Hannon, G.J. (2004). Processing of primary microRNAs by the Microprocessor complex. Nature *432*, 231-235.
Denzler, R., McGeary, S.E., Title, A.C., Agarwal, V., Bartel, D.P., and Stoffel, M. (2016). Impact of MicroRNA Levels, Target-Site Complementarity, and Cooperativity on Competing Endogenous RNA-Regulated Gene Expression. Molecular cell *64*, 565-579.
Edbauer, D., Neilson, J.R., Foster, K.A., Wang, C.F., Seeburg, D.P., Batterton, M.N., Tada, T., Dolan, B.M., Sharp, P.A., and Sheng, M. (2010). Regulation of synaptic structure and function by FMRP-associated microRNAs miR-125b and miR-132. Neuron *65*, 373-384.
Ernst, A., Alkass, K., Bernard, S., Salehpour, M., Perl, S., Tisdale, J., Possnert, G., Druid, H., and Frisen, J. (2014). Neurogenesis in the striatum of the adult human brain. Cell *156*, 1072-1083.
Fiorenza, A., and Barco, A. (2016). Role of Dicer and the miRNA system in neuronal plasticity and brain function. Neurobiol Learn Mem *135*, 3-12.
Friedman, R.C., Farh, K.K., Burge, C.B., and Bartel, D.P. (2009). Most mammalian mRNAs are conserved targets of microRNAs. Genome Res *19*, 92-105.
Fukao, T., Fukuda, Y., Kiga, K., Sharif, J., Hino, K., Enomoto, Y., Kawamura, A., Nakamura, K., Takeuchi, T., and Tanabe, M. (2007). An evolutionarily conserved mechanism for microRNA-223 expression revealed by microRNA gene profiling. Cell *129*, 617-631.
Gao, J., Wang, W.Y., Mao, Y.W., Graff, J., Guan, J.S., Pan, L., Mak, G., Kim, D., Su, S.C., and Tsai, L.H. (2010). A novel pathway regulates memory and plasticity via SIRT1 and miR-134. Nature *466*, 1105-1109.
Garcia, D.M., Baek, D., Shin, C., Bell, G.W., Grimson, A., and Bartel, D.P. (2011). Weak seed-pairing stability and high target-site abundance decrease the proficiency of lsy-6 and other microRNAs. Nature structural & molecular biology *18*, 1139-1146.

Gatfield, D., Le Martelot, G., Vejnar, C.E., Gerlach, D., Schaad, O., Fleury-Olela, F., Ruskeepaa, A.L., Oresic, M., Esau, C.C., Zdobnov, E.M.*, et al.* (2009). Integration of microRNA miR-122 in hepatic circadian gene expression. Genes Dev *23*, 1313-1326.
Gregory, R.I., Yan, K.P., Amuthan, G., Chendrimada, T., Doratotaj, B., Cooch, N., and Shiekhattar, R. (2004). The Microprocessor complex mediates the genesis of microRNAs. Nature *432*, 235-240.
Griffiths-Jones, S., Saini, H.K., van Dongen, S., and Enright, A.J. (2008). miRBase: tools for microRNA genomics. Nucleic Acids Res *36*, D154-158.
Griggs, E.M., Young, E.J., Rumbaugh, G., and Miller, C.A. (2013). MicroRNA-182 regulates amygdala-dependent memory formation. The Journal of neuroscience : the official journal of the Society for Neuroscience *33*, 1734-1740.
Grishok, A., Pasquinelli, A.E., Conte, D., Li, N., Parrish, S., Ha, I., Baillie, D.L., Fire, A., Ruvkun, G., and Mello, C.C. (2001). Genes and mechanisms related to RNA interference regulate expression of the small temporal RNAs that control C. elegans developmental timing. Cell *106*, 23-34.
Gu, Q.H., Yu, D., Hu, Z., Liu, X., Yang, Y., Luo, Y., Zhu, J., and Li, Z. (2015). miR-26a and miR-384-5p are required for LTP maintenance and spine enlargement. Nat Commun *6*, 6789.
Guo, H., Ingolia, N.T., Weissman, J.S., and Bartel, D.P. (2010). Mammalian microRNAs predominantly act to decrease target mRNA levels. Nature *466*, 835-840.
Ha, M., and Kim, V.N. (2014). Regulation of microRNA biogenesis. Nat Rev Mol Cell Biol *15*, 509-524.
Herranz, H., and Cohen, S.M. (2010). MicroRNAs and gene regulatory networks: managing the impact of noise in biological systems. Genes Dev *24*, 1339-1344.
Hou, Q., Ruan, H., Gilbert, J., Wang, G., Ma, Q., Yao, W.D., and Man, H.Y. (2015). MicroRNA miR124 is required for the expression of homeostatic synaptic plasticity. Nature communications *6*, 10045.
Hu, K., Zhang, C., Long, L., Long, X., Feng, L., Li, Y., and Xiao, B. (2011). Expression profile of microRNAs in rat hippocampus following lithium-pilocarpine-induced status epilepticus. Neurosci Lett *488*, 252-257.
Huang, Y.W., Ruiz, C.R., Eyler, E.C., Lin, K., and Meffert, M.K. (2012). Dual regulation of miRNA biogenesis generates target specificity in neurotrophin-induced protein synthesis. Cell *148*, 933-946.
Hwang, H.W., Wentzel, E.A., and Mendell, J.T. (2007). A hexanucleotide element directs microRNA nuclear import. Science *315*, 97-100.
Im, H.I., Hollander, J.A., Bali, P., and Kenny, P.J. (2010). MeCP2 controls BDNF expression and cocaine intake through homeostatic interactions with microRNA-212. Nature neuroscience *13*, 1120-1127.
Kaneko, H., Dridi, S., Tarallo, V., Gelfand, B.D., Fowler, B.J., Cho, W.G., Kleinman, M.E., Ponicsan, S.L., Hauswirth, W.W., Chiodo, V.A.*, et al.* (2011). DICER1 deficit induces Alu RNA toxicity in age-related macular degeneration. Nature *471*, 325-330.
Kawase-Koga, Y., Otaegi, G., and Sun, T. (2009). Different timings of Dicer deletion affect neurogenesis and gliogenesis in the developing mouse central nervous system. Dev Dyn *238*, 2800-2812.
Kim, J., Inoue, K., Ishii, J., Vanti, W.B., Voronov, S.V., Murchison, E., Hannon, G., and Abeliovich, A. (2007). A MicroRNA feedback circuit in midbrain dopamine neurons. Science *317*, 1220-1224.
Kinjo, E.R., Higa, G.S., Santos, B.A., de Sousa, E., Damico, M.V., Walter, L.T., Morya, E., Valle, A.C., Britto, L.R., and Kihara, A.H. (2016). Pilocarpine-induced seizures trigger differential regulation of microRNA-stability related genes in rat hippocampal neurons. Sci Rep *6*, 20969.
Krol, J., Busskamp, V., Markiewicz, I., Stadler, M.B., Ribi, S., Richter, J., Duebel, J., Bicker, S., Fehling, H.J., Schubeler, D.*, et al.* (2010a). Characterizing light-regulated retinal microRNAs reveals rapid turnover as a common property of neuronal microRNAs. Cell *141*, 618-631.
Krol, J., Loedige, I., and Filipowicz, W. (2010b). The widespread regulation of microRNA biogenesis, function and decay. Nature reviews Genetics *11*, 597-610.
Lagos-Quintana, M., Rauhut, R., Lendeckel, W., and Tuschl, T. (2001). Identification of novel genes coding for small expressed RNAs. Science *294*, 853-858.
Laneve, P., Di Marcotullio, L., Gioia, U., Fiori, M.E., Ferretti, E., Gulino, A., Bozzoni, I., and Caffarelli, E. (2007). The interplay between microRNAs and the neurotrophin receptor tropomyosin-related kinase C controls proliferation of human neuroblastoma cells. Proceedings of the National Academy of Sciences of the United States of America *104*, 7957-7962.
Lau, N.C., Lim, L.P., Weinstein, E.G., and Bartel, D.P. (2001). An abundant class of tiny RNAs with probable regulatory roles in Caenorhabditis elegans. Science *294*, 858-862.
Lee, R.C., and Ambros, V. (2001). An extensive class of small RNAs in Caenorhabditis elegans. Science *294*, 862-864.
Lee, R.C., Feinbaum, R.L., and Ambros, V. (1993). The C. elegans heterochronic gene lin-4 encodes small RNAs with antisense complementarity to lin-14. Cell *75*, 843-854.

Lee, Y., Ahn, C., Han, J., Choi, H., Kim, J., Yim, J., Lee, J., Provost, P., Radmark, O., Kim, S.*, et al.* (2003). The nuclear RNase III Drosha initiates microRNA processing. Nature *425*, 415-419.
Lee, Y., Kim, M., Han, J., Yeom, K.H., Lee, S., Baek, S.H., and Kim, V.N. (2004). MicroRNA genes are transcribed by RNA polymerase II. EMBO J *23*, 4051-4060.
Li, J., Li, J., Liu, X., Qin, S., Guan, Y., Liu, Y., Cheng, Y., Chen, X., Li, W., Wang, S.*, et al.* (2013). MicroRNA expression profile and functional analysis reveal that miR-382 is a critical novel gene of alcohol addiction. EMBO Mol Med *5*, 1402-1414.
Lim, L.P., Lau, N.C., Garrett-Engele, P., Grimson, A., Schelter, J.M., Castle, J., Bartel, D.P., Linsley, P.S., and Johnson, J.M. (2005). Microarray analysis shows that some microRNAs downregulate large numbers of target mRNAs. Nature *433*, 769-773.
Lin, Q., Wei, W., Coelho, C.M., Li, X., Baker-Andresen, D., Dudley, K., Ratnu, V.S., Boskovic, Z., Kobor, M.S., Sun, Y.E.*, et al.* (2011). The brain-specific microRNA miR-128b regulates the formation of fear-extinction memory. Nature neuroscience *14*, 1115-1117.
Liu, N., Williams, A.H., Kim, Y., McAnally, J., Bezprozvannaya, S., Sutherland, L.B., Richardson, J.A., Bassel-Duby, R., and Olson, E.N. (2007). An intragenic MEF2-dependent enhancer directs muscle-specific expression of microRNAs 1 and 133. Proceedings of the National Academy of Sciences of the United States of America *104*, 20844-20849.
Lugli, G., Larson, J., Martone, M.E., Jones, Y., and Smalheiser, N.R. (2005). Dicer and eIF2c are enriched at postsynaptic densities in adult mouse brain and are modified by neuronal activity in a calpain-dependent manner. J Neurochem *94*, 896-905.
Lund, E., Guttinger, S., Calado, A., Dahlberg, J.E., and Kutay, U. (2004). Nuclear export of microRNA precursors. Science *303*, 95-98.
Ma, L., Teruya-Feldstein, J., and Weinberg, R.A. (2007). Tumour invasion and metastasis initiated by microRNA-10b in breast cancer. Nature *449*, 682-688.
Mayr, C. (2016). Evolution and Biological Roles of Alternative 3'UTRs. Trends Cell Biol *26*, 227-237.
McNeill, E., and Van Vactor, D. (2012). MicroRNAs shape the neuronal landscape. Neuron *75*, 363-379.
Mellios, N., Sugihara, H., Castro, J., Banerjee, A., Le, C., Kumar, A., Crawford, B., Strathmann, J., Tropea, D., Levine, S.S.*, et al.* (2011). miR-132, an experience-dependent microRNA, is essential for visual cortex plasticity. Nat Neurosci *14*, 1240-1242.
Miura, P., Shenker, S., Andreu-Agullo, C., Westholm, J.O., and Lai, E.C. (2013). Widespread and extensive lengthening of 3' UTRs in the mammalian brain. Genome Res *23*, 812-825.
Mukherji, S., Ebert, M.S., Zheng, G.X., Tsang, J.S., Sharp, P.A., and van Oudenaarden, A. (2011). MicroRNAs can generate thresholds in target gene expression. Nat Genet *43*, 854-859.
Mullokandov, G., Baccarini, A., Ruzo, A., Jayaprakash, A.D., Tung, N., Israelow, B., Evans, M.J., Sachidanandam, R., and Brown, B.D. (2012). High-throughput assessment of microRNA activity and function using microRNA sensor and decoy libraries. Nat Methods *9*, 840-846.
Murchison, E.P., Partridge, J.F., Tam, O.H., Cheloufi, S., and Hannon, G.J. (2005). Characterization of Dicer-deficient murine embryonic stem cells. Proceedings of the National Academy of Sciences of the United States of America *102*, 12135-12140.
Nam, J.W., Rissland, O.S., Koppstein, D., Abreu-Goodger, C., Jan, C.H., Agarwal, V., Yildirim, M.A., Rodriguez, A., and Bartel, D.P. (2014). Global analyses of the effect of different cellular contexts on microRNA targeting. Molecular cell *53*, 1031-1043.
Olde Loohuis, N.F., Kole, K., Glennon, J.C., Karel, P., Van der Borg, G., Van Gemert, Y., Van den Bosch, D., Meinhardt, J., Kos, A., Shahabipour, F.*, et al.* (2015). Elevated microRNA-181c and microRNA-30d levels in the enlarged amygdala of the valproic acid rat model of autism. Neurobiol Dis *80*, 42-53.
Olsen, P.H., and Ambros, V. (1999). The lin-4 regulatory RNA controls developmental timing in Caenorhabditis elegans by blocking LIN-14 protein synthesis after the initiation of translation. Developmental biology *216*, 671-680.
Pan, Q., Shai, O., Lee, L.J., Frey, B.J., and Blencowe, B.J. (2008). Deep surveying of alternative splicing complexity in the human transcriptome by high-throughput sequencing. Nat Genet *40*, 1413-1415.
Remenyi, J., van den Bosch, M.W., Palygin, O., Mistry, R.B., McKenzie, C., Macdonald, A., Hutvagner, G., Arthur, J.S., Frenguelli, B.G., and Pankratov, Y. (2013). miR-132/212 knockout mice reveal roles for these miRNAs in regulating cortical synaptic transmission and plasticity. PLoS One *8*, e62509.
Ruegger, S., and Grosshans, H. (2012). MicroRNA turnover: when, how, and why. Trends Biochem Sci *37*, 436-446.

Rybak-Wolf, A., Jens, M., Murakawa, Y., Herzog, M., Landthaler, M., and Rajewsky, N. (2014). A variety of dicer substrates in human and C. elegans. Cell *159*, 1153-1167.
Salmena, L., Poliseno, L., Tay, Y., Kats, L., and Pandolfi, P.P. (2011). A ceRNA hypothesis: the Rosetta Stone of a hidden RNA language? Cell *146*, 353-358.
Schaefer, A., O'Carroll, D., Tan, C.L., Hillman, D., Sugimori, M., Llinas, R., and Greengard, P. (2007). Cerebellar neurodegeneration in the absence of microRNAs. The Journal of experimental medicine *204*, 1553-1558.
Selbach, M., Schwanhausser, B., Thierfelder, N., Fang, Z., Khanin, R., and Rajewsky, N. (2008). Widespread changes in protein synthesis induced by microRNAs. Nature *455*, 58-63.
Spalding, K.L., Bergmann, O., Alkass, K., Bernard, S., Salehpour, M., Huttner, H.B., Bostrom, E., Westerlund, I., Vial, C., Buchholz, B.A.*, et al.* (2013). Dynamics of hippocampal neurogenesis in adult humans. Cell *153*, 1219-1227.
Thiebes, K.P., Nam, H., Cambronne, X.A., Shen, R., Glasgow, S.M., Cho, H.H., Kwon, J.S., Goodman, R.H., Lee, J.W., Lee, S.*, et al.* (2015). miR-218 is essential to establish motor neuron fate as a downstream effector of Isl1-Lhx3. Nature communications *6*, 7718.
Tognini, P., Napoli, D., and Pizzorusso, T. (2015). Dynamic DNA methylation in the brain: a new epigenetic mark for experience-dependent plasticity. Front Cell Neurosci *9*, 331.
Tsang, J., Zhu, J., and van Oudenaarden, A. (2007). MicroRNA-mediated feedback and feedforward loops are recurrent network motifs in mammals. Molecular cell *26*, 753-767.
Turrigiano, G.G. (2008). The self-tuning neuron: synaptic scaling of excitatory synapses. Cell *135*, 422-435.
van Spronsen, M., van Battum, E.Y., Kuijpers, M., Vangoor, V.R., Rietman, M.L., Pothof, J., Gumy, L.F., van Ijcken, W.F., Akhmanova, A., Pasterkamp, R.J.*, et al.* (2013). Developmental and activity-dependent miRNA expression profiling in primary hippocampal neuron cultures. PLoS One *8*, e74907.
WADDINGTON, C. (1942). CANALIZATION OF DEVELOPMENT AND THE INHERITANCE OF ACQUIRED CHARACTERS. Nature *150*, 563-565.
Yang, J.S., and Lai, E.C. (2011). Alternative miRNA biogenesis pathways and the interpretation of core miRNA pathway mutants. Molecular cell *43*, 892-903.
Yang, J.S., Maurin, T., Robine, N., Rasmussen, K.D., Jeffrey, K.L., Chandwani, R., Papapetrou, E.P., Sadelain, M., O'Carroll, D., and Lai, E.C. (2010). Conserved vertebrate mir-451 provides a platform for Dicer-independent, Ago2-mediated microRNA biogenesis. Proceedings of the National Academy of Sciences of the United States of America *107*, 15163-15168.
Yoo, A.S., Staahl, B.T., Chen, L., and Crabtree, G.R. (2009). MicroRNA-mediated switching of chromatin-remodelling complexes in neural development. Nature *460*, 642-646.
Zehir, A., Hua, L.L., Maska, E.L., Morikawa, Y., and Cserjesi, P. (2010). Dicer is required for survival of differentiating neural crest cells. Developmental biology *340*, 459-467.

Chapter 2:

Dicer maintains the identity and function of proprioceptive sensory neurons

Note: The contents of this chapter have been published in the Journal of Neurophysiology 2017 (March 1st, Vol. 117 no. 3, 1057-1069). I wrote the paper and performed the majority of experiments with assistance from Monica Ferrer, Haihan Zheng and Jennifer Mekonnen. Monica in particular was crucial to getting this project off the ground. Yasuyuki Shima assisted with the analysis of retrotransposable elements. David Ladle was a major contributor who performed the physiology experiments in figures 4 and 6, he also assisted in writing the manuscript. Lastly, Sacha Nelon's advising was vital to many of the directions taken in this study and he helped write the manuscript.

Abstract

Neuronal cell identity is established during development and must be maintained throughout an animal's life (Fishell and Heintz, 2013). Transcription factors critical for establishing neuronal identity can be required for maintaining it (Deneris and Hobert, 2014). Post-transcriptional regulation also plays an important role in neuronal differentiation (Bian and Sun, 2011), but its role in maintaining cell identity is less established. To better understand how post-transcriptional regulation might contribute to cell identity, we examined the proprioceptive neurons in the

dorsal root ganglion (DRG), a highly specialized sensory neuron class, with well established properties that distinguish them from other neurons in the ganglion. By conditionally ablating Dicer in mice, using parvalbumin (Pvalb)-driven cre recombinase, we impaired post-transcriptional regulation in the proprioceptive sensory neuron population. KO animals display a progressive form of ataxia at the beginning of the fourth postnatal week that is accompanied by a cell-death within the DRG. Before cell-loss, expression profiling shows a reduction of proprioceptor specific genes and an increased expression of non-proprioceptive genes normally enriched in other ganglion neurons. Furthermore, although central connections of these neurons are intact, the peripheral connections to the muscle are functionally impaired. Post-transcriptional regulation is therefore necessary to retain the transcriptional identity and support functional specialization of the proprioceptive sensory neurons.

Introduction

The neuronal diversity characteristic of the mature central and peripheral nervous systems arise through progressive stages of proliferation, migration and differentiation, tightly regulated by transcriptional and posttranscriptional mechanisms. Less understood is how neuronal cell types retain their identity after they have differentiated and matured. The identities of specific classes of cells are at least partially determined by transcription factor codes and increasing evidence indicates that these same transcription factors are necessary to maintain identity later in life (Deneris and Hobert, 2014). MicroRNAs, are post-transcriptional regulators that selectively inhibit the translation, stability or polyadenylation of specific transcripts through complimentary base pair recognition encoded within seed regions of the mature microRNAs (Bartel, 2009; Krol et al., 2010b). Like transcription factors, they have been shown to be crucial for several early developmental transitions that establish cell-type specificity (Huang et al., 2010;

Makeyev et al., 2007; Zhao et al., 2009). Less is known, however, about whether this class of molecules, which is highly abundant within the nervous system (Kosik, 2006), may also work to reinforce and maintain neuronal identity after it has been established.

To study mechanisms that maintain neuronal identity we focused on a highly characterized cell type. Proprioceptive sensory neurons, located in the dorsal root ganglion, encode changes in muscle length and tension through innervation of muscle spindles and Golgi tendon organs, specialized compartments in skeletal muscle (Windhorst, 2007). Three distinct subtypes of proprioceptive neurons differ in their central connections with spinal neurons and associated peripheral end organs. The intrafusal fibers in muscle spindles are supplied by primary (group Ia) and secondary (group II) afferents, while Golgi tendon organs are innervated by group Ib afferents. These endings in muscle as well as synaptic terminals in the spinal cord can be visualized by expression of the vesicular glutamate transport 1 (VGluT1; (Wu et al., 2004)). In particular, Ia afferents make strong synaptic connections with motor neurons in the spinal cord innervating homonymous muscle groups (Windhorst, 2007). Proprioceptive sensory neurons can be genetically targeted through their common expression of the calcium binding protein Pvalb (Arber et al., 2000). Disruption of proprioceptor central or peripheral connections trigger easily observable behavioral phenotypes, demonstrated by impairments of neurotrophic or transcription factors such as TrkC, Nt3, Etv1 or Runx3 (Arber et al., 2000; Chen et al., 2002; Ernfors et al., 1994; Klein et al., 1994; Levanon et al., 2002). Additionally, a more comprehensive transcriptional profile of proprioceptors is emerging (Li et al., 2016; Usoskin et al., 2015). Given this functional and genetic knowledge base, proprioceptive sensory neurons lend themselves to the study of how neuronal identity is maintained.

MicroRNAs are crucial for numerous aspects of sensory neuron development, such as determining left/right functional asymmetery in C. elegans taste receptors (Johnston and Hobert, 2003), controlling the number of sensory neuron precursors in drosophila (Li et al., 2006), and ensuring proper inner ear development in mice (Soukup et al., 2009). MicroRNAs, averaging 22 basepairs in size, are generated from longer transcripts derived from intronic or intergenic regions. They are further processed by the Drosha/DGCR8 complex or by the splicesome, transported out of the nucleus and then terminally processed by the microRNA biogenesis enzyme Dicer (Krol et al., 2010b), with one notable exception being mir-451 which uses Argonaute-2 for its terminal processing step (Cheloufi et al., 2010; Cifuentes et al., 2010; Yang et al., 2010). In order to better tackle how microRNAs contribute to cell identity in proprioceptive sensory neurons, we conditionally ablated Dicer (Harfe et al., 2005) through a Pvalb cre driver (Hippenmeyer et al., 2005). By conditionally ablating Dicer from Pvalb positive neurons, we can ask how proprioceptive sensory neuron identity is affected by global impairment of post-transcriptional regulation. Dicer KO animals displayed a clear behavioral decline, reminiscent of other proprioceptive mutants. This decline in behavior was accompanied by cell death within the ganglion. Prior to the onset of cell death there was a loss of transcriptional identity as well as reduced transmission at peripheral but not central connections.

Materials and Methods:

Mice and Genotyping

All mice were acquired from Jackson labs. All procedures for animal experiments were approved by the Brandeis University and Wright State University Animal Care and Use Committees. The tdTomato reporter line Ai9 (Madisen et al., 2010) was mated to floxed Dicer animals (Harfe et

al., 2005) along with parvalbumin-ires-cre mice (Hippenmeyer et al., 2005). After several generations, $Pvalb^{cre/cre}$, $Ai9^{+/+}$, $Dicer^{flx/wt}$ parents were bred to generate experimental animals, of either sex, that were either homozygous or WT for the floxed allele. All genotyping was done using the extract and amp PCR kit (Sigma-Aldrich) with the primers and PCR programs recommended by Jackson labs for each line.

Behavioral Analysis

Animals were observed daily using two behavioral tests in order to examine motor function from p20-30. First, each animal was subjected to a cylinder test (Brooks and Dunnett, 2009; Fleming et al., 2013). Briefly, mice were placed into a small transparent cylinder (diameter, 12.7 cm; height, 15.5 cm) and were scored for the number of rears during a three-minute observation. Rears were scored when the mouse stood on its hindlimbs and pressed both forepaws against the side of the glass. Subsequently, each mouse was subjected to a modified form of footprint analysis (Brooks and Dunnett, 2009; Carter et al., 1999) using a custom-built, elevated linear track (length, 26 cm; width, 5 cm). The bottom of the track was transparent, enabling us to film the animals with an iphone video camera using a minimum frame rate of 120 Fps. Gait patterns were analyzed using FIJI. The central position of each paw placement was used to measure the average distance between left and right limbs for each static position of the animal (width), and the average forward movement for each step (stride; Fig1C). Statistical analyses were performed in R using a two-way repeated measures ANOVA. Additionally, post-hoc tests were performed using a student's T-Test with a Šidák correction.

DRG Cell Count and Area Analysis

Tissue Collection. At p20, 25 and 30, animals were deeply anesthetized with isofluorane, followed by a mixture of Ketamine and Xylazine (equal to or greater than 80 and 10 mg/kg, ip), and transcardially perfused with ice-cold phosphate buffered saline (PBS) followed by 4% paraformaldehyde in PBS. The spinal column with some muscle and portions of the rib cage still attached was pinned down onto a sylgard coated glass dish containing ice cold PBS and a laminectomy was performed under a dissection microscope. The spinal cord was carefully removed while keeping the dorsal root ganglion attached to the remaining portions of the vertebrae. The lumbar 4 dorsal root ganglion (L4 DRG) was identified relative to lumbar 1, the first ganglion past the rib cage. The DRG was placed in PBS and the roots were partially trimmed. It was then placed in ice cold 4% PFA for one hour at 4° C, subjected to gentle rotation and protected from light. The DRG was washed (3X) in 30% sucrose, and suspended in PBS over night at 4° C. Ganglia equilibrated in Tissue-TEK O.C.T. compound (VWR), for at least 20 minutes, and were then flash frozen in 2-methylbutane with CO2 pellets and sectioned at 14 μM on a Leica CM3050 cryostat. Sections were adhered to Fisherbrand Colorfrost Plus slides.

Staining and Quantification. Nissl stained slides (NeuroTrace® 640/660 Deep-Red Fluorescent Nissl Stain, Invitrogen) were counterstained with DAPI (Vector Laboratories), mounted (Vectashield HardSet Mounting Medium). and imaged (Leica SP5 confocal microscope) within several days of staining to prevent decreased signal and increased background. Total numbers of $tdTomato^+$ and $Nissl^+$ neurons were counted in FIJI in at least five sections. The average ratio of $tdTomato^+$ neurons to $Nissl^+$ cells was compared across ages using a two-way Anova followed by a post-hoc Tukey test in R. Cell areas were measured in thresholded tdTomato images using the FIJI analyze particles plugin (circularity=0.3, area > 100

μm^2). Overlapping cells were excluded. Area measurements were excluded from one animal due to high background. Comparisons of the mean and overall distributions for KO and WT were performed in R using a Welch's t-test and a Kolmogorov–Smirnov test respectively.

RNA Sequencing and Expression Analysis

RNA collection and library construction. Both L4 DRGs were dissected from animals perfused with PBS (without PFA) and were placed into a 1.5 ml low retention microtube (Phenix Research Products), containing 1 mL 1X PBS with 1 mg type XIV protease and 1 mg of Collagenase (Sigma-Aldrich), and then placed in a 37 ° C water bath for ten minutes. Subsequently, L4 DRGs were subjected to manual cell sorting as previously described (Hempel et al., 2007; Sugino et al., 2006). DRGs were washed in ice-cold artificial cerebral spinal fluid (ACSF; containing in mM: 126 NaCl, 3 KCl, 1.25 NaH2PO4, 20 Dextrose, 20 NaHCO3, 2 MgSO4 and 2 CaCl2, 0.05 APV, 0.02 DNQX and 0.0001 TTX; pH = 7.35; osmolarity = 320 mOsm; 1 % fetal bovine serum). The ganglia were triturated using fire polished Pasteur pipettes with successfully smaller inner diameters (~600, 300 and 150 μm) and then diluted in 20 mL of ACSF. Individual $tdTomato^+$ neurons were sorted manually using a micropipette with an inner diameter of 30-50 μm. Fluorescent cells were then passed through three subsequent petri dishes to increase sample purity and to dilute any RNA released during dissociation. For each sample, approximately 150 to 200 neurons were sorted, transferred into 50 μL of extraction buffer, processed using the picopure RNA isolation kit (Life Technologies), and subjected to on-column DNAse digestion. RNA samples were amplified using the Ovation RNA-seq system (NuGEN). The cDNA was sonicated into ~200 base pair fragments using a Covaris S 220 Shearing Device and then converted into sequencing libraries with the Ovation Rapid DR Multiplex System

(Nugen). RNA library concentration was quantified with a qPCR based Library Quantification Kit (KAPA biosystems) and then sequenced on an Illumina Nextseq.

Expression Analysis. Sequencing data was trimmed and quality filtered with cutAdapt (Martin, 2011). Subsequently ribosomal, mitochondrial and low complexity reads were removed and the data were mapped using RSEM (Li and Dewey, 2011). Expression of previously described proprioceptor- and other DRG sensory neuron-enriched genes (Usoskin et al., 2015) were filtered to remove those expressed at very low levels (sum of KO and WT expression < 2 transcripts per million), or that were common to both sets. Expression changes were calculated as the difference between KO and WT samples divided by the sum. Monte Carlo simulations were performed using in-house software written in python and R to assess the likelihood of observing changes in the expression of enriched genes by chance. For both lists, the summed expression changes were compared to summed expression changes of randomly selected genes, matching the approximate WT expression level of the enriched genes. Distributions of expected expression changes for expression matched gene lists were generated from one million points. The accession number for the RNAseq data is GSE86019.

Spinal Cord and Muscle Physiology

Spinal cord preparation. P21 control (Dicer WT and heterozygous) and mutant animals were used for both ventral root recording and muscle/nerve preparations. Animals were anesthetized and transcardially perfused with 5ml of ice-cold oxygenated (95% O2-5% CO2) artificial cerebrospinal fluid (ACSF; containing in mM: 127 NaCl, 1.9 KCl, 1.2 KH2PO4, 1 MgSO4·7H2O, 26 NaHCO3, 16.9 D(+)-glucose monohydrate, and 2 CaCl2). The spinal column and attached lower limbs were dissected free and immersed in a recirculating bath of cold (16-18°C), oxygenated ACSF. To improve preparation viability for ventral root recordings,

dissection was performed in ACSF in which NaCl was replaced by equal osmolar sucrose (254mM). The spinal cord was exposed via l laminectomy and hemisected to increase its oxygenation (Jiang et al., 1999). The preparation was transferred to a recording chamber and allowed to recover for 1 h in recirculating, oxygenated standard ACSF while the temperature was slowly brought to the recording temperature of 25°C.

Ventral root recordings. The ventral root of the fifth lumbar (L5) segment was drawn into a glass capillary and sealed against the ventral surface of the spinal cord by applied suction (A-M Systems, Sequim, WA). Stimulation of the dorsal root of the same segment (L5) was accomplished via a constant current stimulator (0.1ms pulse duration, A365 stimulus isolator, World Precision Instruments, Sarasota, FL). Threshold intensity required to evoke ventral root potentials ranged from 8-15μA. A standardized stimulation intensity of 2x threshold was used in these experiments. Differential recordings of ventral root potentials were recorded with an EX4-400 quad channel amplifier (1000x gain, 2Hz low cut, 500Hz high cut; Dagan, Minneapolis, MN) and digitized at 20kHz with WinLTP software (WinLTP, Bristol, UK). Peak amplitude, peak latency, and maximum slope of the rising phase of the response were determined offline using analysis tools in WinLTP (Anderson and Collingridge, 2007). Student's t-test was used to compare genotype responses. Mean responses ± standard deviation (SD) are presented.

Muscle and nerve preparation. Initial dissection procedures were similar to those for ventral root recordings preparations, but sucrose-replaced ACSF was not required. The nerve supply to the rectus femoris muscle of the quadriceps group was maintained up to the level of the 3rd and 4th lumbar roots (L3 and L4). All other muscles were dennervated. Tendons anchoring the rectus femoris on the ischial bone were preserved intact, while the tibia bone was cut free at the region of the insertion of the patellar tendon. Numerous minutiae pins were placed to

stabilize the femur and hip bone to minimize compliance of the joints during muscle stretch or contraction. A 6-0 silk suture was tied at the distal end of the patellar tendon and attached to the lever arm of a force-transducing micro-stepping motor (300C dual-mode muscle lever, Aurora Scientific, Ontario, Canada). Movements were controlled and digitized with Spike2 software (CED, Cambridge, UK).

The spinal cord was cut away in these preparations, but the peripheral ends of both dorsal and ventral roots were placed in suction electrodes. The force-length relationship was determined for each preparation to find the level of baseline tension (a function of muscle length) that generated the largest force during contraction. Muscle contraction was initiated by supra-threshold stimulation of motor axons innervating the rectus femoris. In our experience, the majority of motor axons supplying quadriceps muscles traveled through the L3 ventral root, and we found the greatest muscle force (monitored by the force-transducing motor) was generated when stimulating this root. One second vibration sequences were repeated 3 times with 3-5 second intervening rest periods. A variety of amplitude (20, 40, 80, and 120μm) and frequency (10, 20, 50, 100Hz) combinations were used with background stretches of ~110% of the baseline tension. Recordings of rectus femoris sensory responses were made via a suction electrode placed on L4 dorsal root (DRL4). We observed sensory axons supplying the quadriceps were found in both DRL3 and DRL4, but the majority of axons pass through DRL4. Recordings were made at room temperature (21-23^{0}C). Analysis was performed offline using custom scripts in Spike2 and MATLAB (The MathWorks, Natick, MA). Main effects and interactions between genotype, vibration frequency, and vibration amplitude were analyzed with a three-way ANOVA in SPSS (version 23, IBM). Data is presented as mean ± standard deviation (SD).

Muscle Immunohistochemistry

Tissue Collection. P30 mice were anesthetized with isofluorane and Ketamine/Xylazene and the Gastrocnemius and Tibialis Anterior were dissected. For VGluT1 staining of proprioceptive sensory endings, animals were transcardially perfused with ice cold PFA, followed by PBS. Muscles were fixed in PFA overnight at 4° C, then washed (3X) and equilibrated overnight in 30% sucrose, and then embedded in Tissue-TEK O.C.T. compound (VWR).

Immunhistochemisty. Muscles stained for S46 (intrafusal fibers) were flash frozen and not fixed. All sections were cut longitudinally, at 60 μm (S46) or 35 μm (VGluT1) and were mounted on Fisherbrand Colorfrost Plus slides. Intrafusal fibers were visualized as previously described (Taylor et al., 2005) with some modifications. Sections were blocked with 0.5% porcine gelatin (Sigma-Aldrich), 1.5% goat serum (Invitrogen) in 1% Triton-X-100 (Fisher) in Superblock buffer (Thermo Scientific) for at least two hours. Muscle tissue was stained overnight at 4° C with a mouse monoclonal S46 antibody (Developmental Studies Hybridoma Bank), along with a chicken anti neurofilament-h polyclonal antibody (Aves Labs), at 1:50 and 1:1000 respectively. Sections were washed in PBS and stained using goat anti-mouse Alexafluor 546 and goat anti-chicken alexafluor 488 (Invitogen) secondary antibodies at a 1:500 dilution, followed by three washes in PBS. Slides were mounted using Vectashield HardSet Mounting Medium with Dapi (VWR). The staining procedure for vGluT1 was similar except sections were incubated in the primary antibody, guinea pig anti vGluT1 (Millipore) at 1:1000 for at least two days at 4° C. Secondary incubations were performed at room temperature for three hours with Rhodamine Red goat anti-guinea pig (Jackson ImmunoResearch). Subsequently, sections were washed four times for 30 minutes. Statistics were done in R using a Welch's t-test.

Results

Parvalbumin-driven conditional ablation of Dicer leads to progressive ataxia in the 4th post-natal week

To better understand the role of Dicer in proprioception, Pvalb-Ires-Cre mice (Hippenmeyer et al, 2005) were mated to floxed dicer animals (Harfe et al, 2005), and, in most cases, to a conditional reporter line, Ai9 (Madisen et al, 2010), for visualization and isolation of the Pvalb positive population. Most experimental animals were generated from matings between $Pvalb^{cre/cre}$, $Ai9^{+/+}$, $Dicer^{flx/wt}$ parents, to generate animals that were either WT or homozygous for the floxed allele. These animals displayed a number of noticeable phenotypes, as observed previously (Valdez et al, 2014), Dicer KOs displayed clear ataxia, easily noticeable at post-natal day 30 (Fig.1A). Additionally, as early as p20 KO animals were hyperactive and occasionally displayed circling behavior. Also, KO animals were typically smaller and more emaciated than their WT littermates. Almost all KO animals appeared to be scoliotic and some animals experienced epileptic bouts that would occasionally lead to death. However, these animals were also highly uncoordinated in a manner similar to, but perhaps more severe than, that seen when proprioceptive sensory neurons conditionally express diptheria toxin (Akay et al., 2014). These animals were also reminiscent of the Etv1 and Neurotrophin3 mutants (Arber et al., 2000; Ernfors et al., 1994) as well as mice lacking Piezo2 in proprioceptive sensory neurons (Woo et al., 2015). Animals were born in normal Mendelian ratios becoming progressively more symptomatic and displaying reduced weight that worsened during the fourth postnatal week (data not shown), additionally animals rarely survived after age p70 without the aid of food pellets and hydrogel on the cage floor. To better characterize the onset of ataxia, two behavioral assays were performed. First, rearing behavior was assayed in a transparent cylinder. WT animals reared at a

roughly equal rate across ages, while KOs after some initial hyperactivity exhibited no rearing beginning at age p27 (Fig.1B). A repeated-measures ANOVA suggested that the effect of age was not significant (p=0.058), while genotype as well as an interaction between genotype and age were significant (p= 1.4×10^{-4}, 2.1×10^{-3}) suggesting that loss of Dicer impairs the use of hindlimbs for rearing and that the deficit increases with age. Furthermore a post-hoc t-Test with a Sidák correction suggested significant differences at p26-p28 (p = 3.3×10^{-3}) and p29-p30 (p = 6.7×10^{-3}). The gait of WT and KO animals was characterized by filming the movements of animals on a clear linear track (Fig.2.1C), and measuring the position of their fore- and hindlimbs. This enabled the quantification of both the average stance width (Fig.1D), the separation between forelimbs or hindlimbs in the x-axis (example in Fig. 1C), and stride length (Fig.1E), the forward distance travelled by a single limb in the y-axis. A repeated measures ANOVA for forelimb stance width showed significant effects for genotype and age as well as an interaction between these variables (p = 0.03, 1.23×10^{-5}, 8.86×10^{-4}). Genotype and age effects were also significant for the hindlimbs but showed no interaction (p = 0.046, 0.011,0.067). A post-hoc test suggested that only the p27 hindlimb and p30 forelimb results were significant (p = 1.9×10^{-3}, 1.1×10^{-4}). Changes in hindlimb stride length were not significant for genotype but were significant for age as well as an interaction between age and genotype (p=0.09, 2.47×10^{-3}, 9.56×10^{-5}). Lastly forelimb stride length was significant for genotype, age and an interaction between these two (p = 0.039, 2.22×10^{-3}, 9.66×10^{-5}). Post-hoc tests suggested that hindlimb and forelimb effects were significant at both p27 (p = 5.5×10^{-3}, 3.5×10^{-3}) and p30 (p = 2.2×10^{-4}, 1.7×10^{-5}). This data suggests that loss of Dicer leads to a progressive ataxia that largely incapacitates the animals by the end of the fourth post-natal week.

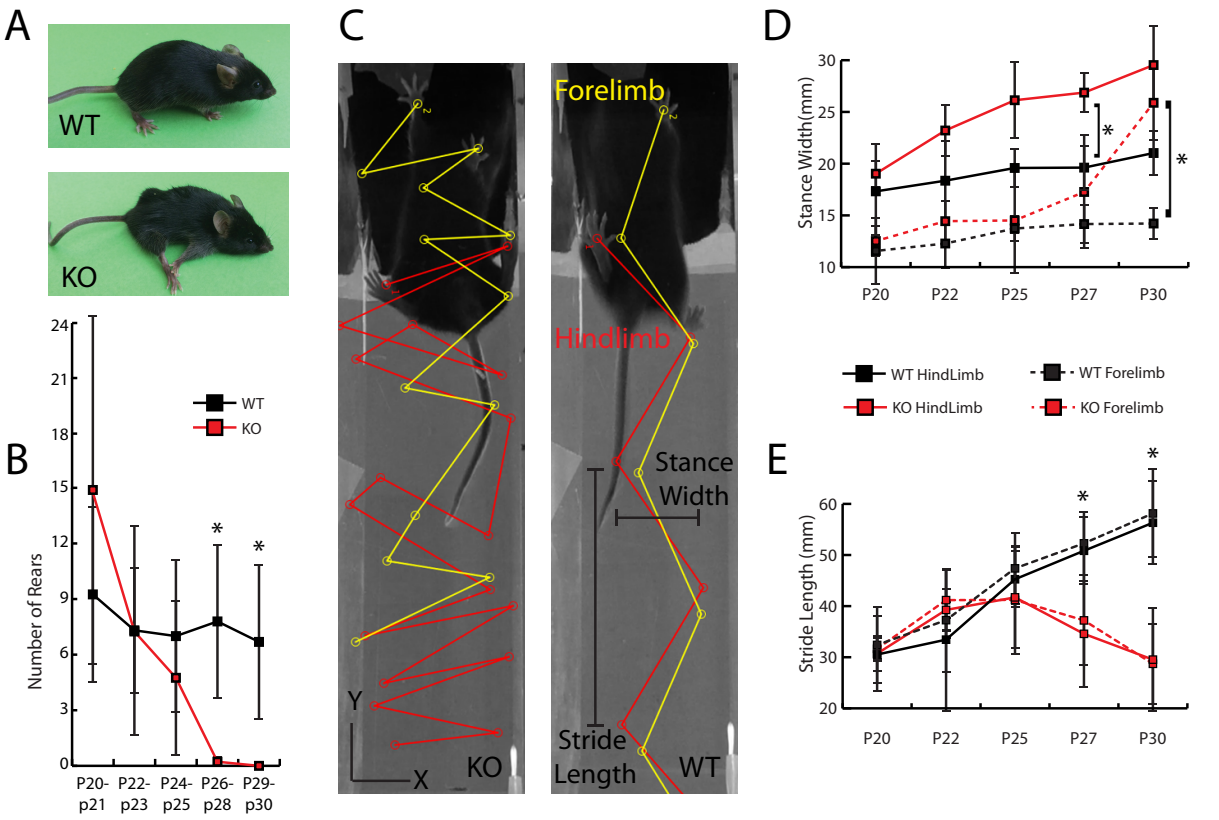

Figure 1. Conditional ablation of Dicer in parvalbumin positive (Pvalb^{+}) neurons elicits progressive ataxia. A, Photos of Pvalbcre/cre,Ai9+/+,Dicerwt/wt, WT mice (top) and Pvcre/cre,Ai9+/+,Dicerflx/flx, KO (bottom). B, Number of rears per 3-minute session at p20-p30 for both WT (n=8, black) and KO (n=6, red), error bars are standard deviation, asterisks in all panels show ages at which T-Test p-values were less than 0.05 after a Šidák correction C, Example images of mice walking on a linear track while filmed from below (KO on Left, WT is right). Paw patterns were measured for hind- and forelimbs, and separated into horizontal (stance width) and vertical (stride length) components. D, Stance width (mm), defined as the average difference in the x axis between either the fore or hind paws, increased progressively between p20 and p30, but the increase was much greater for KO than WT. E, WT stride length, calculated as the average distance (in the y axis) between movements within a limb, increased over the same developmental period, but KO stride length began to decrease after P25.

Progressive ataxia is accompanied by a loss of proprioceptive sensory neurons in the dorsal root ganglion

Since deletion of Dicer in other cell types can lead to cell death (Davis et al., 2008; Schaefer et al., 2007; Zehir et al., 2010) and since the behavioral phenotype was reminiscent of mutations affecting proprioceptive sensory neurons within the DRG (Arber et al., 2000; Ernfors et al., 1994; Tourtellotte and Milbrandt, 1998); we decided to look at the number of td-tomato positive neurons labeled by cre activity within the lumbar 4 DRG, a segmental level carrying sensory input from many hindlimb muscles, at p20, p25 and p30. DRGs were isolated, cryosectioned and then Nissl stained, and the numbers of tdTomato-positive neurons per section was counted. Due to variability between sections and animals we normalized the number of tdTomato-positive neurons to the number of Nissl-positive cells within each section to quantify the fractional change in the labeled population (examples shown in Fig. 2A). The results reveal that the fraction of tdTomato-positive neurons decline with age (Fig. 2B). A two way ANOVA demonstrated a significant effect for genotype ($p = 2.62 \times 10^{-4}$), and a post-hoc Tukey test showed that the effect of genotype was insignificant at ages p20 and p25 ($p = 0.95, 0.34$) but was significant at P30 ($p = 2.9 \times 10^{-3}$). It should also be mentioned that as expected there were no significant differences across ages for the Nissl-positive tdTomato-negative population (WT 178.4 ± 35.3, n = 16; KO 162.7 ± 53.0, n = 16, t-test: p = 0.33). Since $Pvalb^{+}$ neurons vary in size, the distribution of cross-sectional areas was measured at each age. Although, the area distributions are slightly different (Fig. 2C), as shown with a Kolmogov-Smirnov test (p = 0.041), the mean values for each animal were not significantly different (WT, n=16, mean = 564.7 ± 25.8; KO, n=16, mean= 557.5 ± 18.9; p = 0.82). These data suggest that cell loss occurs roughly equally for all subgroups within the $Pvalb^{+}$ population. Therefore, over

time, conditional ablation of dicer within Pvalb^{+} cells leads to a loss of the proprioceptive sensory neurons.

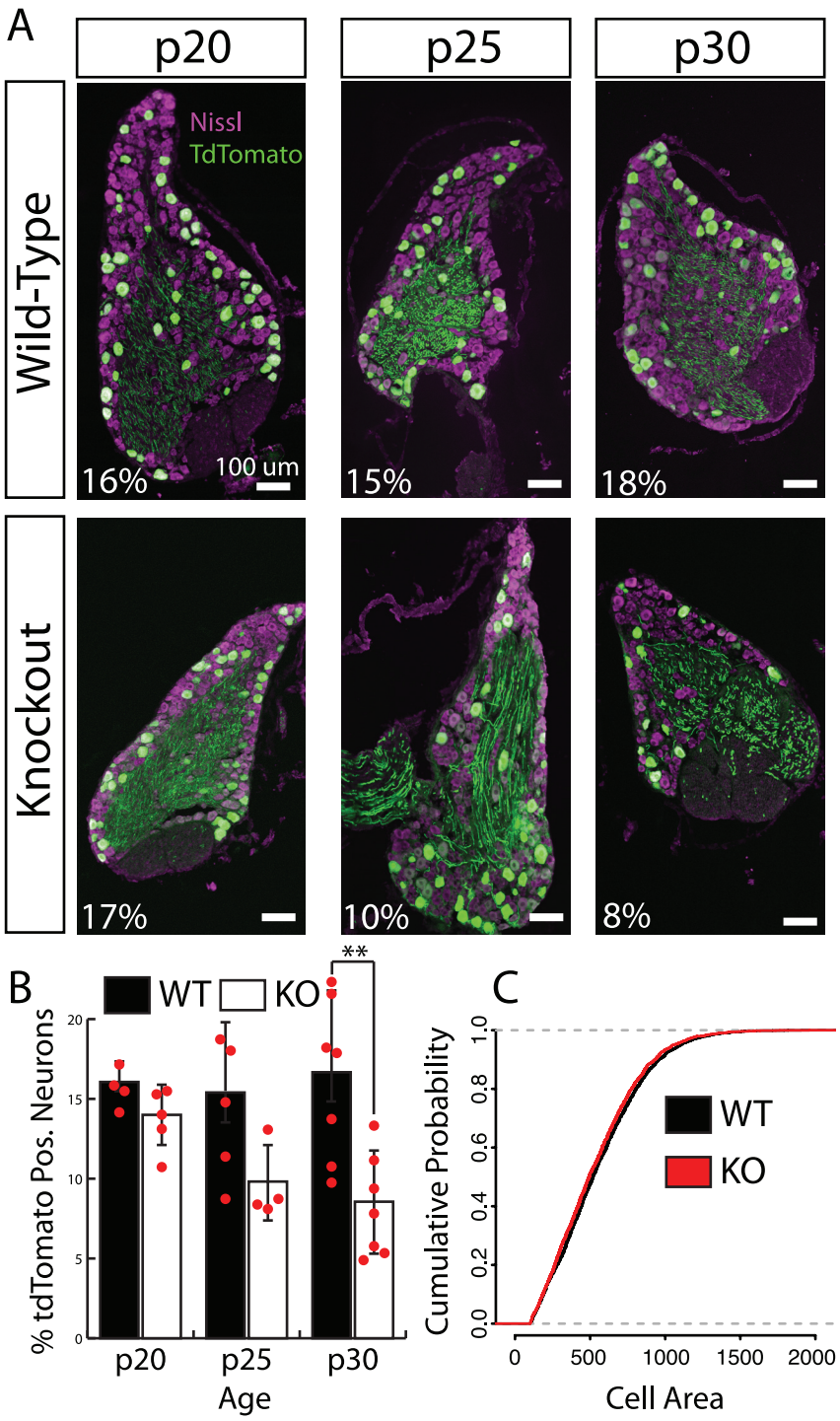

Figure 2 Dicer KO animals progressively lose Pvalb^{+} neurons within the dorsal root ganglion (DRG). A, Example images of L4 DRG cryosections from WT and KO animals at postnatal ages, 20, 25 and 30. Cre-activated tandem dimer tomato (tdTomato) labeled neurons

are shown in green, Nissl counterstain in magenta. % of td-tomato+ neurons (of total in section) indicated (bottom left), scale bar (bottom right) 100 μm. B, Average % tdTomato+ neurons for WT (black; n=4,5,7) and KO (red; n=5,5,7) for p20, p25, and p30, error bars are standard deviation and individual data points are represented by red dots. A two way ANOVA determined that the effect of genotype was significant ($p= 2.6 \times 10\text{-}4$). Post-hoc Tukey test demonstrated a significant reduction at p30 ($p=2.9 \times 10\text{-}3$) but not at p20 or p25 (p=0.951, 0.167). C, Cumulative probability distributions of cell areas for WT (16 animals, 2840 cells) and KO (16 animals, 2081 cells).

A loss of transcriptional specificity precedes proprioceptor cell death

To gain insight into the etiology of ataxia in KO animals, proprioceptive sensory neurons were isolated from lumbar 4, prior to the onset of cell death, at p21, and then subjected to RNA extraction and deep sequencing. It has been reported in retinal pigment epithelial cells, that loss of Dicer can cause global transcriptional misregulation and cell death as a result of runaway accumulation of transcribed Alu elements (Kaneko et al., 2011). To assess whether or not loss of Dicer in proprioceptive neurons causes accumulation of Alu elements or other transcribed retrotransposons, we aligned the sequencing data to the repeat masker track from the UCSC genome browser and normalized the read count for each motif to the total number of mapped reads. This revealed no significant differences in the abundance of SINE elements or of other categories of retrotransposons in KO vs. WT mice.

Having ruled out retrotransposons, the mRNA profiles of the KO cells were examined. Reads were mapped with RSEM (Li and Dewey, 2011) and differential expression was assessed using edgeR with a false discovery rate of 5% and a minimum baseline expression value of 20 transcripts per million (TPM). Overall, 2146 genes were down-regulated while 1728 were up-

regulated in the KO. The 15 up- and downregulated genes displaying the largest fold changes are shown in figure 3A. More than half (8 of 15) of the highly down-regulated genes (Pln, Tuba8, Relt, Heatr5a , Wls, Vstm2b, Kcnc1, and Nxph1) are highly enriched in proprioceptive sensory neurons relative to other neurons of the DRG (Usoskin et al., 2015). This prompted us to examine other genes strongly linked to proprioceptor survival or function. Etv1, TrkC, Runx3 and Sad-B were all downregulated (Fold Changes:-1.83, -3.39, -1.39 and -1.43). Piezo2, Tmem150C and Asic3 were either upregulated or unchanged (Fold Changes: 1.17 1.07, 2.17), and Pea3 (Etv4) was expressed at very low levels (<1 TPM) in both WT and KO. Together, these data suggest a widespread loss of proprioceptor-enriched genes.

In order to more quantitatively characterize the effect of Dicer KO on transcriptional identity, we used data from a previously published study (Usoskin et al., 2105), in which DRG sensory neurons were clustered into 11 groups, including two proprioceptive groups. We aggregated the top 50 genes that best defined each cluster in Usoskin et al., (after removing genes expressed at very low levels in both WT and KO), into two non-redundant lists of genes, enriched in proprioceptors (n=69) and non-proprioceptors (n=251) respectively. Proprioceptor enriched genes were much more likely to be downregulated in the KO neurons (Fig. 3B). In order to assess the likelihood that this downregulation could occur by chance, we performed a Monte Carlo simulation by repeatedly calculating expression changes for other randomly selected genes expressed at similar levels in proprioceptors, but not identified as proprioceptor-enriched. The observed expression change of the proprioceptor group (Fig. 3C, EC = -0.38) greatly exceeded that observed by chance (mean = -0.035; S.D. = 0.019, $n=10^6$). Conversely, genes enriched in other sensory neurons were largely upregulated (Fig. 3D) and this value (Fig. 3E, EC = 0.078) was more than eight SD from the mean of the randomized distribution (mean =

-0.022; S.D. = 0.012, n=10^6). These data suggest a loss of cell-type specific identity for the proprioceptive sensory neurons in response to Dicer KO.

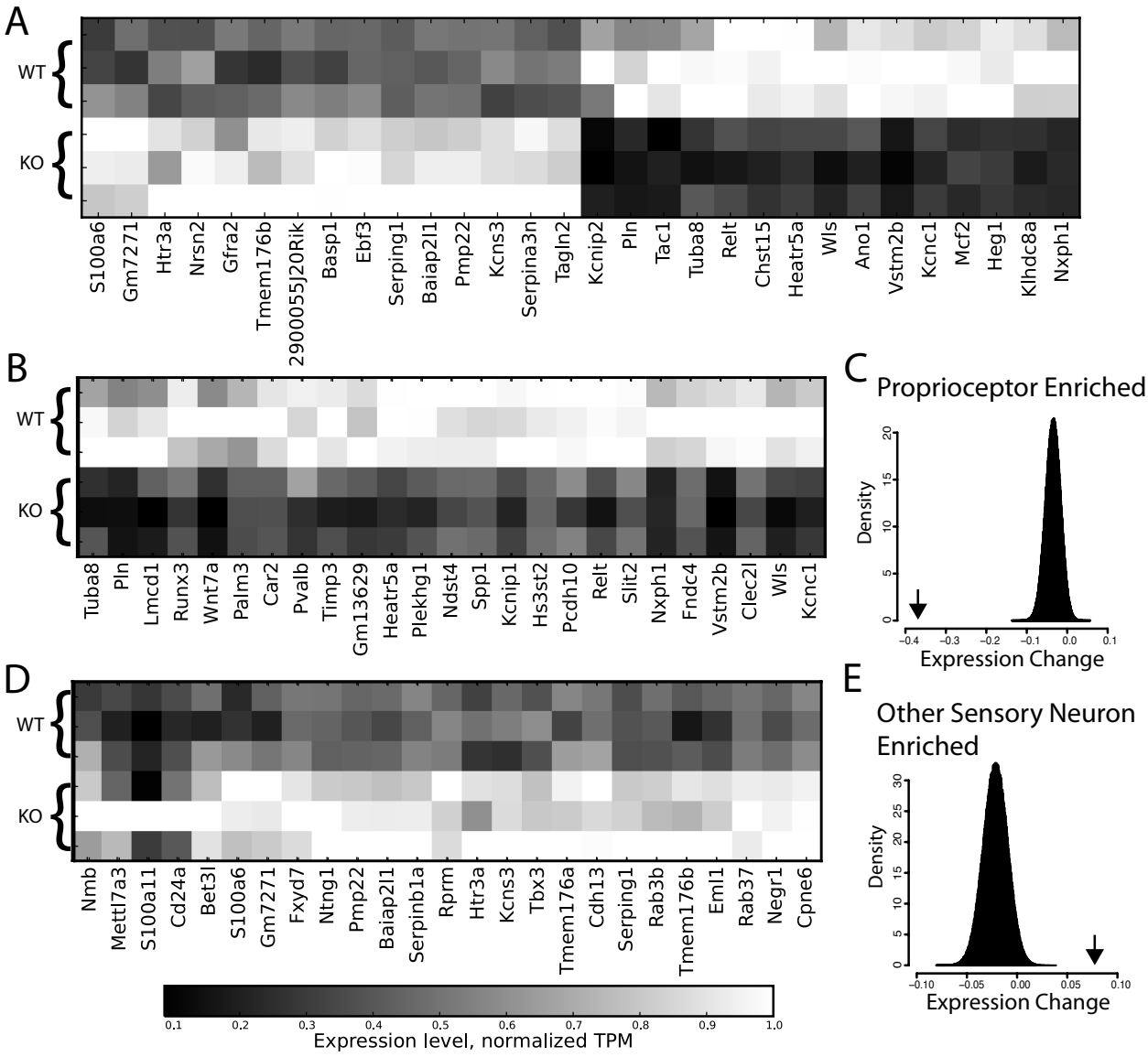

Figure 2 Pvalb$^+$ sensory neurons display a loss of propriocepor-specific gene (PSG) expression identity. A, Heat map of the top 15 up and down-regulated genes whose expression values were greater than 20 transcripts per million (TPM), the expression value for each biological replicate (n=3) is normalized to the maximum value within the column and calculated as the log base 2 of that value plus 1, the color map is shown at the bottom. B, An additional heat

map of expression values for selected PSGs (Usokin et al, 2015), n=3 for both genotypes. C, Monte Carlo simulation showing that down-regulation of PSGs, (-0.38, arrow) is greater than that for randomly selected genes matched for expression level (mean = -0.035; S.D. = 0.019, n=106). D, As in A, except for genes selectively enriched in DRG sensory neurons excluding proprioceptors. E, as in C but for non-proprioceptor genes and random selections matched to these expression levels. Modest up-regulation of these genes (0.078, arrow) is greater than expected by chance for randomly selected genes (mean = -0.022; S.D. = 0.012, n=106).

Group Ia sensory neurons maintain their connection with motor neurons despite Dicer KO

To better understand the functional consequences of the KO, synaptic connections between Ia proprioceptive afferents and motor neurons in the spinal cord were examined through measurements of ventral root potentials (Fig. 4A) following dorsal root stimulation using an *ex vivo* preparation (Mears and Frank, 1997). Ventral root responses increased with stimulus intensity from threshold (T), the current required to evoke a measurable response in the ventral root recordings, to 2xT and then plateaued (data not shown). Consequently, comparisons were made with data from 2xT stimulation. Unexpectedly, motor neuron responses were not reduced in KOs (Fig. 4B). While differences in peak amplitude (control 67.2 ± 21.5μV, n = 5; KO 107.9 ± 54.9μV, n = 8, t-test: p = 0.09) and maximum slope of the rising phase of the response (control 21 ± 10μV/ms, n = 5; KO 51 ± 40μV/ms, n = 8, t-test: p = 0.08) were not significant, the data suggests responses in KOs may, if anything, be larger than in control animals. The peak latencies were comparable in control (5.8 ± 0.9ms, n = 5) and KO (5.4 ± 1.5ms, n = 8; t-test: p = 0.577) animals, suggesting central action potential conduction and synaptic delays are not affected in KOs. These data suggest that any functional impairment prior to cell loss, is not present at central

proprioceptor synapses and suggests the phenotype of the KO animals may be largely driven by a deficit in the periphery.

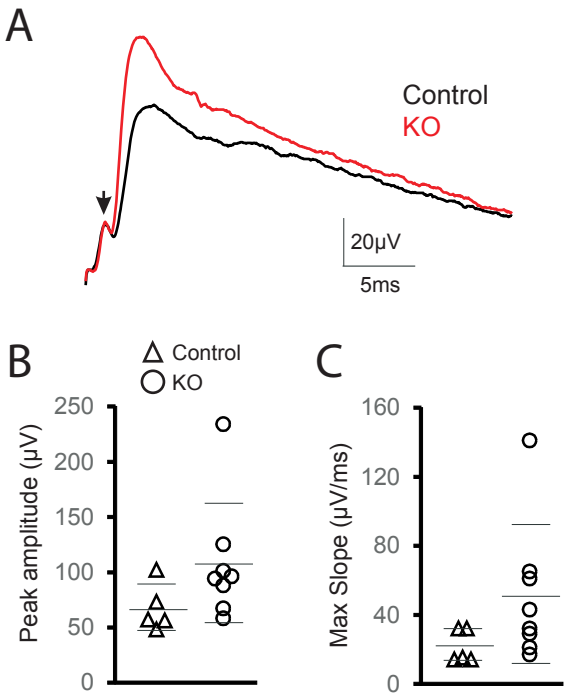

Figure 3: L5 motor neuron responses recorded in the L5 dorsal root following stimulation of sensory afferents. A, Representative average traces (15 individual sweeps at 0.2Hz) from control and mutant preparations illustrating compound motor neuron responses. Arrow highlights depolarization immediately preceding synaptic potential caused by synchronized sensory axon action potentials arriving in ventral horn of spinal cord. This potential is unaffected by high frequency sensory stimulation, while the synaptic potential is depressed (data not shown). Panels B and C show peak amplitude and maximum slope measurements for control (triangles, n=5) and KO (circles, n=8) animals (bars indicate mean ± SD). Stimulation intensity for all data shown was 2x threshold intensity required to elicit a measurable ventral root response.

By post-natal day 30 VGluT1+ sensory endings are largely absent from the muscle

Considering that the gene expression data demonstrated a loss of cell type specific expression (Fig3), relative to other DRG sensory neurons, and that proprioceptive sensory neurons are distinguished from other sensory neurons by their ability to innervate and transduce information about the muscles, sensory neuron connectivity to intrafusal muscle fibers was assessed using immunohistochemistry. The experiments were performed at p30 when all KO animals exhibited a robust phenotype. Since Pvalb is expressed postnatally in extrafusal muscle fibers (Celio and Heizmann, 1982), it was necessary to use another marker to determine if the intrafusal fibers, the targets of the Ia afferents, were still present, as a lack of these structures might explain the behavioral deficits we observed in the KO animals (Fig. 1). These intrafusal fibers can be specifically labeled with the S46 antibody (Miller et al., 1985) which targets a specialized form of myosin (Kucera and Walro, 1995). Annulospiral endings were also visualized using the neurofilament-h antibody in conjunction with S46 (Fig5A). $S46^{+}$ fibers were readily observed in both WT and KO animals (Fig5B and C). S46 counts were performed on both the gastrocnemius as well as the tibialis anterior to rule out the possibility that conditional Dicer ablation might have differential effects on antagonistic muscle groups as seen in the ETV1 mutant (de Nooij et al., 2013). The observations suggested that intrafusal fibers were largely unaffected (Fig. 5G) in the tibialis ($p = 0.904$) as well as the gastrocnemius ($p = 0.255$). Although large differences in the weight of both muscles were observed (Fig. 5I, $p = 2.28 \times 10^{-5}$, 0.01), these differences paralleled differences in the weight of KO animals. In order to ask if the loss of muscle mass might be related to mal-nourishment and/or some global problem with growth we normalized muscle weights to body weights (Fig. 5J) and found that if body mass is taken into account there were no significant differences in both muscle groups ($p = 0.11$, 0.56), suggesting that the loss of

muscle mass was driven globally, most likely by malnourishment, rather than by some process intrinsic to the muscles themselves. These data suggest that the intrafusal fibers remain intact upon conditional ablation of Dicer.

To further evaluate the effect of conditional ablation of Dicer on proprioceptive sensory neuron connectivity to the muscle, we examined VGluT1 expression in the tibialis and gastrocnemius. VGluT1 specifically labels proprioceptive sensory neurons at the site of their innervation of intrafusal fibers (Wu et al., 2004). Although, VGluT1 is thought to not be directly responsible for the mechanotransductive ability of these sensory neurons, it may serve a secondary signal-amplification role (Bewick et al., 2005). Disruption of staining for this marker can indicate a problem with proprioceptive connectivity in the muscle (de Nooij et al., 2013). Numerous VGluT1 positive sensory endings were observed in the WT (Fig. 5D) but staining was largely absent from the KO animals (Fig. 5E,F). The number of $VGluT1^{+}$ sensory endings observed per muscle section was steeply reduced (Fig. 5H) both in the tibialis ($p = 5.41 \times 10^{-5}$) and in the gastrocnemius ($p = 0.025$). These data support the conclusion that a Pvalb driven KO of Dicer specifically affects sensory endings of proprioceptive sensory neurons while leaving their target intrafusal fibers intact.

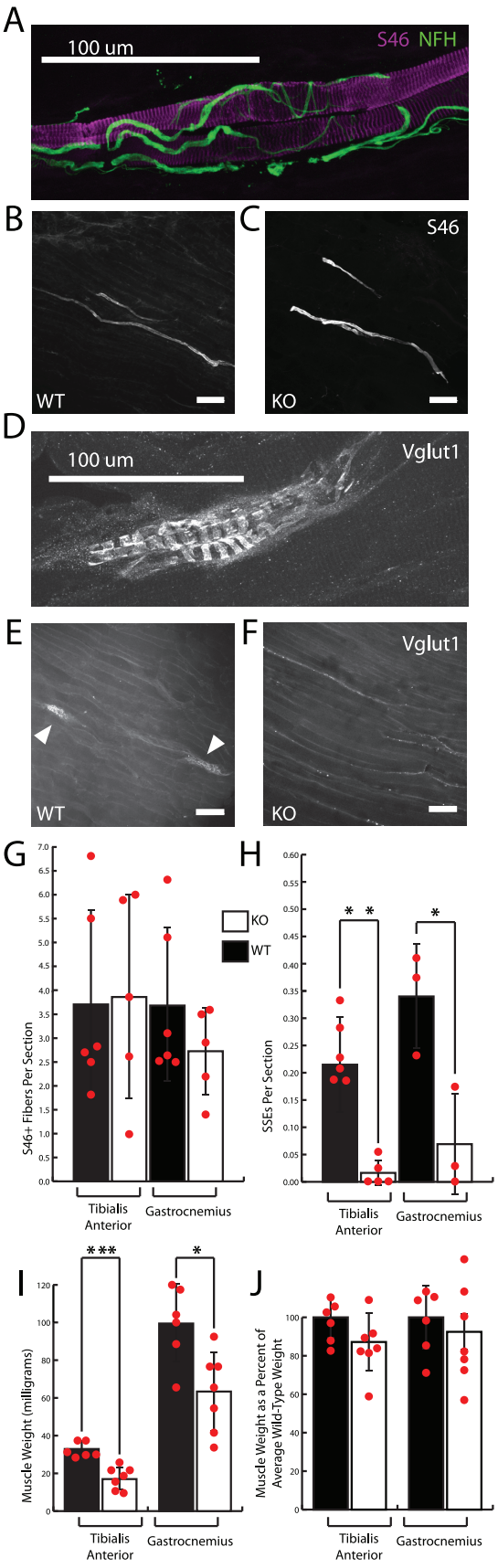
A
100 um
S46 NFH
B
WT
C
S46
KO
D
100 um
Vglut1
E
WT
F
Vglut1
KO
G
KO
WT
S46+ Fibers Per Section
Tibialis Anterior
Gastrocnemius
H
SSEs Per Section
Tibialis Anterior
Gastrocnemius
I
Muscle Weight (milligrams)
Tibialis Anterior
Gastrocnemius
J
Muscle Weight as a Percent of Average Wild-Type Weight
Tibialis Anterior
Gastrocnemius

Figure 5: Hindlimb muscles lose proprioceptive connectivity despite conservation of intrafusal fibers at post-natal day 30. A, Example image of an annulospiral ending from a WT p30 gastrocnemius muscle, intrafusal fiber labeled by S46 antibody (magenta), sensory axon labeled with neurofilament-h antibody (green), scale bars are 100 μm. B and C, Example WT and KO S46 positive fibers at p30. D, Close-up image of Vglut1 image from a p30 animal showing adjacent annulospiral endings. E, lower magnification of two spindle associated sensory endings (SSEs) in WT. F, An example section from a KO muscle displaying no SSEs. G, S46 fibers per section for the gastrocnemius and tibialis anterior muscle groups for WT (black; n=6) KO (white; n=5) are not significantly different (p= 0.90, 0.25), error bars are standard deviation, while red dots show individual data points. H, The average number of spindle associated sensory endings (SSEs) per muscle section was determined for the WT (black, n=3) and KO (white,n=3), in the tibialis anterior, and gastrocnemius WT (n=6), KO (n=7). Both differences were significant (p= 5 × 10-5, 0.025). I, Muscle weights (mg) for both WT (n=6) and KO (n=7) were significantly different for the tibialis and gastrocnemius (p = 2.3 × 10-4, 0.01), but were not significant when normalized to body weight (muscle weight/body weight), and expressed as a percentage of the average normalized WT value, J, (p= 0.11, 0.5455).

Dicer is necessary for maintaining functional Ia afferent connectivity with muscle spindles

Having established that Ia afferents can make functional connections with motor neurons, and that VGluT1 sensory afferents are absent in KO mice after the behavioral deficit is fully established, the peripheral sensitivity of these afferents was investigated at p21, prior to the onset of cell loss. Passive, small amplitude tendon vibrations selectively activate Ia afferents, but do not drive secondary spindle or Golgi tendon organ afferents (Brown et al., 1967).We assayed the sensitivity of these afferents in the rectus femoris (a knee extensor) muscle using a modified *ex*

vivo preparation (Franco et al., 2014; Wilkinson et al., 2012).Small amplitude stretches of the patellar tendon were delivered at various frequencies using a force-transducing motor and the compound responses of Ia afferents in the rectus femoris were measured by extracellular recordings at the L4 dorsal root.

A variety of amplitude (20, 40, 80, and 120μm) and frequency (10, 20, 50, 100Hz) combinations were used to probe Ia afferent sensitivity to vibration in control and KO animals. Representative examples of afferent responses to 100Hz vibration at 80μm amplitude are shown in Figure 6A. Compound action potentials were reliably observed with each vibration cycle in controls with little variability in amplitude throughout the 1- second vibration sequences. Deficits in KO animals were observed in two key parameters. Compound action potential amplitude was dramatically reduced in KOs animals at all vibration frequencies and amplitudes (Fig. 6A, B; $F(1,174) = 555.3$, $p < 0.0001$). Thus, fewer Ia afferents responded to this natural stimulus in KOs. The reduced cohort of responding afferents also failed to encode every vibration cycle, with unresponsive cycles observed with even the largest amplitude vibrations (see Fig. 6A for example, and Fig. 6B for quantification at all frequency and amplitude combinations; genotype effect $F(1,174) = 129.9$, $p < 0.0001$). Encoding failures occurred less frequently at lower frequency vibrations (see responses at 20 and 10Hz, for examples).

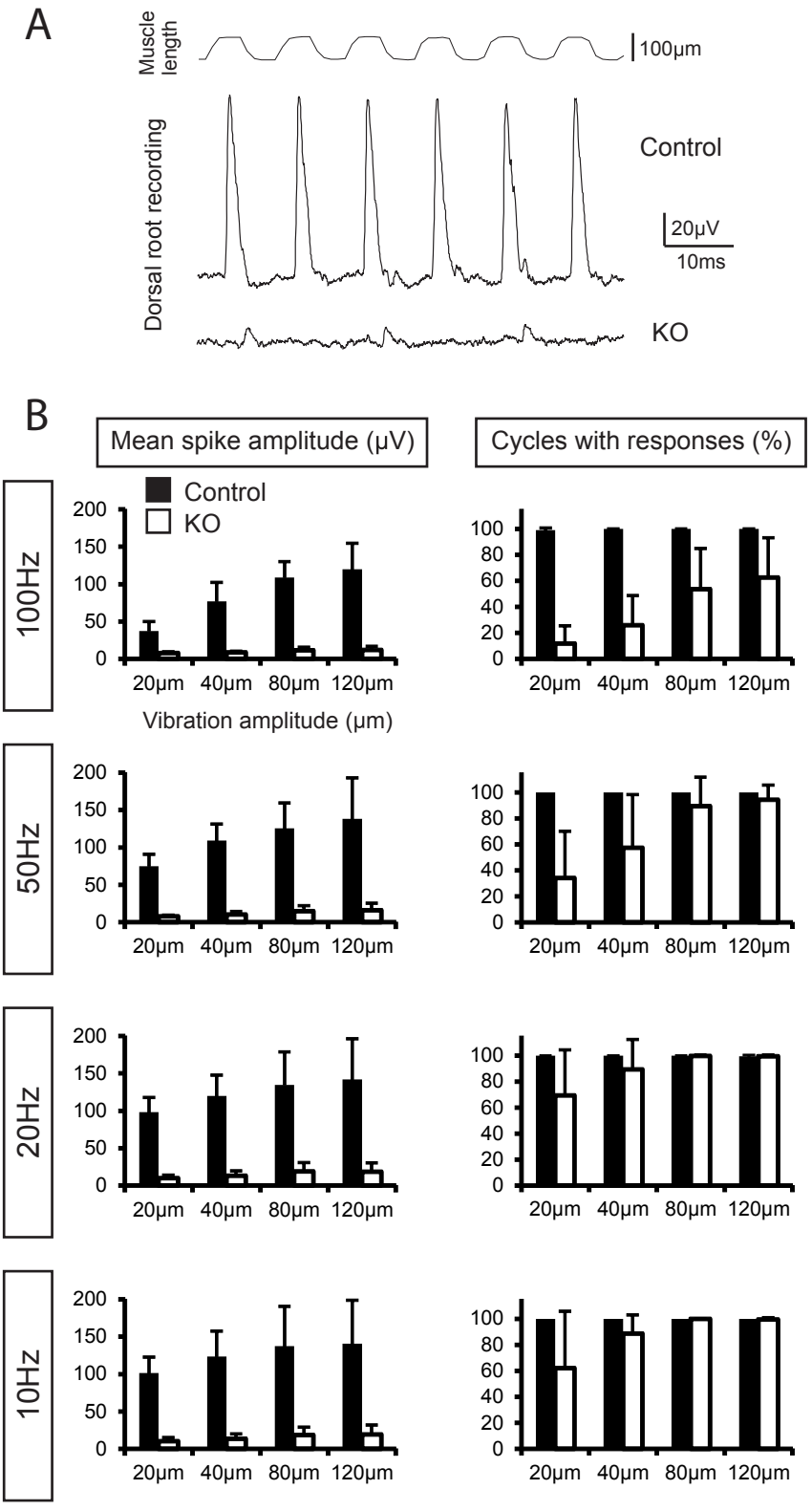
A
Muscle length
100µm
Dorsal root recording
Control
20µV
10ms
KO
B
Mean spike amplitude (µV)
Cycles with responses (%)
Control
KO
100Hz
50Hz
20Hz
10Hz
200
150
100
50
0
100
80
60
40
20
0
20µm 40µm 80µm 120µm
Vibration amplitude (µm)

Figure 6: Group responses of proprioceptive neurons to small-amplitude tendon vibration. A, Representative traces from control and mutant preparations illustrating responses to 6 cycles of 100Hz vibration with an amplitude of 80μm. Upper trace indicates changes in muscle length during vibration. Middle and lower traces show extracellular recordings of proprioceptive afferent responses measured at the L4 dorsal root in control and KO preparations, respectively. Note lack of response during some vibration cycles and overall diminished response amplitude in the KO trace. The left column of panel B shows average responses for control (n=6) and KO (n=5) animals to 100, 50, 20 and 10 Hz vibrations at varying amplitudes (± SD). Average compound action potential amplitudes increase with increasing vibration amplitude in control animals, but mutant responses are significantly reduced compared to controls at all vibration amplitudes and frequencies. The right column of panel B illustrates average consistency of responses to vibration. Greater deficits in response fidelity are observed at lower vibration amplitudes (20 and 40μm) in KO animals at all frequencies tested.

Discussion

We have demonstrated that conditional ablation of Dicer in Pvalb^{+} neurons leads to a progressive ataxia beginning during the fourth postnatal week. Development of the ataxia is accompanied by a loss of td-tomato labeled Pvalb^{+} neurons in the DRG. Before cell loss, however, these neurons lose aspects of their mature identity, showing a down-regulation of proprioceptor-specific genes and an up-regulation of genes that are specific to other sensory neurons within the ganglion. Although, afferents remain connected to spinal neurons in the KOs, deficits appear in the peripheral connections of these cells, culminating in a near complete loss of the proprioceptive

sensory ending marker VGluT1 during the fifth post-natal week. These data suggest Dicer is necessary to maintain the identity and function of proprioceptive sensory neurons.

Although we have focused on the role of proprioceptors, parvalbumin is also expressed in other parts of the motor system including Purkinje cells in the cerebellum, motorneurons and a subset of interneurons within the spinal cord, and the muscles themselves. There are several lines of evidence that lead us to believe that the observed ataxia results primarily from loss of function of proprioceptors rather than deficits in these other cell types. First, conditionally ablating Dicer solely in the parvalbumin-positive Purkinje cells with a Pcp2-cre driver causes degeneration of the Purkinje neurons. But cell loss and the resulting mild ataxia occur at several months of age rather than within the first several weeks (Schaefer et al. 2007). Second, a prior study found that Pvalb driven dicer KO does not alter the initial formation and maintenance of NMJs (Valdez et al., 2014), and we observed intact ventral root responses at P21 (Fig. 4) when compound responses of IA afferents are already highly abnormal (Fig. 6). Both of these findings argue against a primary defect in the motoneurons. Furthermore, some of the intrafusal fibers innervated by proprioceptors also express parvalbumin and therefore also potentially contribute to the behavior. Arguing against this is our observation that the S46 marker for intrafusal fibers remains stable. Finally, although the loss of $Pvalb^{+}$ neurons and the downregulation of Etv1 expression (Fig. 3) are reminiscent of those observed following loss of muscle NT3 (Patel et al., 2003) this is not likely to occur following Pvalb-driven loss of dicer. Of the intrafusal fibers, only bag fibers express NT3 (Copray and Brouwer, 1994), but bag fibers do not express Pvalb (Celio and Heizmann, 1982), therefore we can rule out a cell autonomous involvement of Dicer in spindle NT3 secretion. Note that although it is unlikely that an initial malfunction in spindles causes loss of proprioceptor connectivity, this does not rule out the possibility that loss of

connectivity may cause loss of trophic support of the proprioceptors. If a Dicer KO were to destabilize these connections, causing them to withdraw, this might then lead to a drop in TrkC signaling, due to a lack of contact with the NT3 secreting bag fibers, and a resulting increase in apoptosis and a decline in Etv1 expression.

Most directly and importantly, while this paper was being revised, Imai and colleagues (2016) reported similar ataxia and changes in proprioceptor survival and connectivity both following Dicer deletion using Pvalb-cre and using Advillin-Cre (which targets trigeminal and DRG sensory neurons). This strongly argues against a major contribution from Dicer expressed in other structures including both extra- and intrafusal muscle fibers, and argues that the motor symptoms reported here arise from a loss of Dicer in Pvalb-positive sensory neurons including proprioceptors.

Although this report focused on the ataxia phenotype these animals display this was not the only deficit we observed. For example, the weight loss, circling behavior, hyperactivity and bouts of epilepsy potentially point towards involvement of other circuits. Parvalbumin-positive neurons in structures such as the hypothalamus, inner ear, striatum and neocortex, as well as others, could potentially contribute to aspects of the observed aberrant behavior.

The timing of the behavioral phenotype during the fourth post-natal week contrasts with mutants reported in the literature. Etv1 mutants display noticeable ataxia days after birth (Arber et al., 2000), Runx3 mutants are also ataxic after birth. Although the precise onset is not reported (Levanon et al., 2002), these mutants do display a loss of proprioceptive afferents within the spinal cord at p0. Animals lacking TrkC, which is critical to proprioceptive sensory neuron survival, show abnormal movements as early as p4 (Klein et al., 1994). Additionally, knockout of Egr3, a gene essential for the induction of intrafusal fibers, produces a noticeable phenotype

by p5 (Tourtellotte and Milbrandt, 1998). The onset of these effects is much earlier than that observed in the Dicer KO described here, although, we cannot exclude the possibility that more sensitive tests may have revealed problems at an earlier age. Although Pvalb is expressed relatively late in some brain structures, it occurs in the DRG as early as E16.5 (Hippenmeyer et al., 2005) and parvalbumin-cre conditional ablation of Piezo2, the principal mechanotransduction channel of the proprioceptors, also produces abnormal motor behavior as early as p7 (Woo et al., 2015). It is also possible that the effects of impaired microRNA processing, may be delayed, due to the stability of the microRNAs themselves (Guo et al., 2015). However, studies in other systems demonstrate that such delays often do not occur. For example, loss of Dicer can produce strong and rapid deficits in the development of dopaminergic neurons (Huang et al., 2010), and can increase neuronal apoptosis days after Dicer deletion through Emx1-Cre (De Pietri Tonelli et al., 2008). The results presented here suggest the possibility that the late phenotype of the Dicer KO animals reflects a role in late functional maturation or in maintenance of the adult identity, rather than a role in the initial differentiation and early survival attributed to genes giving rise to earlier phenotypes. What is also interesting is that the timing of the stance width effect appears different between the forelimbs and hindlimbs. This difference might reflect differences in developmental periods between these two sets of appendages. Finally, it is tempting to speculate that a functional role for Dicer in late development might involve balancing the expression, post-transcriptionally, of critical components involved in mechanotransduction at the periphery of the proprioceptive axons in order to maintain and reliably transduce useful information about the muscle groups they innervate.

One surprising feature of the late behavioral deficit is the degree to which the connections onto the muscle are impaired prior to a measureable difference in the gait. We observed a large

difference in the group response of the proprioceptive sensory neurons during small amplitude vibrations of the rectus femorus at p21, but no significant changes in the behavior at this age. This could reflect central compensation for a peripheral deficit. Such compensation has been demonstrated in studies showing that chronically blocking transmission from sensory afferents elevates the ventral EPSP in response to dorsal root stimulation (Webb and Cope, 1992). However, we did not observe a significant difference in the ventral EPSP. It is possible that other aspects of central function not assessed here, such as motoneuron excitability, contributed to behavioral compensation, or that the behavior has a large functional reserve making it robust in the face of early losses of peripheral input.

Two other conditional knockouts also produce late effects on proprioceptors, and interestingly, both affect their peripheral, but not central connections, as observed following Dicer knockout. Targeted deletion of Erbb2 in the muscle produces an observable effect on behavior by around p15, as does selective elimination of NT3 from intrafusal fibers (Shneider et al., 2009). Both mutants affect the differentiation and/or trophic signaling from the intrafusal fibers and, like Dicer KO, produce modest or no effects on the central connections of proprioceptors.

How then does Dicer KO in the proprioceptors lead to deficits in muscle connectivity and transcriptional identity? In mammals, Dicer has several reported roles, processing microRNA precursors into mature transcripts, the generation of endogenous siRNAs, and in some instances preventing the accumulation of transcribed retro-transposons (Kurzynska-Kokorniak et al., 2015). We were able to eliminate the latter function, as our RNA sequencing data did not demonstrate an increase in SINE elements or other categories of retrotransposons. This suggests that a microRNA, siRNA or group of either is responsible for the decline in identity and

function. Unfortunately, isolating and sequencing the small RNA population from the proprioceptor population proved difficult and effects at the level of mRNA were widespread, precluding identification of a specific set of microRNAs or siRNAs responsible.

Loss of Dicer produced highly significant, but distributed changes in the proprioceptor transcriptome. Genes previously identified as critically important to proprioceptor development such as Etv1, Runx3, TrkC were modestly downregulated (1.4 to 3.4-fold) and on average proprioceptive enriched genes declined by 40%. This more distributed deficit is consistent with the effects of microRNAs in other systems (Bartel, 2009). Although we could not test the effects of each of these genes, one of us has found previously that a parvalbumin driven knockout of Etv1 produced no observable behavioral deficit (D. R. Ladle, personal communication).

The decline in cell type-specific expression within proprioceptors is reminiscent of the effects of loss of microRNA function in retinal cone cells (Busskamp et al., 2014), which leads to a decline in cone-enriched genes and a loss of their primary cellular specializations, the outer segment. A similar post-transcriptional regulation of identity and function has also been demonstrated in motor neurons (Amin et al., 2015; Thiebes et al., 2015) in which developmental expression of mir-218, is required to suppress a network of genes expressed in surrounding interneuron cell types. It seems feasible that proprioceptive sensory neurons require active post-transcriptional suppression of transcripts normally enriched in other DRG cell types as this would help explain the up-regulation of this gene group (Fig. 3D,E). Finally, in the work reported here, it is intriguing that the loss of cell identity at the transcriptional level is accompanied by a loss of functional muscle connectivity but an at least initial preservation of the central connections. An appealing explanation is that because all sensory neurons within the ganglion ultimately innervate the spinal cord, this property is more hardwired than some of the

sensory specializations these groups acquire. While there is ample evidence for genetic and epigenetic specification of neuronal cell types, the present results highlight the possibility that post-transcriptional regulation may serve to fine-tune and further specialize specific properties of neuronal cell types.

References:

Akay, T., Tourtellotte, W.G., Arber, S., and Jessell, T.M. (2014). Degradation of mouse locomotor pattern in the absence of proprioceptive sensory feedback. Proceedings of the National Academy of Sciences of the United States of America *111*, 16877-16882.

Amin, N.D., Bai, G., Klug, J.R., Bonanomi, D., Pankratz, M.T., Gifford, W.D., Hinckley, C.A., Sternfeld, M.J., Driscoll, S.P., Dominguez, B.*, et al.* (2015). Loss of motoneuron-specific microRNA-218 causes systemic neuromuscular failure. Science *350*, 1525-1529.

Anderson, W.W., and Collingridge, G.L. (2007). Capabilities of the WinLTP data acquisition program extending beyond basic LTP experimental functions. Journal of neuroscience methods *162*, 346-356.

Arber, S., Ladle, D.R., Lin, J.H., Frank, E., and Jessell, T.M. (2000). ETS gene Er81 controls the formation of functional connections between group Ia sensory afferents and motor neurons. Cell *101*, 485-498.

Bartel, D.P. (2009). MicroRNAs: target recognition and regulatory functions. Cell *136*, 215-233.

Bewick, G.S., Reid, B., Richardson, C., and Banks, R.W. (2005). Autogenic modulation of mechanoreceptor excitability by glutamate release from synaptic-like vesicles: evidence from the rat muscle spindle primary sensory ending. The Journal of physiology *562*, 381-394.

Bian, S., and Sun, T. (2011). Functions of noncoding RNAs in neural development and neurological diseases. Molecular neurobiology *44*, 359-373.

Brooks, S.P., and Dunnett, S.B. (2009). Tests to assess motor phenotype in mice: a user's guide. Nature reviews Neuroscience *10*, 519-529.

Brown, M.C., Engberg, I., and Matthews, P.B. (1967). The relative sensitivity to vibration of muscle receptors of the cat. The Journal of physiology *192*, 773-800.

Busskamp, V., Krol, J., Nelidova, D., Daum, J., Szikra, T., Tsuda, B., Juttner, J., Farrow, K., Scherf, B.G., Alvarez, C.P.*, et al.* (2014). miRNAs 182 and 183 are necessary to maintain adult cone photoreceptor outer segments and visual function. Neuron *83*, 586-600.

Carter, R.J., Lione, L.A., Humby, T., Mangiarini, L., Mahal, A., Bates, G.P., Dunnett, S.B., and Morton, A.J. (1999). Characterization of progressive motor deficits in mice transgenic for the human Huntington's disease mutation. The Journal of neuroscience : the official journal of the Society for Neuroscience *19*, 3248-3257.

Celio, M.R., and Heizmann, C.W. (1982). Calcium-binding protein parvalbumin is associated with fast contracting muscle fibres. Nature *297*, 504-506.

Cheloufi, S., Dos Santos, C.O., Chong, M.M., and Hannon, G.J. (2010). A dicer-independent miRNA biogenesis pathway that requires Ago catalysis. Nature *465*, 584-589.

Chen, H.H., Tourtellotte, W.G., and Frank, E. (2002). Muscle spindle-derived neurotrophin 3 regulates synaptic connectivity between muscle sensory and motor neurons. The Journal of neuroscience : the official journal of the Society for Neuroscience *22*, 3512-3519.

Cifuentes, D., Xue, H., Taylor, D.W., Patnode, H., Mishima, Y., Cheloufi, S., Ma, E., Mane, S., Hannon, G.J., Lawson, N.D.*, et al.* (2010). A novel miRNA processing pathway independent of Dicer requires Argonaute2 catalytic activity. Science *328*, 1694-1698.

Copray, J.C., and Brouwer, N. (1994). Selective expression of neurotrophin-3 messenger RNA in muscle spindles of the rat. Neuroscience *63*, 1125-1135.

Davis, T.H., Cuellar, T.L., Koch, S.M., Barker, A.J., Harfe, B.D., McManus, M.T., and Ullian, E.M. (2008). Conditional loss of Dicer disrupts cellular and tissue morphogenesis in the cortex and hippocampus. The Journal of neuroscience : the official journal of the Society for Neuroscience *28*, 4322-4330.

de Nooij, J.C., Doobar, S., and Jessell, T.M. (2013). Etv1 inactivation reveals proprioceptor subclasses that reflect the level of NT3 expression in muscle targets. Neuron *77*, 1055-1068.
De Pietri Tonelli, D., Pulvers, J.N., Haffner, C., Murchison, E.P., Hannon, G.J., and Huttner, W.B. (2008). miRNAs are essential for survival and differentiation of newborn neurons but not for expansion of neural progenitors during early neurogenesis in the mouse embryonic neocortex. Development *135*, 3911-3921.
Deneris, E.S., and Hobert, O. (2014). Maintenance of postmitotic neuronal cell identity. Nature neuroscience *17*, 899-907.
Ernfors, P., Lee, K.F., Kucera, J., and Jaenisch, R. (1994). Lack of neurotrophin-3 leads to deficiencies in the peripheral nervous system and loss of limb proprioceptive afferents. Cell *77*, 503-512.
Fishell, G., and Heintz, N. (2013). The neuron identity problem: form meets function. Neuron *80*, 602-612.
Fleming, S.M., Ekhator, O.R., and Ghisays, V. (2013). Assessment of sensorimotor function in mouse models of Parkinson's disease. Journal of visualized experiments : JoVE.
Franco, J.A., Kloefkorn, H.E., Hochman, S., and Wilkinson, K.A. (2014). An in vitro adult mouse muscle-nerve preparation for studying the firing properties of muscle afferents. Journal of visualized experiments : JoVE, 51948.
Guo, Y., Liu, J., Elfenbein, S.J., Ma, Y., Zhong, M., Qiu, C., Ding, Y., and Lu, J. (2015). Characterization of the mammalian miRNA turnover landscape. Nucleic acids research *43*, 2326-2341.
Harfe, B.D., McManus, M.T., Mansfield, J.H., Hornstein, E., and Tabin, C.J. (2005). The RNaseIII enzyme Dicer is required for morphogenesis but not patterning of the vertebrate limb. Proceedings of the National Academy of Sciences of the United States of America *102*, 10898-10903.
Hempel, C.M., Sugino, K., and Nelson, S.B. (2007). A manual method for the purification of fluorescently labeled neurons from the mammalian brain. Nature protocols *2*, 2924-2929.
Hippenmeyer, S., Vrieseling, E., Sigrist, M., Portmann, T., Laengle, C., Ladle, D.R., and Arber, S. (2005). A developmental switch in the response of DRG neurons to ETS transcription factor signaling. PLoS biology *3*, e159.
Huang, T., Liu, Y., Huang, M., Zhao, X., and Cheng, L. (2010). Wnt1-cre-mediated conditional loss of Dicer results in malformation of the midbrain and cerebellum and failure of neural crest and dopaminergic differentiation in mice. Journal of molecular cell biology *2*, 152-163.
Jiang, Z., Carlin, K.P., and Brownstone, R.M. (1999). An in vitro functionally mature mouse spinal cord preparation for the study of spinal motor networks. Brain research *816*, 493-499.
Johnston, R.J., and Hobert, O. (2003). A microRNA controlling left/right neuronal asymmetry in Caenorhabditis elegans. Nature *426*, 845-849.
Kaneko, H., Dridi, S., Tarallo, V., Gelfand, B.D., Fowler, B.J., Cho, W.G., Kleinman, M.E., Ponicsan, S.L., Hauswirth, W.W., Chiodo, V.A*., et al.* (2011). DICER1 deficit induces Alu RNA toxicity in age-related macular degeneration. Nature *471*, 325-330.
Klein, R., Silos-Santiago, I., Smeyne, R.J., Lira, S.A., Brambilla, R., Bryant, S., Zhang, L., Snider, W.D., and Barbacid, M. (1994). Disruption of the neurotrophin-3 receptor gene trkC eliminates la muscle afferents and results in abnormal movements. Nature *368*, 249-251.
Kosik, K.S. (2006). The neuronal microRNA system. Nature reviews Neuroscience *7*, 911-920.
Krol, J., Loedige, I., and Filipowicz, W. (2010). The widespread regulation of microRNA biogenesis, function and decay. Nature reviews Genetics *11*, 597-610.
Kucera, J., and Walro, J.M. (1995). An immunocytochemical marker for early type I muscle fibers in the developing rat hindlimb. Anatomy and embryology *192*, 137-147.
Kurzynska-Kokorniak, A., Koralewska, N., Pokornowska, M., Urbanowicz, A., Tworak, A., Mickiewicz, A., and Figlerowicz, M. (2015). The many faces of Dicer: the complexity of the mechanisms regulating Dicer gene expression and enzyme activities. Nucleic acids research *43*, 4365-4380.
Levanon, D., Bettoun, D., Harris-Cerruti, C., Woolf, E., Negreanu, V., Eilam, R., Bernstein, Y., Goldenberg, D., Xiao, C., Fliegauf, M*., et al.* (2002). The Runx3 transcription factor regulates development and survival of TrkC dorsal root ganglia neurons. The EMBO journal *21*, 3454-3463.
Li, B., and Dewey, C.N. (2011). RSEM: accurate transcript quantification from RNA-Seq data with or without a reference genome. BMC bioinformatics *12*, 323.
Li, C.L., Li, K.C., Wu, D., Chen, Y., Luo, H., Zhao, J.R., Wang, S.S., Sun, M.M., Lu, Y.J., Zhong, Y.Q*., et al.* (2016). Somatosensory neuron types identified by high-coverage single-cell RNA-sequencing and functional heterogeneity. Cell research *26*, 83-102.
Li, Y., Wang, F., Lee, J.A., and Gao, F.B. (2006). MicroRNA-9a ensures the precise specification of sensory organ precursors in Drosophila. Genes & development *20*, 2793-2805.

Madisen, L., Zwingman, T.A., Sunkin, S.M., Oh, S.W., Zariwala, H.A., Gu, H., Ng, L.L., Palmiter, R.D., Hawrylycz, M.J., Jones, A.R.*, et al.* (2010). A robust and high-throughput Cre reporting and characterization system for the whole mouse brain. Nature neuroscience *13*, 133-140.
Makeyev, E.V., Zhang, J., Carrasco, M.A., and Maniatis, T. (2007). The MicroRNA miR-124 promotes neuronal differentiation by triggering brain-specific alternative pre-mRNA splicing. Molecular cell *27*, 435-448.
Martin, M. (2011). Cutadapt removes adapter sequences from high-throughput sequencing reads. 2011 *17*.
Mears, S.C., and Frank, E. (1997). Formation of specific monosynaptic connections between muscle spindle afferents and motoneurons in the mouse. The Journal of neuroscience : the official journal of the Society for Neuroscience *17*, 3128-3135.
Miller, J.B., Crow, M.T., and Stockdale, F.E. (1985). Slow and fast myosin heavy chain content defines three types of myotubes in early muscle cell cultures. The Journal of cell biology *101*, 1643-1650.
Patel, T.D., Kramer, I., Kucera, J., Niederkofler, V., Jessell, T.M., Arber, S., and Snider, W.D. (2003). Peripheral NT3 signaling is required for ETS protein expression and central patterning of proprioceptive sensory afferents. Neuron *38*, 403-416.
Schaefer, A., O'Carroll, D., Tan, C.L., Hillman, D., Sugimori, M., Llinas, R., and Greengard, P. (2007). Cerebellar neurodegeneration in the absence of microRNAs. The Journal of experimental medicine *204*, 1553-1558.
Shneider, N.A., Mentis, G.Z., Schustak, J., and O'Donovan, M.J. (2009). Functionally reduced sensorimotor connections form with normal specificity despite abnormal muscle spindle development: the role of spindle-derived neurotrophin 3. The Journal of neuroscience : the official journal of the Society for Neuroscience *29*, 4719-4735.
Soukup, G.A., Fritzsch, B., Pierce, M.L., Weston, M.D., Jahan, I., McManus, M.T., and Harfe, B.D. (2009). Residual microRNA expression dictates the extent of inner ear development in conditional Dicer knockout mice. Developmental biology *328*, 328-341.
Sugino, K., Hempel, C.M., Miller, M.N., Hattox, A.M., Shapiro, P., Wu, C., Huang, Z.J., and Nelson, S.B. (2006). Molecular taxonomy of major neuronal classes in the adult mouse forebrain. Nature neuroscience *9*, 99-107.
Taylor, M.D., Holdeman, A.S., Weltmer, S.G., Ryals, J.M., and Wright, D.E. (2005). Modulation of muscle spindle innervation by neurotrophin-3 following nerve injury. Experimental neurology *191*, 211-222.
Thiebes, K.P., Nam, H., Cambronne, X.A., Shen, R., Glasgow, S.M., Cho, H.H., Kwon, J.S., Goodman, R.H., Lee, J.W., Lee, S.*, et al.* (2015). miR-218 is essential to establish motor neuron fate as a downstream effector of Isl1-Lhx3. Nature communications *6*, 7718.
Tourtellotte, W.G., and Milbrandt, J. (1998). Sensory ataxia and muscle spindle agenesis in mice lacking the transcription factor Egr3. Nature genetics *20*, 87-91.
Usoskin, D., Furlan, A., Islam, S., Abdo, H., Lonnerberg, P., Lou, D., Hjerling-Leffler, J., Haeggstrom, J., Kharchenko, O., Kharchenko, P.V.*, et al.* (2015). Unbiased classification of sensory neuron types by large-scale single-cell RNA sequencing. Nature neuroscience *18*, 145-153.
Valdez, G., Heyer, M.P., Feng, G., and Sanes, J.R. (2014). The role of muscle microRNAs in repairing the neuromuscular junction. PloS one *9*, e93140.
Webb, C.B., and Cope, T.C. (1992). Modulation of la EPSP amplitude: the effects of chronic synaptic inactivity. The Journal of neuroscience : the official journal of the Society for Neuroscience *12*, 338-344.
Wilkinson, K.A., Kloefkorn, H.E., and Hochman, S. (2012). Characterization of muscle spindle afferents in the adult mouse using an in vitro muscle-nerve preparation. PloS one *7*, e39140.
Windhorst, U. (2007). Muscle proprioceptive feedback and spinal networks. Brain research bulletin *73*, 155-202.
Woo, S.H., Lukacs, V., de Nooij, J.C., Zaytseva, D., Criddle, C.R., Francisco, A., Jessell, T.M., Wilkinson, K.A., and Patapoutian, A. (2015). Piezo2 is the principal mechanotransduction channel for proprioception. Nat Neurosci *18*, 1756-1762.
Wu, S.X., Koshimizu, Y., Feng, Y.P., Okamoto, K., Fujiyama, F., Hioki, H., Li, Y.Q., Kaneko, T., and Mizuno, N. (2004). Vesicular glutamate transporter immunoreactivity in the central and peripheral endings of muscle-spindle afferents. Brain research *1011*, 247-251.
Yang, J.S., Maurin, T., Robine, N., Rasmussen, K.D., Jeffrey, K.L., Chandwani, R., Papapetrou, E.P., Sadelain, M., O'Carroll, D., and Lai, E.C. (2010). Conserved vertebrate mir-451 provides a platform for Dicer-independent, Ago2-mediated microRNA biogenesis. Proceedings of the National Academy of Sciences of the United States of America *107*, 15163-15168.
Zehir, A., Hua, L.L., Maska, E.L., Morikawa, Y., and Cserjesi, P. (2010). Dicer is required for survival of differentiating neural crest cells. Developmental biology *340*, 459-467.
Zhao, C., Sun, G., Li, S., and Shi, Y. (2009). A feedback regulatory loop involving microRNA-9 and nuclear receptor TLX in neural stem cell fate determination. Nature structural & molecular biology *16*, 365-371.

Chapter 3:

Mir-7 controls cortical interneuron excitability in an activity and experience dependent manner.

Note: The contents of this chapter represent a preliminary manuscript that after some additional work I plan to submit for publication during summer, 2017. I performed most of the work highlighted in this manuscript with only one exception: Praveen Taneja collected some of the Dicer physiology data in slice Culture.

Abstract

How neurons regulate their intrinsic excitability has an impact on the transfer of information, the excitability of the network and the health of the animal. Much is known about how excitatory neurons regulate their excitability, however, very little is understood about inhibitory neuron plasticity. Fast-spiking (FS) cells represent the largest group of neocortical inhibitory neurons and understanding their properties has implications for the treatment of epilepsy, autism and schizophrenia. This study addresses the degree to which post-transcriptional regulation contributes to FS cell excitability. Mir-7 is differentially regulated in FS cells but not excitatory neurons by activity deprivation. Furthermore, TTX treatment in culture or reduction of activity with sensory deprivation controls FS cell excitability in a Dicer and mir-7 dependent manner. Sequencing of mRNA from FS cells reveals that activity deprivation affects hundreds of

different transcripts. Furthermore, this data suggests that mir-7 may control FS cell excitability through the regulation of PIP_2 metabolism.

Introduction:

During the course of development, all neurons experience drastically changing activity patterns. These changing activity patterns interact with complex regulatory networks encoded in the genome. How the neuron responds to a constantly shifting activity environment occurs at numerous cellular loci. For example, neurons may adjust the postsynaptic sensitivity of their excitatory connections, their intrinsic excitability or the release properties of their presynaptic terminals (Davis and Bezprozvanny, 2001; Desai et al., 1999; Turrigiano et al., 1998). The adjustment of these properties are thought to endow neural networks with the ability to robustly propagate internally generated as well as external sensory signals, while simultaneously restricting activity patterns from entering pathological regimes that may lead to epilepsy, autism, schizophrenia and other disease states.

Understanding and cataloging the molecular mechanisms governing global plasticity is complicated by the breadth of cellular diversity within the nervous system. Several studies have shown that the response of differing cell types can vary given the same activity perturbation. For example, visual deprivation during the critical period produces an increase in the strength of excitatory connections between pyramidal neurons while decreasing the strength of monosynaptic connections from fast-spiking (FS) to excitatory cells (Maffei et al., 2004). Visual experience can also generate vastly differing gene expression responses in different cortical cell types (Mardinly et al., 2016). Additionally, the function of these activity-regulated genes can differ depending on their context. The activity responsive transcription factor Npas4, is induced

in both excitatory and inhibitory neurons, but enacts differing downstream genetic programs between cell types (Spiegel et al., 2014). Lastly, from a network homeostasis standpoint, increasing excitatory output onto excitatory cells would raise network activity, while increasing excitatory output onto FS cells should decrease network activity. Hence robust network stability may require excitatory and inhibitory neurons to possess at least partially opposing plasticity programs.

In the cortex, the most of our understanding of cellular and synaptic plasticity comes from excitatory neurons. Reasonably so, as these cells are the predominant neuronal population and prior to the advent of transgenic and knock-in animals the examination of rare neuronal populations was often technologically infeasible. Understanding FS cell plasticity is of particular importance as these neurons are the largest population of cortical inhibitory neurons (Rudy et al., 2011), exert a large amount of control over pyramidal neuron firing through potent perisomatic inhibition and heavily shape network activity (Cardin et al., 2009). Additionally, FS cell dysfunction is thought to drive a number of nervous system disorders. Impairment of the Neuregulin-Erbb4 system in FS cells produce schizophrenia like symptoms in mice (Del Pino et al., 2013) and is also related to epilepsy in humans (Li et al., 2011). An improved mechanistic understanding of FS cell plasticity may offer hope for targeted therapeutic approaches in the future.

Post-transcriptional regulation through microRNAs has already been implicated in multiple forms of Hebbian as well as homeostatic plasticity (Cohen et al., 2011; Qureshi and Mehler, 2012). Using organotypic slice culture, where it was possible to precisely control activity patterns pharmacologically, it was asked if there were any activity responsive microRNAs in FS cells during chronic TTX treatment. It was found that mir-7 was differentially

regulated in FS cells and not excitatory neurons. Also, FS cells adjust their intrinsic excitability in a Dicer and mir-7 dependent manner. Furthermore, this mechanism is conserved *in vivo* during whisker deprivation in barrel cortex. mRNA sequencing in culture implicated mir-7 control of Phosphatidylinositol 4,5-bisphosphate (Pip_2) metabolism as the target for mir-7 control of FS cell excitability. A Pip_2 related mechanism is consistent with observed changes in inward rectifying and two-pore potassium channel currents as both have already been demonstrated to be affected by Pip_2 levels.

Materials and Methods

Mice and genotyping: All procedures for animal experiments were approved by the Brandeis University Animal Care and Use Committee. Most animals were obtained from Jackson labs, including the tdTomato reporter line Ai9 strain (Madisen et al., 2010), parvalbumin-ires-cre mice (Hippenmeyer et al., 2005), Emx-ires-cre animals (Gorski et al., 2002), Camk2a-Cre transgenics (Tsien et al., 1996) and the floxed Dicer animals (Harfe et al., 2005). The mir-7 sponge line was a gift from Dr. Tao Sun at Cornell (Pollock et al., 2014). Experimental animals were obtained by mating $Pvalb^{cre/cre}$, $Ai9^{+/+}$ or $Pvalb^{cre/cre}$, $Ai9^{+/+}$, $Dicer^{flx/wt}$ mice to either $Dicer^{flx/wt}$ or $mir\text{-}7p^{+/-}$ parents, or mating either $Camk2a\text{-}Cre^{+/+}$ or $Emx\text{-}ires\text{-}cre^{+/+}$ to $Ai9^{+/+}$ mice. Animals were genotyped using the extract and amp PCR kit (Sigma-Aldrich) or the Mouse Direct PCR Kit (Biotools) using primers and PCR programs recommended by Jackson labs or using primers targeting destabilized EGFP for the sponge mice.

Whisker plucking: Animals were subjected to whisker plucking at p21 (± 1 day). Mice were anesthetized with isofluorane (~0.3%), initially via a chamber and subsequently through a nose-cone. The D-row and γ whiskers, on the animal's right side, were identified under a microscope

and carefully plucked with forceps as previously described (Fox, 1992). The animals were sacrificed for recordings approximately 1 to 2 days later (p23).

Slice Culture: Organotypic slice cultures were generated as previously reported (Stoppini et al., 1991) with some modifications. In brief, animals ~postnatal day 7, were anesthetized with isofluorane, followed by a mixture of Ketamine and Xylazine (equal to or greater than 80 and 10 mg/kg, ip). Pups were decapitated; the brains were then extracted and blocked perpendicular to the somatosensory cortex, with the cerebellum removed. The tissue was encased in 2% low melt agarose dissolved in ACSF and transferred to a VF-200 compresstome (precisionary instruments). The brains were sliced in ice cold (~4°C) ACSF ([in mM] , NaCl 126, KCl 3, $MgSO_4$ 2, $NaH_2PO_4H_2O$ 1, $NaHCO_3$ 25, $CaCl_2$ 2, Dextrose 25). Subsequently, 300 μm sections from somatosensory cortex were transferred to prewarmed (35°C) millicell membrane inserts (EMD-Millipore, PICMORG50; 0.4 μm) sitting on top of slice culture medium (Minimum Essential Medium Eagle supplemented with 20% Horse Serum, Insulin 1 mg/ml and [in mM]: HEPES 30, NaHCO3 5.2, d-Glucose 12.9, l- Ascorbate 0.5, $MgSO_4$ 2, Glutamine 1, $CaCl_2$ 1; pH = 7.35, ~315 mOsm). Slices were placed in an incubator (~90% relative humidity, 95% O_2, 5% CO_2 at 35°C) and the media was exchanged every other day. Tetrototoxin (TTX) treatment (0.5 μM, Tocris) began at estimated post-natal day 18 (ep18) and lasted for approximately four days.

Slice Physiology:

Acute slice preparation: Juvenile mice were anesthetized with isofluorane, decapitated and their brains removed and placed into ice cold oxygenated ACSF. The brain was then blocked as previously described for thalamocortical slices (Finnerty et al., 1999), on a 10° ramp with the anterior portion facing down-hill. The blocking cut was made at 50° angle relative to the midline,

such that the left hemisphere of the cortex was preserved (to facilitate recording from the deprived barrels). The brain was glued to a platform and cut using a Leica VT 1000 S vibratome in ice cold oxygenated ACSF. Around 1.6 mm was removed from the top half of the brain (the anterior portion facing upwards) and subsequently several 300 μm slices were collected and transferred to warmed (35°C) ACSF for 15 minutes of recovery, prior to being placed at room temperature and continuously oxygenated prior to recordings. Barrels were identified as previously reported (Welker and Woolsey, 1974), by examining the slices under IR illumination and identifying the five primary barrels, with the E barrel closest to the midline. All acute slice recordings were done in layer 5 FS cells.

Patch clamp recordings: Slices were continuously perfused, 2 to 3 ml/minute, with ACSF (pH=7.35, osmolarity = 310 mOsm), warmed to 33°C,oxygenated, and supplemented with 50 μM picrotoxin, to block Gaba-A receptors, 20 μM 6,7-dinitroquinoxaline-2,3- dione, (DNQX), to block AMPA and Kainate receptors, and 50 μM 2-amino-5- phosphonovaleric acid (AP-V), to prevent NMDA receptor activation (ultimately preventing synaptic transmission during recordings). Borosilicate glass pipettes (1B100F-4, World Precision Instruments), pulled on a P-97 pipette puller (Sutter Instrument Co.) had a tip resistance of 3-7 MΩ and were filled with a K-Gluconate internal solution (Biocytin 0.5%, [in mM] , KCl 20, K-Glu 100, K-Hepes 10, Mg-ATP ,4 Na-GTP 0.3, Na-Phosphocreatine 10, with sucrose added for an osm = 295 mOsm, pH=7.35). Recordings were amplified by an Axoclamp 700A amplifier (Molecular devices), digitized at 40 kHz, and acquired through custom Igor-pro software (Wavemetrics). Recorded neurons had a series resistance less than 20 MΩ, and series resistance was stable within 20% across recordings. Cells had a resting potential less than -60 mV (for acute slices) or -55 mV (for culture). Cells were held at either -70 mV (acute) or -60 mV (culture). Cultured cells, on average, had a more

depolarized resting potential and a lower membrane resistance. A -50 pA or -10 mV square (for current or voltage clamp) pulse was applied at the beginning of each trace to measure the membrane resistance. For firing-current (FI) curves, all cells were given an initial series of current pulses to provide an estimate of the rheobase prior to the initiation of an FI curve protocol with stimulating pulses selected to range from 100 to 200 pA below the rheobase of the neuron to 0.6 (acute) or 1.2 (slice culture) nA above the initial stimulus. Rectangular current pulses were delivered in either 50 (acute) or 100 (culture) pA increments, lasted 1 second, and each stimulation was separated by 30 seconds. FI curves were analyzed using custom software written in IGOR, while statistics were performed in R using a linear mixed effects model to compare FI curves or a student's t-test to for examining the membrane resistance and capacitance within a genotype. Cells recorded for IV ramps met similar standards to those acquired in current clamp. However, neurons were recorded in pairs (a spared and deprived layer 5 FS cell). At the beginning of each IV ramp experiment, the rheobase was measured with a series of square current pulses separated by 50 pA amp intervals (similar to the FI curve experiments). Afterwards, Zd-728 and TTX (10 μM and 0.4 μM, respectively) were added to the bath to block the hyperpolarization activated channels (Ih) and voltage gated sodium channels respectively. Approximately 10 minutes post-perfusion, the cells were subjected to a voltage ramp (-125 to -25 mV, 20 mV/s) that was performed in triplicate. Following this initial acquisition, additional voltage ramps were acquired after application of 10 μM Barium to block inward rectifier potassium channels, followed by 40 μM 4-AP to block a subset of voltage gated potassium channels (most likely including KV1 and KV3 family members), with at least 20 minutes separating each acquisition from the drug's application. IV curve data was imported and

analyzed using a custom scripts written in python. All mean values for electrophysiology data are expressed with ± S.E.M throughout the text.

RNA seq:

Cell sorting: Slice cultures were converted into a single cell suspension as previously described (Sugino et al., 2006), with some modifications. After TTX treatment, organotypic slice cultures were placed in ice cold, oxygenated ACSF with 1% FBS and 5% Trehalose (Saxena et al., 2012), that had been 0.4 μm filtered, containing blockers (APV, DNQX and TTX) to prevent excito-toxicity. The slice culture was gently removed from the membrane and the cortex was micro-dissected under a Leica MZ 16-F fluorescent microscope and placed in an oxygenated room temperature bath, supplemented with 1 mg/ml type XIV protease (Sigma-Aldrich), for 45 minutes. Afterwards, the tissue was moved back to the ACSF solution (without protease) and triturated with fire polished Pasteur pipettes of successively smaller diameters (~600, 300 and 150 μm). Then, samples were either manually sorted (mRNA sequencing of PV cells) or subjected to FACS (all other samples) with a bd FACSaria machine. Manual sorting followed the protocol previously published in our lab (Sugino et al., 2006). All isolated material for mRNA sequencing was harvested using the picopure RNA isolation kit (Life Technologies) and subjected to an on column DNAase digestion. mRNA libraries were prepared as previously described (O'Toole et al., 2017). In brief, samples were amplified with the Ovation RNA-seq system (Nugen), sonicated with a Covaris S 220 Shearing Device, then libraries were constructed with the Ovation Rapid DR multiplex System (Nugen), the concentration of which was determined with the Illumina library quantification kit (KAPA biosystems). Small RNAs were harvested with the Qiagen RNeasy microKit. Within excitatory or parvalbumin cell populations, roughly comparable numbers of neurons were used to prepare libraries to reduce amplification

and purification biases (~1000 for PV cells and ~2000 for excitatory). The small RNA libraries were constructed with the TailorMix miRNA Sample Preparation Kit V2 (Seqmatic), all samples underwent 17 cycles of amplification and were quantified similarly to the mRNA libraries. Samples were sequenced on either an Illumina Nextseq or Hiseq sequencer. mRNA libraries had around 25 million reads, while sRNA libraries had at least half a million reads.

RNA seq analysis: mRNA sequencing data was trimmed and quality filtered with cutAdapt (Martin, 2011), afterwards low complexity, ribosomal and mitochondrial reads were filtered. Reads were mapped with RSEM (Li and Dewey, 2011), differential expression and data plotting was performed with custom-python scripts. Small RNA sequencing was also trimmed and quality filtered with cutAdapt. The data was then mapped with Bowtie2 (Langmead and Salzberg, 2012) and microRNAs were counted with featureCounts (Liao et al., 2014). Differential expression analysis was performed with edgeR (Robinson et al., 2010). Annotation of small RNA content was performed with annotateBed (Quinlan and Hall, 2010). All small RNA data was plotted with Matplotlib in python. Finally, fold-change (FC) was calculated as the number of TTX reads divided by the control condition.

Results:

Activity profiling of microRNAs in neocortical excitatory and pvalb$^+$ neurons:

To study the post-transcriptional regulation of FS cells, we asked how microRNA expression was affected by activity deprivation and how this response differed from that in excitatory cells. Pvalb-Ires-Cre mice (Hippenmeyer et al., 2005) were crossed to a tdTomato expressing conditional reporter line, Ai9 (Madisen et al., 2010), to label the Pvalb$^+$ positive population. Camk2a-cre (Tsien et al., 1996) animals were also crossed to the Ai9 line for labeling excitatory cells. Organotypic slice cultures were generated at around p7, subjected to

TTX treatment at ep18 and then RNA was harvested at ep22 via FACS of tdTomato positive neurons, from either excitatory or Pvalb labeled cultures (~1K neurons collected for FS cell samples, ~2K for excitatory). Small RNA libraries generated from these samples, when examined on a poly-acryalimde gel, contained bands at the expected positions for miRNAs as well as piRNAs (data not shown). After sequencing the mapped read-length distribution contained a prominent peak at 22 bp (example shown in Fig. 1a). Additionally, annotation of mapped sequences demonstrated that the majority of reads corresponded to microRNAs (Fig. 1b). For differential expression analysis, microRNAs below an average of 100 counts per million were excluded as it has been reported that low abundance microRNAs (less than 1000 RPM) have no detectable effect on gene repression (Mullokandov et al., 2012).

Amidst the 226 microRNAs examined in FS cells (ctl n =4, TTX n =3, where each sample was from a pool of at least two animals, with cultured slices divided up between activity drug conditions) that fell above threshold, several met the predetermined criteria ($Log_2(FC)<-1$ or >1, $p < 0.01$ at an FDR = 0.01) for differential expression (Fig. 2C). Mir-92a-3p, mir-212-3p, mir-21a-5p and mir-129-5p were all down regulated by TTX ($Log_2(FC) = -2.54, -2.41, -1.67, -1.5$; $p = 8.1 \times 10^{-4}$, 2.7×10^{-5}, 5.8×10^{-3}, 7.7×10^{-3}, respectively). Mir-129 has already been identified as a microRNA that is destabilized by activity (Krol et al., 2010a), while mir-92 has been shown to control neuronal excitability in *Drosophila* (Chen and Rosbash, 2017). Only a single microRNA was found to be upregulated by activity deprivation in FS cells, mir-7b-5p changed by 5.24 fold ($p = 2.4 \times 10^{-11}$). In excitatory cells, 268 microRNAs were above threshold (ctl n =4, TTX n=4). Mir-129 and mir-132 were downregulated ($Log_2(FC) = -1.33, -1.27$; $p = 8.6 \times 10^{-7}$, 3.6×10^{-3}, respectively), while mir-708 was upregulated ($Log_2(FC) = 1.48$, 3.6×10^{-3}). Mir-132 had been previously demonstrated to be downregulated by dark rearing and monocular

deprivation in mice (Mellios et al., 2011). It was decided to focus on mir-7 for the remainder of the study, as it exhibited the largest significant change in FS cells (FC=3.09 across mir-7 family members) and was unchanging in excitatory cells (FC = 1.02). It should also be noted that the mir-7 family members were expressed at much lower levels in FS cells (Excitatory, ctl = 2.45×10^5, TTX = 2.52×10^5; FS cell, ctl =5.05×10^3, TTX = 1.56×10^4), an observation which that will be of use later.

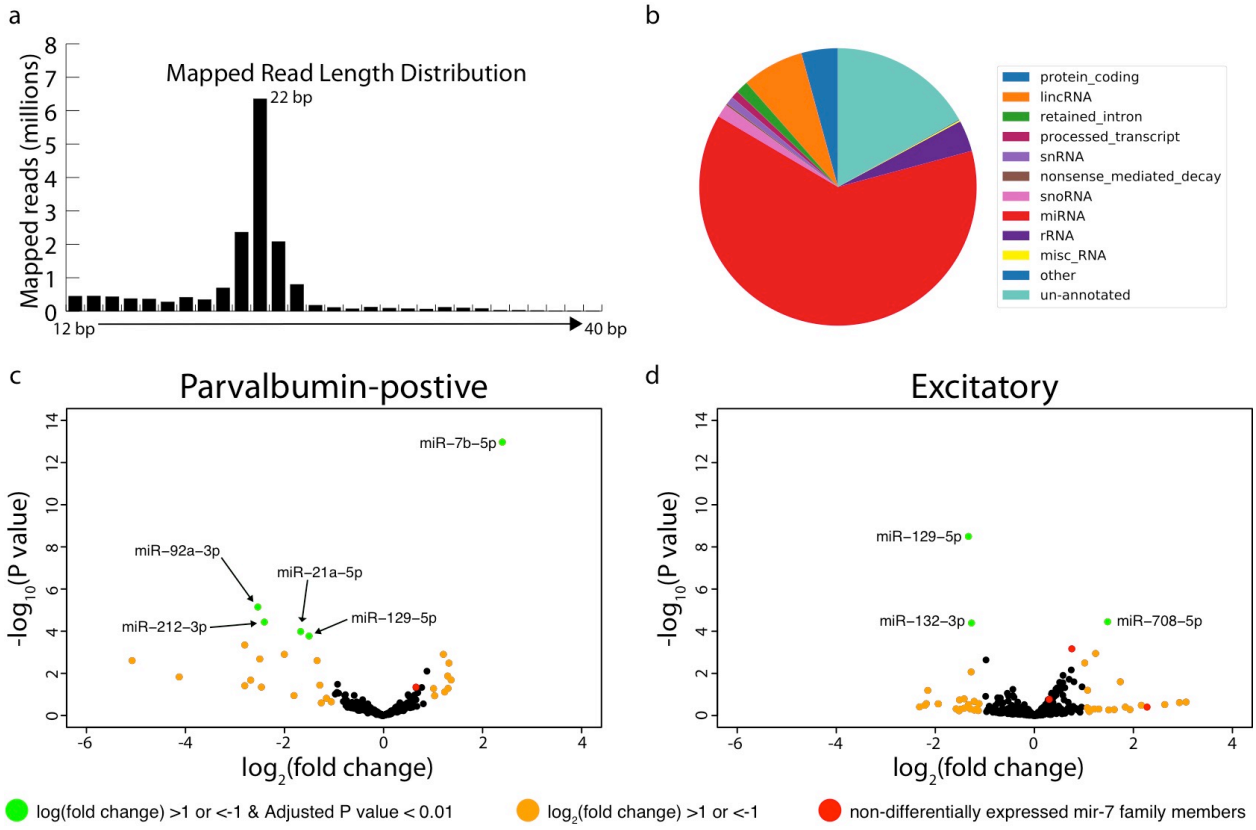

Figure 1: Cell-type specific activity regulated microRNAs in Pvalb+ and Excitatory cortical neurons. (a) Example distribution of mapped reads from a single sample (Excitatory/Control), as a function of read-length (after trimming and mapping) showing a peak at 22 bp. (b) The distribution of RNA classes found within the example shown in (a), reads were annotated based on all known RNA classes from the ensemble database. (c) A volcano plot for the differential expression (TTX vs control) for all microRNAs sequenced from Pvalb neurons, with mean

expression above 100 CPM. The x-axis is the log of the fold-change (TTX over control), while the y-axis is the –log10 of the P value (after adjusting for an FDR of 0.01). Orange dots are microRNAs with a log2(FC) > 1 or < -1, those in green are similar but pass an FDR threshold of 0.01, red-dots display mir-7 family members that are not differential expressed. All differentially expressed microRNAs are labelled. (d) The same as in (c) except libraries were generated from excitatory neurons.

Activity dependent plasticity of FS cell intrinsic excitability is Dicer and mir-7 dependent:

To examine fast spiking cell plasticity, we made use of a cortical organotypic slice culture preparation (De Simoni and Yu, 2006). This system offered the advantage of easy pharmacological manipulation while largely preserving many aspects of neocortical architecture. Pvalb-Ires-Cre labeled cells displayed a localization pattern similar to that seen *in vivo* (Fig. 2a). Sparse labeling of $Pvalb^{+}$ cells in organotypic slice culture through delivery of a cre-dependent eGFP vector (Matsuda and Cepko, 2007) via gene bullet transfection (Fig. 2b) revealed that these neurons retain their multipolar dendritic morphology (Fig 2C) and are capable of firing at rates as high as 200 Hz (Fig. 2g-i). In order to induce FS cell plasticity, complete silencing of action potential firing via TTX was used beginning at ep18 (time course in Fig. 2d). Numerous studies have demonstrated that multiple properties are affected by TTX treatment, including synaptic scaling, EPSC and IPSC frequency, as well as intrinsic excitability (Bartley et al., 2008; Desai et al., 1999; Turrigiano et al., 1998). Considering that fast-spiking cell intrinsic excitability had already been demonstrated to change during muscimol treatment *in vivo* in the absence of major changes in transcription (Miller et al., 2011), it seemed to be the most logical property to examine.

Layer V fast spiking cells increased their intrinsic excitability in response to TTX treatment (Fig 2g-o). Using a linear mixed-effects model, it was determined that TTX affected firing rate ($\chi 2$ =9.9, p= 0.0016), shifting the FI curve parallel to the frequency axis by 33.4 HZ (Fig. 2). This change in firing rate correlated with a significant change in membrane resistance at rest (ctl = 40.6 ± 3.1 MΩ, TTX = 69.2 ± 5.6 MΩ, p = 8.87×10^{-5}, Fig. 2e), in the absence of a change in capacitance (ctl = 169 ± 23 pF,TTX = 130 ± 23 pF, p = 0.14, Fig. 2f). To determine if the activity dependent shift of FS cell excitability was regulated by microRNAs, cultures from $Pvalb^{cre/wt}$, $Ai9^{+/-}$,$Dicer^{flx/flx}$ mice were generated. The floxed Dicer allele, when excised, removes exon 23, containing the 2^{nd} ribonuclease III domain, rendering the enzyme inert (Harfe et al., 2005). Conditional ablation of Dicer prevented any noticeable change in the FI curve during TTX treatment ($\chi 2$ =0.37, p= 0.54), and did not alter the membrane resistance (ctl = 48.6 MΩ ± 6.5, TTX = 42.3 MΩ ±3.9, p = 0.41, Fig2e) or the capacitance (ctl = 137 pF ± 16,TTX = 123 pF ± 14, p = 0.61, fig 2f). Considering that mir-7 was differentially regulated in FS cells, $Pv^{cre/wt}$, $Ai9^{+/-}$, $mir\text{-}7sp^{+/-}$ animals were bred and used for slice cultures. This allowed for the conditional expression of a mir-7 sponge (Pollock et al., 2014) specifically within FS cells. Expression of the mir-7 sponge partially blocked an increase in FS cell excitability (fig 2m-o), TTX affected sponge-expressing cells ($\chi 2$ =5.39, p= 0.02) by 17.6 Hz (compared to 33.4 in WT). However, as observed following Dicer deletion, the sponge completely blocked the increase in membrane resistance at rest (ctl = 42.2 ± 3.0 MΩ, TTX = 50.3 ± 4.5 MΩ, p = 0.61, Fig. 2e) with no significant change in the capacitance (ctl = 189 ± 32 pF, TTX = 145 ± 28 pF, p = 0.31, Fig. 2f). These data support the hypothesis that activity dependent changes in FS cell excitability are regulated by mir-7. Additionally, we observed that the Dicer cells displayed an increase in

baseline excitability. This suggests that the effect of Dicer ablation FS cell excitability is more complex than impairment of mir-7 alone.

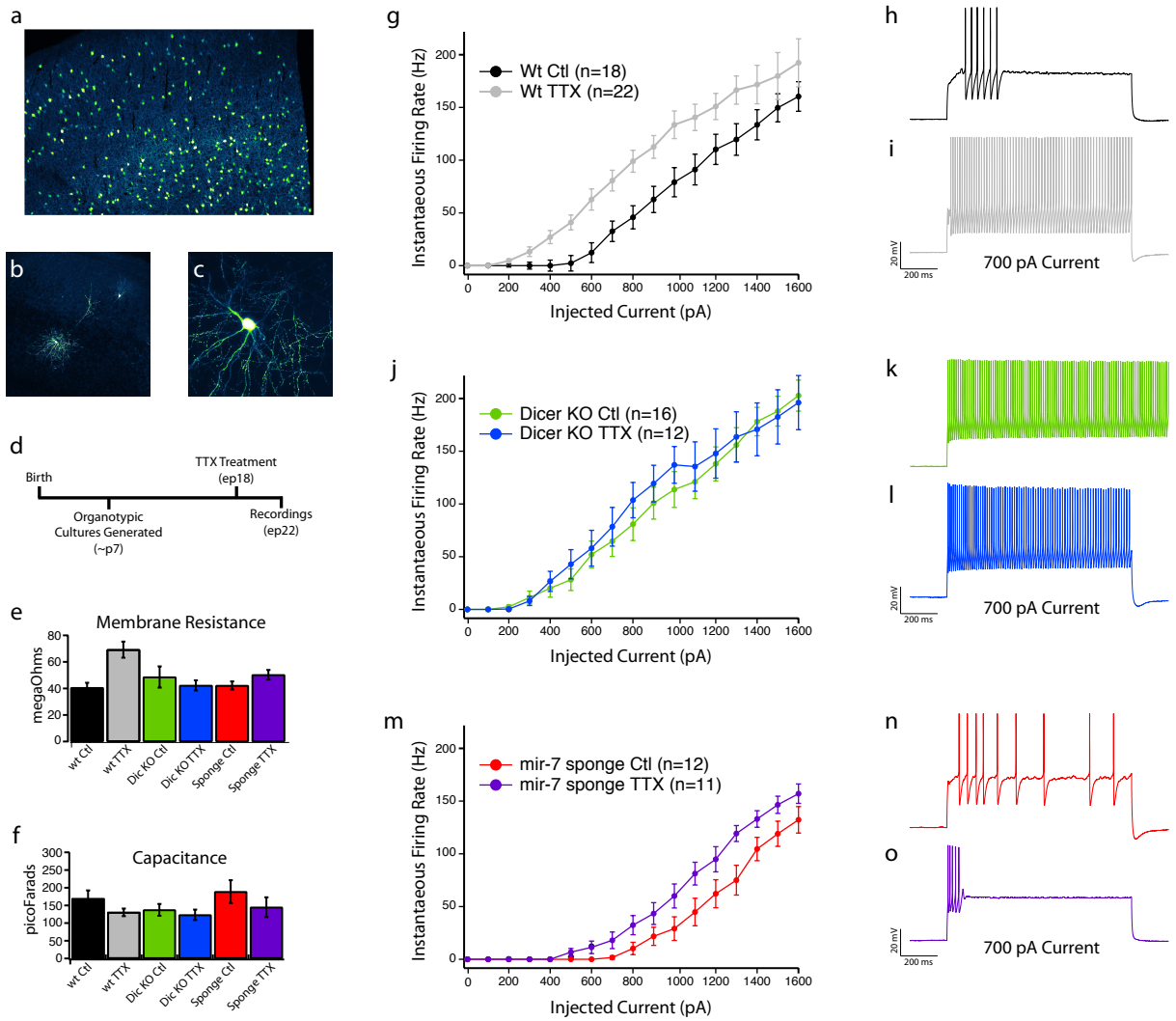

Figure 2: Chronic activity blockade in slice culture modulates layer V FS cell excitability in a Dicer and mir-7 dependent manner. (a) Example image of organotypic slice culture from Pvalb$^{cre/wt}$, Ai9$^{+/wt}$ showing tdTomato-positive cell distribution at ~ep22. (b) Two FS cells labeled with gene bullets expressing eGFP. (c) A close-up of the Pvalb^{+} cell in the lower portion of B, displaying multipolar dendritic morphology typical of basket cells. (d) Experimental time-course. (e-o) current clamp recordings of layer V FS cell recordings in organotypic slice culture

for wt-Ctl, Pvalb$^{cre/wt}$, Ai9$^{+/-}$ (black), and wt-TTX (grey), Dicer-Ctl and Pvalb$^{cre/wt}$, Ai9$^{+/-}$,Dicer$^{flx/flx}$ (green) and Dicer KO-TTX (blue), sponge Ctl, Pvalb$^{cre/cre}$,Ai9$^{+/+}$, mir-7sp$^{+/-}$,(red) and sponge TTX (purple). (e) Membrane resistance, in megOhms, for all conditions, error bars here and elsewhere are SEM unless noted otherwise. (f) Capacitance measurements, in pF. (g) FI curves from WT animals, plot instantaneous firing rate (Hz; y-axis) against current injected (pA; x-axis), TTX affected firing rate ($\chi 2$ =9.9, p= 0.0016), shifting the frequency by 33.4 HZ, (h) and (i) are representative traces at 700 pA of current injection. (j-l) same as previous three panels for the Dicer KO cultures, TTX did not affect the firing rate ($\chi 2$ =0.37, p= 0.54). (m-o) Current clamp data from mir-7 Sponge animals, TTX did affect the firing rate ($\chi 2$ =5.39, p= 0.02), by 17.6 Hz.

MicroRNA mediated regulation of FS cell excitability is conserved *in vivo*:

Is the mechanism for activity-regulated control of layer V FS cell excitability conserved *in vivo*? The whisker-barrel system provides a convenient means of asking this question, as barrels corresponding to specific whisker rows are readily identifiable in acute slices (Finnerty et al., 1999; Welker and Woolsey, 1974). Subsequent to whisker trimming, numerous plasticity changes rapidly occur throughout barrel cortex (Gainey and Feldman, 2017). Furthermore, it's been demonstrated that whisker-evoked activity of bursting and regular spiking layer V pyramidal neurons, drops within a day after whisker trimming (Glazewski et al., 2017; Jacob et al., 2012), suggesting a global drop in layer 5 activity analogous to (though perhaps milder than) the activity changes induced pharmacologically in slice culture. At p21 the D-row and γ whiskers were plucked. 36 to 48 hours later patch clamp recordings were made from layer V FS cells in the deprived or spared barrel (Fig. 3a-c).

We first determined which, if any, changes in intrinsic excitability occurred in wild-type layer 5 FS cells. Contrary to findings in layers 2/3 and 4 where FS cell excitability decreases (Gainey and Feldman, 2017; Sun, 2009), whisker deprivation increased FS cell excitability (Fig3g-i). Sensory deprivation significantly increased the firing rate of wild-type FS cells by 38.7 HZ ($\chi 2$ =6.57, p= 1.03×10^{-2}). Additionally, there was a change in membrane resistance at rest (spared = 81.9 ± 4.7 MΩ, deprived = 129.0 ±14.5 MΩ, p = 1.05×10^{-2}, Fig3e), without any change in capacitance (spared = 79 ± 3.8 pF , deprived = 76 ± 7.5 pF, p = 0.76, fig 3f). The intrinsic excitability of Dicer KO FS cells (Fig. 3j-l) was unaffected by sensory deprivation ($\chi 2$ = 5.51×10^{-4}, p= 0.98), similarly there were no significant changes in membrane resistance (spared = 99.6 ± 10.4 MΩ, deprived = 117 ± 18.3 MΩ, p = 0.43, Fig3e) or capacitance (spared = 81.3 ± 7.0 pF, deprived = 81.9 ± 7.4 pF, p = 0.95, fig 3f). Sponge cells (Fig. 3m-o) were also unaffected ($\chi 2$ =0.36, p= 0.54) by sensory deprivation and similarly exhibited no change in membrane resistance (spared = 90.7 ± 7.6 MΩ, deprived = 86.6 ± 6.4 MΩ, p = 0.68, Fig3e) or capacitance (spared = 74.6 ± 5.8 pF, deprived = 73.5 ± 3.0 pF, p = 0.95, Fig. 3f). This data support the notion that layer V FS cell activity regulation *in vivo* is comparable, qualitatively and mechanistically, to that observed in slice culture.

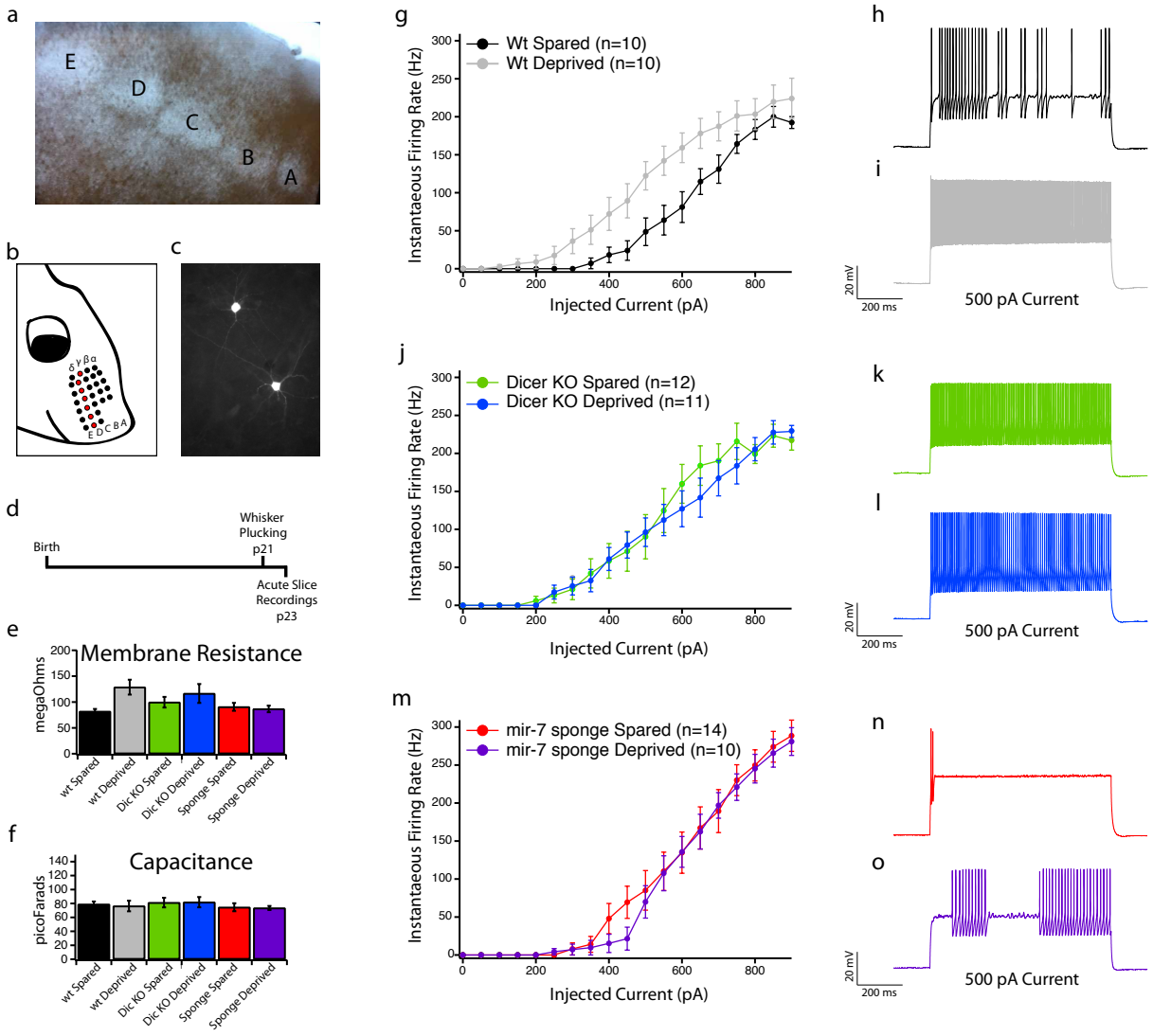

Figure 3: Sensory deprivation also modulates layer V FS cell excitability in a Dicer and mir-7 dependent manner. (a) Example of an acute slice, from a deprived animal, barrels A through E are easily visible, Deprived: recordings from D or γ barrels, Spared: recordings from the E or C barrel. (b) Cartoon showing whisker layout on animal's right side, the D-row along with the γ whisker (red) were plucked at p21 (c) Two biocytin filled FS cells imaged post-recording. (d) Experimental time-course for deprivation and recordings. (e-o) current clamp recordings of layer V FS cell recordings in acute slice for wt-Ctl, Pvalb$^{cre/wt}$, Ai9$^{+/-}$ (black), and wt-TTX (grey), Dicer KO-Ctl and Pvalb$^{cre/wt}$, Ai9$^{+/-}$,Dicer$^{flx/flx}$ (green) and Dicer KO-TTX (blue),

sponge Ctl, Pvalb$^{cre/cre}$,Ai9$^{+/+}$, mir-7sp$^{+/-}$, (red) and sponge TTX (purple). (e) Membrane resistance, in MΩ, for all conditions. (f) Capacitance measurements, in pF. (g) FI curves from WT animals, sensory deprivation affected firing rate ($\chi 2 = 6.57$, $p = 0.01$), increasing the frequency by 19.7 HZ, (h) and (i) are representative traces at 500 pA of current injection, scale bar: 20 mV, 200 ms. (j-l) same as previous three panels for Dicer KO, sensory deprivation did not affect the firing rate ($\chi 2 = 0.00055$, $p = 0.98$). (m-o) Current clamp data from mir-7 Sponge animals, sensory deprivation did not affect the firing rate ($\chi 2 = 0.36$, $p= 0.54$).

mRNA sequencing to screen for putative mir-7 targets controlling FS cell excitability:

In mammals, microRNA mediated repression usually changes mRNA levels in addition to decreasing protein levels (Guo et al., 2010). Hence, we used differential expression profiling through deep sequencing to identify candidate mir-7 targets responsible for altering FS cell intrinsic excitability. Organotypic slice cultures were used, as opposed to sensory deprivation *in vivo*, due to the greater degree of control over the activity levels of all neurons within each slice. To distinguish cell type-specific and global changes, neurons were manually sorted from Pv$^{cre/wt}$, Ai9$^{+/-}$ cultures (FS cells) or isolated through FACS for EMX$^{cre/wt}$, Ai9$^{+/-}$ cultures (excitatory cells). Despite the differences in cell isolation, these samples should still be comparable as others have found high correlations between FACS and manually collected samples within cell-types (Okaty et al., 2011). In both cases cell-type specific mRNAs were harvested, subjected to SPIA amplification followed by library construction. The multidimensional scaling plot, in figure 4a, demonstrates that samples clustered according to activity and cell-type. As expected, excitatory neuron markers, Vglut1 and Tbr1 were enriched in the excitatory population (Fig. 4b), while Gabt1, Gad1 and Gad2 were exclusive to the Pvalb^{+} population (Fig. 4b), thus demonstrating the purity of each sample.

The expression profiles of excitatory and Pvalb$^+$ cells were both altered by activity deprivation. To isolate activity-regulated genes from genes differentially expressed across cell types, comparisons were made within a cell-type as opposed to across all conditions. With an FDR of 0.05 and a minimum expression threshold of 10 transcripts per million (TPM), 758 genes were upregulated and 1182 genes were downregulated in the EMX$^+$ population. While 1679 genes were up and 1100 genes were downregulated in the Pvalb$^+$ neurons. Interestingly, the top 20 up and down regulated genes for either cell type (as determined by fold-change) typically displayed highly cell-type specific induction patterns (Fig. 4c-d). Also, several genes displayed on the heat maps have already been demonstrated to be activity regulated, such as Elk, Egr1 and Nnat (Oyang et al., 2011; Schaukowitch et al., 2017; Spiegel et al., 2014). The expression of genes predicted to have conserved mir-7 binding sites, according to Targetscan (Agarwal et al., 2015), were examined (Fig. 4e). Considering that mir-7 was upregulated by TTX in FS cells (Fig. 1c), not affected in excitatory neurons, but, generally more abundant in excitatory cells, genes that were activity regulated in FS neurons and not excitatory cells while displaying less overall expression in excitatory neurons were emphasized. One such example is highlighted in figure 4e. There were six genes, that were differentially expressed in FS cells, and matched this pattern: Adam11, Pitpna, Ppif, Pde4d, Raf1 and Iglon5 (Fig. 4f). Of particular interest was Pitpna (phosphatidyl inositol transporter protein) because of its known impact on PIP_2 levels , a lipid whose presence in the membrane affects multiple potassium channels (Suh and Hille, 2008). It should also be noted that Adam11 is also reported to impact potassium channel localization, while Pde4d, might potentially affect potassium channel conductance through cyclic-Amp regulation (Kole et al., 2015; Siegelbaum et al., 1982).

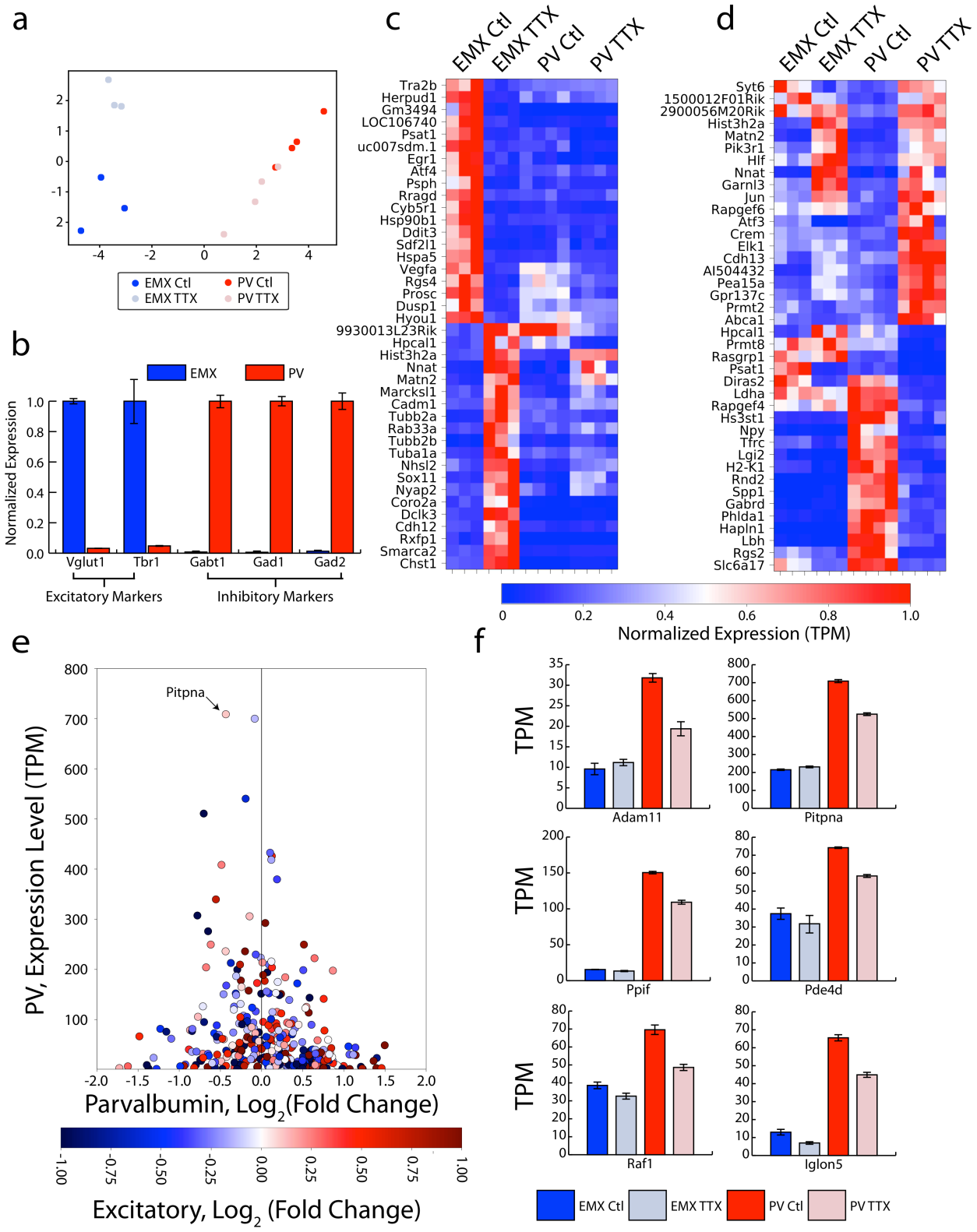
a
EMX Ctl
EMX TTX
PV Ctl
PV TTX
b
EMX
PV
Normalized Expression
Vglut1
Tbr1
Gabt1
Gad1
Gad2
Excitatory Markers
Inhibitory Markers
c
EMX Ctl
EMX TTX
PV Ctl
PV TTX
Tra2b
Herpud1
Gm3494
LOC106740
Psat1
uc007sdm.1
Egr1
Atf4
Psph
Rragd
Cyb5r1
Hsp90b1
Ddit3
Sdf2l1
Hspa5
Vegfa
Rgs4
Prosc
Dusp1
Hyou1
9930013L23Rik
Hpcal1
Hist3h2a
Nnat
Matn2
Marcksl1
Cadm1
Tubb2a
Rab33a
Tubb2b
Tuba1a
Nhsl2
Sox11
Nyap2
Coro2a
Dclk3
Cdh12
Rxfp1
Smarca2
Chst1
d
EMX Ctl
EMX TTX
PV Ctl
PV TTX
Syt6
1500012F01Rik
2900056M20Rik
Hist3h2a
Matn2
Pik3r1
Hlf
Nnat
Garnl3
Jun
Rapgef6
Atf3
Crem
Elk1
Cdh13
AI504432
Pea15a
Gpr137c
Prmt2
Abca1
Hpcal1
Prmt8
Rasgrp1
Psat1
Diras2
Ldha
Rapgef4
Hs3st1
Npy
Tfrc
Lgi2
H2-K1
Rnd2
Spp1
Gabrd
Phlda1
Hapln1
Lbh
Rgs2
Slc6a17
Normalized Expression (TPM)
e
Pitpna
PV, Expression Level (TPM)
Parvalbumin, Log2(Fold Change)
Excitatory, Log2 (Fold Change)
f
TPM
Adam11
Pitpna
Ppif
Pde4d
Raf1
Iglon5
EMX Ctl
EMX TTX
PV Ctl
PV TTX

Figure 4: mRNA sequencing of FS cells and excitatory cells in slice culture during chronic TTX treatment. (a) Multi-dimensional scaling plot comparing sorted samples from $EMX^{cre/wt}$, $Ai9^{+/-}$ and $Pvalb^{cre/wt}$, $Ai9^{+/-}$ animals from either a control condition or after four days of TTX treatment. (b) Normalized expression for marker genes from control samples for either EMX or PV control samples, Vglut1 and Tbr1 are excitatory markers, Gabt1, Gad1 and Gad2 label inhibitory neurons. (c) Heat map for the top 20 genes in $EMX^{cre/wt}$, $Ai9^{+/-}$ cells (as determined by fold-change) that were either up or down regulated (top and bottom of heat map respectively) and were statistically significant (FDR = 0.05), color value map for normalized expression values shown below. (d) same as in (c) but for $Pvalb^{cre/wt}$, $Ai9^{+/-}$ cells. (e) Scatter plot displaying the expression level, transcripts per million (TPM), and Log_2(Fold Change) in the $Pvalb^{+}$ cells for all predicted conserved mir-7 targets (according to Targetscan). Imposed on each point is a color map of that gene's regulation in Emx^{+} population, Log_2(Fold Change) in response to TTX treatment (f) Bar plots (TPM values) of candidate genes: Atpb2, Ppif, Scn2b, Pde4d, Pitpna and Raf1 that are predicted targets of mir-7, and whose expression patterns match the following criteria: down-regulated in FS cells, unaffected by TTX in Emx^{+} neurons, and net expression lower in excitatory compared to FS cells.

Sensory deprivation modulates multiple potassium conductances in layer V FS cells:

Neuronal firing thresholds are governed by channels active at rest, and by voltage gated channels activated or inactivated as the neuron depolarizes. The observed shift in the FI curve is reminiscent of a change in subthreshold conductances, as shown previously {Ulrich, 2003 #75}, where the effect is subtractive with regards to the firing rate and has a minimal effect on the FI curve's slope. Considering that membrane resistance at rest correlated with changes in the rheobase (Fig. 2 & 3) and the mRNA expression screen implicated several genes that are known

to modulate potassium channel function (Fig. 4f), whole cell currents were measured in voltage clamp. As before, spared and deprived barrels were identified. Pairs of neurons (one spared, one deprived) were recorded simultaneously in slices from WT animals. Preliminarily (n=3), each pair displayed a difference in rheobase and membrane resistance comparable to the effect seen in figure 3 (Fig. 5a-b). After the firing properties had been established, TTX and Zd7288 were perfused into the bath. Subsequently, the cells were subjected to an IV ramp (example in Fig. 5C). Then, to examine inward rectifying potassium currents, 10 μm barium (Goldberg et al., 2011) was added to the bath (Fig 5C). The average subtracted current, obtained from these two voltage ramps, displayed a profile typical of inwardly rectifying potassium channels. Furthermore, this current differed between spared and deprived conditions (Fig5e). The 4-AP (40 μm) sensitive current, which in FS cells is likely mediated by KV3 channels (Bean, 2007), was also examined (Fig. 5d). The averaged subtracted 4-AP sensitive current also exhibited a clear change across spared and deprived conditions (Fig. 5f). Finally, after application of all blockers, there were still residual differences between spared and deprived layer V FS cells. This residual difference had a linear relationship with voltage (Fig. 5G), suggesting that leak currents may account for the remaining difference.

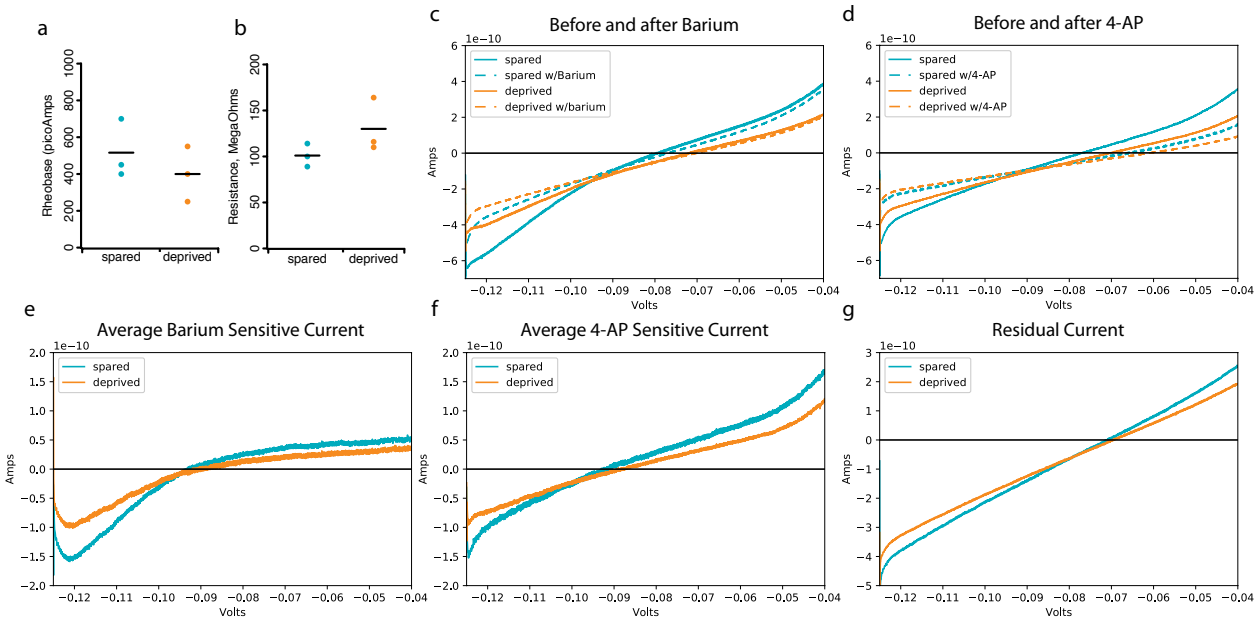

Figure 3.5: Alteration of multiple potassium conductances underlie sensory deprivation driven changes in layer V FS excitability. (a) Rheobase (current necessary to elicit an action potential) in 3 pairs of cells simultaneously recorded from spared (blue) and deprived (orange) barrels in whisker plucked Pvalb$^{cre/wt}$, Ai9$^{+/-}$ animals. (b) Rheobase (MΩ). (c) IV plot from an example pair subjected to a 5 second voltage ramp from -125 to -40 mV, spared (blue) and deprived (orange) are shown before (solid line) and after (dotted line) treatment with 10 μM barium. (d) Same as in C except curves are before and after 40 μM 4-AP treatment, note, the initial curves are identical to the post-barium curves in C. (e) Averaged subtracted current values for the barium sensitive current and (f) 4-AP current. (g) Average residual current (after Barium and 4-AP).

Discussion:

Here we demonstrate that mir-7 expression is regulated in a cell type-specific manner during activity deprivation. Mir-7 is upregulated in FS cells, but its expression is unaffected by activity in excitatory neocortical neurons, although it is expressed at substantially higher levels in these

cells. Furthermore, the changes in intrinsic excitability within FS cells are Dicer as well as mir-7 dependent. Additionally, there is a conservation of this regulatory mechanism *in vivo*, as experience-dependent changes in layer 5 FS cell excitability move in a comparable manner within barrel cortex during whisker plucking, and also depend on Dicer and mir-7. These activity dependent physiological changes are accompanied by gene expression changes within FS cells. Although, it is difficult (presently) to determine how many of these changes contribute to FS cell excitability, it can be postulated that one or several mir-7 targets, down-regulated by activity, in FS cells, and not activity regulated in excitatory neurons are responsible. Currently, Pitpna represents the strongest candidate for mir-7 driven control of excitability.

Phosphatidylinositol transfer protein is thought to be a rate-limiting factor in the control of PIP_2 levels (Cunningham et al., 1995), so it is reasonable to suspect a reduction in [PIP_2] in response to down-regulation of Pitpna. If PIP_2 levels are affected, then a number of potassium channels might be expected to decrease their conductance. PIP_2 acts as a cofactor for numerous potassium channels (Suh and Hille, 2008), affecting inward rectifiers (Huang et al., 1998) as well as two pore leak potassium channels (Lopes et al., 2005) in other cell types. A decline in PIP_2 levels due to mir-7 mediated destabilization of Pitpna mRNAs may therefore, cause an increase in the membrane resistance by reducing the function of either or both inwardly rectifying and two-pore leak potassium channels. The voltage clamp data is consistent with this hypothesis (Fig. 5). Finally this increase in membrane resistance would increase the excitability of the neuron. Interestingly, Vibrator mice, which express 65 to 85% less Pitpna have an “unusually rapid (18–20 Hz) postural action tremor expressed in juvenile homozygotes” (Monaco et al., 2004). This phenotype is attributed to a large, spontaneous, insertion of 6 kb intracisternal A particle in the fourth intron of Pitpna (Monaco et al., 2004). We can speculate that this postural

action tremor might be associated with a defect in neuronal excitability directly mediated changes in Pip_2 levels altering ion channel function, although, Vibrator mice also suffer from neurodegeration (Hamilton et al., 1997), muddying any direct interpretations of this phenotype. Further work will determine if mir-7 controls Pitpna expression and by extension PIP_2 levels. Additionally, destabilization of Pip_2 concentration through the application of Wortmannin or by providing an abundance of phosphatidyl inositol intracellularly should have predictable effects on FS cell excitability. Future experiments will test the proposed links between mir-7, PIP_2 metabolism and FS cell excitability.

In addition to understanding the mechanism of mir-7 related control of FS cell excitability, a critical question remains. Is an increase in mir-7 expression sufficient to increase FS cell excitability? Activity blockade not only affects mir-7 but also hundreds of other genes. The differential expression of mir-7 might be one piece in an elaborate genetic program that controls FS cell excitability, many parts of which could be necessary. If mir-7 is sufficient to alter FS cell excitability, then it could be used to treat alterations of FS cell excitability such as Dravet syndrome (Bender et al., 2012). Increasing FS cell excitability, in the absence of compensatory changes, may decrease network excitability. However, it would also be necessary to know how mir-7 affects other aspects of FS cell physiology. For example, mir-7 is predicted to target the Erbb pathway. Erbb signalling contributes to the control of excitatory input onto FS cells (Del Pino et al., 2013), and is postulated to contribute to the timing of the critical period (Gu et al., 2016; Sun et al., 2016). If mir-7 negatively regulated mEPSC frequency while increasing FS cell intrinsic excitability the net effect on the network could be minimal. This possibility is intriguing as it would suggest that mir-7 is a cell-autonomous homeostatic regulator of neuronal firing, balancing excitatory input against intrinsic excitability. Finally, we know that

mir-7 expression is strong in early development, but declines as the animal matures (Pollock et al., 2014). Given the data reported here, mir-7 might also have a role in gradually decreasing the neuron's membrane resistance as the net number of active inputs the neuron receives gradually increases (during development) therefore balancing the firing rate of the neuron against it's developmentally regulated excitatory input.

Although, this study narrowed its focus to mir-7, the differences in baseline excitability, between the mir-7 sponge, wild-type and Dicer knockout neurons suggest that other microRNAs also contribute to the control of neuronal excitability. Furthermore, there may be some mechanistic similarities between FS cells and pyramidal neurons in this regard, as short-term ablation of Dicer also raises excitatory neuron excitability (Fiorenza et al., 2016). It remains unclear though, if Dicer mediated control of baseline excitability is linked to a microRNA(s).. A number of non-microRNA related functions have been attributed to Dicer (Yang and Lai, 2011). For example, Dicer has been shown to control the accumulation of double stranded RNA in the retinal pigment epithelium (Kaneko et al., 2011). Increased quantities of double stranded RNA could affect the function of the ds-RNA dependent kinase PKR and lead to a change in neuronal excitability, as loss of PKR triggers an increase in synchronous network activity (Zhu et al., 2011). Examining the conditional knockout of DGCR8 in neocortical neurons might shed some light on Dicer's control of neuronal excitability.

Finally, it should be noted that an increase in layer 5 FS cell plasticity during sensory deprivation is itself a novel finding. It suggests the existence of differences in FS cell plasticity between layers during sensory deprivation. Prior work demonstrated that layer 4 fast spiking cells lower their excitability after whisker trimming in barrel cortex (Sun, 2009). Although, the time course of the deprivation was quite long (three weeks) as opposed to the two days of

deprivation used here. However, there is a preliminary report of a rapid decrease in layer 2/3 FS cell excitability (Gainey and Feldman, 2017). Still, it would be necessary to re-examine layer 2/3 or layer 4 plasticity with methods identical to those performed in this study to rule out non-biological reasons for this contrast. For example, the slice preparation protocol used in the examination of FS cell plasticity in layer 4 uses a sodium replacement solution for the cutting and recovery of the brain slices. Prolonged exposure to low sodium might have an impact on the neuron's firing properties. However, the idea that there may be differences in the plasticity properties of cells in different layers is not unprecedented, and cortical Pvalb^{+} neurons are reported to be heterogeneous across layers (Tasic et al., 2016), for example differing in their expression of Etv1 (Dehorter et al., 2015). If we take these reported differences in FS cell plasticity at face value, what might this say about the role that fast spiking cells play across layers during global changes in activity? In the simplest of all worlds, increased FS cell excitability would negatively control the response of layer 5, while its decreased excitability in the granular and supragranular layers would increase the response to incoming sensory stimuli (within these layers). The net effect would be that the gain is increased for layers that receive and then integrate sensory information from adjacent barrels and other cortical regions, while, the gain of the cortex's output (layer 5) would decrease, possibly acting to filter out less coherent stimuli arriving from layer 2/3.

References:

Agarwal, V., Bell, G.W., Nam, J.W., and Bartel, D.P. (2015). Predicting effective microRNA target sites in mammalian mRNAs. Elife *4*.

Bartley, A.F., Huang, Z.J., Huber, K.M., and Gibson, J.R. (2008). Differential activity-dependent, homeostatic plasticity of two neocortical inhibitory circuits. J Neurophysiol *100*, 1983-1994.

Bean, B.P. (2007). The action potential in mammalian central neurons. Nat Rev Neurosci *8*, 451-465.

Bender, A.C., Morse, R.P., Scott, R.C., Holmes, G.L., and Lenck-Santini, P.P. (2012). SCN1A mutations in Dravet syndrome: impact of interneuron dysfunction on neural networks and cognitive outcome. Epilepsy Behav *23*, 177-186.

Cardin, J.A., Carlen, M., Meletis, K., Knoblich, U., Zhang, F., Deisseroth, K., Tsai, L.H., and Moore, C.I. (2009). Driving fast-spiking cells induces gamma rhythm and controls sensory responses. Nature *459*, 663-667.
Chen, X., and Rosbash, M. (2017). MicroRNA-92a is a circadian modulator of neuronal excitability in Drosophila. Nat Commun *8*, 14707.
Cohen, J.E., Lee, P.R., Chen, S., Li, W., and Fields, R.D. (2011). MicroRNA regulation of homeostatic synaptic plasticity. Proc Natl Acad Sci U S A *108*, 11650-11655.
Cunningham, E., Thomas, G.M., Ball, A., Hiles, I., and Cockcroft, S. (1995). Phosphatidylinositol transfer protein dictates the rate of inositol trisphosphate production by promoting the synthesis of PIP2. Curr Biol *5*, 775-783.
Davis, G.W., and Bezprozvanny, I. (2001). Maintaining the stability of neural function: a homeostatic hypothesis. Annu Rev Physiol *63*, 847-869.
De Simoni, A., and Yu, L.M. (2006). Preparation of organotypic hippocampal slice cultures: interface method. Nat Protoc *1*, 1439-1445.
Dehorter, N., Ciceri, G., Bartolini, G., Lim, L., del Pino, I., and Marin, O. (2015). Tuning of fast-spiking interneuron properties by an activity-dependent transcriptional switch. Science *349*, 1216-1220.
Del Pino, I., Garcia-Frigola, C., Dehorter, N., Brotons-Mas, J.R., Alvarez-Salvado, E., Martinez de Lagran, M., Ciceri, G., Gabaldon, M.V., Moratal, D., Dierssen, M.*, et al.* (2013). Erbb4 deletion from fast-spiking interneurons causes schizophrenia-like phenotypes. Neuron *79*, 1152-1168.
Desai, N.S., Rutherford, L.C., and Turrigiano, G.G. (1999). Plasticity in the intrinsic excitability of cortical pyramidal neurons. Nat Neurosci *2*, 515-520.
Finnerty, G.T., Roberts, L.S., and Connors, B.W. (1999). Sensory experience modifies the short-term dynamics of neocortical synapses. Nature *400*, 367-371.
Fiorenza, A., Lopez-Atalaya, J.P., Rovira, V., Scandaglia, M., Geijo-Barrientos, E., and Barco, A. (2016). Blocking miRNA Biogenesis in Adult Forebrain Neurons Enhances Seizure Susceptibility, Fear Memory, and Food Intake by Increasing Neuronal Responsiveness. Cereb Cortex *26*, 1619-1633.
Fox, K. (1992). A critical period for experience-dependent synaptic plasticity in rat barrel cortex. J Neurosci *12*, 1826-1838.
Gainey, M.A., and Feldman, D.E. (2017). Multiple shared mechanisms for homeostatic plasticity in rodent somatosensory and visual cortex. Philos Trans R Soc Lond B Biol Sci *372*.
Glazewski, S., Greenhill, S., and Fox, K. (2017). Time-course and mechanisms of homeostatic plasticity in layers 2/3 and 5 of the barrel cortex. Philos Trans R Soc Lond B Biol Sci *372*.
Goldberg, E.M., Jeong, H.Y., Kruglikov, I., Tremblay, R., Lazarenko, R.M., and Rudy, B. (2011). Rapid developmental maturation of neocortical FS cell intrinsic excitability. Cereb Cortex *21*, 666-682.
Gorski, J.A., Talley, T., Qiu, M., Puelles, L., Rubenstein, J.L., and Jones, K.R. (2002). Cortical excitatory neurons and glia, but not GABAergic neurons, are produced in the Emx1-expressing lineage. J Neurosci *22*, 6309-6314.
Gu, Y., Tran, T., Murase, S., Borrell, A., Kirkwood, A., and Quinlan, E.M. (2016). Neuregulin-Dependent Regulation of Fast-Spiking Interneuron Excitability Controls the Timing of the Critical Period. J Neurosci *36*, 10285-10295.
Guo, H., Ingolia, N.T., Weissman, J.S., and Bartel, D.P. (2010). Mammalian microRNAs predominantly act to decrease target mRNA levels. Nature *466*, 835-840.
Hamilton, B.A., Smith, D.J., Mueller, K.L., Kerrebrock, A.W., Bronson, R.T., van Berkel, V., Daly, M.J., Kruglyak, L., Reeve, M.P., Nemhauser, J.L.*, et al.* (1997). The vibrator mutation causes neurodegeneration via reduced expression of PITP alpha: positional complementation cloning and extragenic suppression. Neuron *18*, 711-722.
Harfe, B.D., McManus, M.T., Mansfield, J.H., Hornstein, E., and Tabin, C.J. (2005). The RNaseIII enzyme Dicer is required for morphogenesis but not patterning of the vertebrate limb. Proc Natl Acad Sci U S A *102*, 10898-10903.
Hippenmeyer, S., Vrieseling, E., Sigrist, M., Portmann, T., Laengle, C., Ladle, D.R., and Arber, S. (2005). A developmental switch in the response of DRG neurons to ETS transcription factor signaling. PLoS Biol *3*, e159.
Huang, C.L., Feng, S., and Hilgemann, D.W. (1998). Direct activation of inward rectifier potassium channels by PIP2 and its stabilization by Gbetagamma. Nature *391*, 803-806.
Jacob, V., Petreanu, L., Wright, N., Svoboda, K., and Fox, K. (2012). Regular spiking and intrinsic bursting pyramidal cells show orthogonal forms of experience-dependent plasticity in layer V of barrel cortex. Neuron *73*, 391-404.
Kaneko, H., Dridi, S., Tarallo, V., Gelfand, B.D., Fowler, B.J., Cho, W.G., Kleinman, M.E., Ponicsan, S.L., Hauswirth, W.W., Chiodo, V.A.*, et al.* (2011). DICER1 deficit induces Alu RNA toxicity in age-related macular degeneration. Nature *471*, 325-330.

Kole, M.J., Qian, J., Waase, M.P., Klassen, T.L., Chen, T.T., Augustine, G.J., and Noebels, J.L. (2015). Selective Loss of Presynaptic Potassium Channel Clusters at the Cerebellar Basket Cell Terminal Pinceau in Adam11 Mutants Reveals Their Role in Ephaptic Control of Purkinje Cell Firing. J Neurosci *35*, 11433-11444.
Krol, J., Busskamp, V., Markiewicz, I., Stadler, M.B., Ribi, S., Richter, J., Duebel, J., Bicker, S., Fehling, H.J., Schubeler, D.*, et al.* (2010). Characterizing light-regulated retinal microRNAs reveals rapid turnover as a common property of neuronal microRNAs. Cell *141*, 618-631.
Langmead, B., and Salzberg, S.L. (2012). Fast gapped-read alignment with Bowtie 2. Nat Methods *9*, 357-359.
Li, B., and Dewey, C.N. (2011). RSEM: accurate transcript quantification from RNA-Seq data with or without a reference genome. BMC Bioinformatics *12*, 323.
Li, K.X., Lu, Y.M., Xu, Z.H., Zhang, J., Zhu, J.M., Zhang, J.M., Cao, S.X., Chen, X.J., Chen, Z., Luo, J.H.*, et al.* (2011). Neuregulin 1 regulates excitability of fast-spiking neurons through Kv1.1 and acts in epilepsy. Nat Neurosci *15*, 267-273.
Liao, Y., Smyth, G.K., and Shi, W. (2014). featureCounts: an efficient general purpose program for assigning sequence reads to genomic features. Bioinformatics *30*, 923-930.
Lopes, C.M., Rohacs, T., Czirjak, G., Balla, T., Enyedi, P., and Logothetis, D.E. (2005). PIP2 hydrolysis underlies agonist-induced inhibition and regulates voltage gating of two-pore domain K+ channels. J Physiol *564*, 117-129.
Madisen, L., Zwingman, T.A., Sunkin, S.M., Oh, S.W., Zariwala, H.A., Gu, H., Ng, L.L., Palmiter, R.D., Hawrylycz, M.J., Jones, A.R.*, et al.* (2010). A robust and high-throughput Cre reporting and characterization system for the whole mouse brain. Nat Neurosci *13*, 133-140.
Maffei, A., Nelson, S.B., and Turrigiano, G.G. (2004). Selective reconfiguration of layer 4 visual cortical circuitry by visual deprivation. Nat Neurosci *7*, 1353-1359.
Mardinly, A.R., Spiegel, I., Patrizi, A., Centofante, E., Bazinet, J.E., Tzeng, C.P., Mandel-Brehm, C., Harmin, D.A., Adesnik, H., Fagiolini, M.*, et al.* (2016). Sensory experience regulates cortical inhibition by inducing IGF1 in VIP neurons. Nature *531*, 371-375.
Martin, M. (2011). Cutadapt removes adapter sequences from high-throughput sequencing reads. 2011 *17*.
Matsuda, T., and Cepko, C.L. (2007). Controlled expression of transgenes introduced by in vivo electroporation. Proc Natl Acad Sci U S A *104*, 1027-1032.
Mellios, N., Sugihara, H., Castro, J., Banerjee, A., Le, C., Kumar, A., Crawford, B., Strathmann, J., Tropea, D., Levine, S.S.*, et al.* (2011). miR-132, an experience-dependent microRNA, is essential for visual cortex plasticity. Nat Neurosci *14*, 1240-1242.
Miller, M.N., Okaty, B.W., Kato, S., and Nelson, S.B. (2011). Activity-dependent changes in the firing properties of neocortical fast-spiking interneurons in the absence of large changes in gene expression. Dev Neurobiol *71*, 62-70.
Monaco, M.E., Kim, J., Ruan, W., Wieczorek, R., Kleinberg, D.L., and Walden, P.D. (2004). Lipid metabolism in phosphatidylinositol transfer protein alpha-deficient vibrator mice. Biochem Biophys Res Commun *317*, 444-450.
Mullokandov, G., Baccarini, A., Ruzo, A., Jayaprakash, A.D., Tung, N., Israelow, B., Evans, M.J., Sachidanandam, R., and Brown, B.D. (2012). High-throughput assessment of microRNA activity and function using microRNA sensor and decoy libraries. Nat Methods *9*, 840-846.
O'Toole, S.M., Ferrer, M.M., Mekonnen, J., Zhang, H., Shima, Y., Ladle, D.R., and Nelson, S.B. (2017). Dicer maintains the identity and function of proprioceptive sensory neurons. J Neurophysiol *117*, 1057-1069.
Okaty, B.W., Sugino, K., and Nelson, S.B. (2011). A quantitative comparison of cell-type-specific microarray gene expression profiling methods in the mouse brain. PLoS One *6*, e16493.
Oyang, E.L., Davidson, B.C., Lee, W., and Poon, M.M. (2011). Functional characterization of the dendritically localized mRNA neuronatin in hippocampal neurons. PLoS One *6*, e24879.
Pollock, A., Bian, S., Zhang, C., Chen, Z., and Sun, T. (2014). Growth of the developing cerebral cortex is controlled by microRNA-7 through the p53 pathway. Cell Rep *7*, 1184-1196.
Quinlan, A.R., and Hall, I.M. (2010). BEDTools: a flexible suite of utilities for comparing genomic features. Bioinformatics *26*, 841-842.
Qureshi, I.A., and Mehler, M.F. (2012). Emerging roles of non-coding RNAs in brain evolution, development, plasticity and disease. Nat Rev Neurosci *13*, 528-541.
Robinson, M.D., McCarthy, D.J., and Smyth, G.K. (2010). edgeR: a Bioconductor package for differential expression analysis of digital gene expression data. Bioinformatics *26*, 139-140.
Rudy, B., Fishell, G., Lee, S., and Hjerling-Leffler, J. (2011). Three groups of interneurons account for nearly 100% of neocortical GABAergic neurons. Dev Neurobiol *71*, 45-61.
Saxena, A., Wagatsuma, A., Noro, Y., Kuji, T., Asaka-Oba, A., Watahiki, A., Gurnot, C., Fagiolini, M., Hensch, T.K., and Carninci, P. (2012). Trehalose-enhanced isolation of neuronal sub-types from adult mouse brain. Biotechniques *52*, 381-385.

Schaukowitch, K., Reese, A.L., Kim, S.K., Kilaru, G., Joo, J.Y., Kavalali, E.T., and Kim, T.K. (2017). An Intrinsic Transcriptional Program Underlying Synaptic Scaling during Activity Suppression. Cell Rep *18*, 1512-1526.
Siegelbaum, S.A., Camardo, J.S., and Kandel, E.R. (1982). Serotonin and cyclic AMP close single K+ channels in Aplysia sensory neurones. Nature *299*, 413-417.
Spiegel, I., Mardinly, A.R., Gabel, H.W., Bazinet, J.E., Couch, C.H., Tzeng, C.P., Harmin, D.A., and Greenberg, M.E. (2014). Npas4 regulates excitatory-inhibitory balance within neural circuits through cell-type-specific gene programs. Cell *157*, 1216-1229.
Stoppini, L., Buchs, P.A., and Muller, D. (1991). A simple method for organotypic cultures of nervous tissue. J Neurosci Methods *37*, 173-182.
Sugino, K., Hempel, C.M., Miller, M.N., Hattox, A.M., Shapiro, P., Wu, C., Huang, Z.J., and Nelson, S.B. (2006). Molecular taxonomy of major neuronal classes in the adult mouse forebrain. Nat Neurosci *9*, 99-107.
Suh, B.C., and Hille, B. (2008). PIP2 is a necessary cofactor for ion channel function: how and why? Annu Rev Biophys *37*, 175-195.
Sun, Q.Q. (2009). Experience-dependent intrinsic plasticity in interneurons of barrel cortex layer IV. J Neurophysiol *102*, 2955-2973.
Sun, Y., Ikrar, T., Davis, M.F., Gong, N., Zheng, X., Luo, Z.D., Lai, C., Mei, L., Holmes, T.C., Gandhi, S.P.*, et al.* (2016). Neuregulin-1/ErbB4 Signaling Regulates Visual Cortical Plasticity. Neuron *92*, 160-173.
Tasic, B., Menon, V., Nguyen, T.N., Kim, T.K., Jarsky, T., Yao, Z., Levi, B., Gray, L.T., Sorensen, S.A., Dolbeare, T.*, et al.* (2016). Adult mouse cortical cell taxonomy revealed by single cell transcriptomics. Nat Neurosci *19*, 335-346.
Tsien, J.Z., Chen, D.F., Gerber, D., Tom, C., Mercer, E.H., Anderson, D.J., Mayford, M., Kandel, E.R., and Tonegawa, S. (1996). Subregion- and cell type-restricted gene knockout in mouse brain. Cell *87*, 1317-1326.
Turrigiano, G.G., Leslie, K.R., Desai, N.S., Rutherford, L.C., and Nelson, S.B. (1998). Activity-dependent scaling of quantal amplitude in neocortical neurons. Nature *391*, 892-896.
Ulrich, D. (2003). Differential arithmetic of shunting inhibition for voltage and spike rate in neocortical pyramidal cells. Eur J Neurosci *18*, 2159-2165.
Welker, C., and Woolsey, T.A. (1974). Structure of layer IV in the somatosensory neocortex of the rat: description and comparison with the mouse. J Comp Neurol *158*, 437-453.
Yang, J.S., and Lai, E.C. (2011). Alternative miRNA biogenesis pathways and the interpretation of core miRNA pathway mutants. Mol Cell *43*, 892-903.
Zhu, P.J., Huang, W., Kalikulov, D., Yoo, J.W., Placzek, A.N., Stoica, L., Zhou, H., Bell, J.C., Friedlander, M.J., Krnjevic, K.*, et al.* (2011). Suppression of PKR promotes network excitability and enhanced cognition by interferon-gamma-mediated disinhibition. Cell *147*, 1384-1396.

Chapter 4:

In the opening chapter of this dissertation, in addition to a broad overview of the microRNA system, two important requirements of fully differentiated neurons were addressed. They must rigidly adhere to their identity, actively maintaining a highly specialized role within the neural circuit, while also adapting to changes in local activity, so that internally generated and external sensory signals successfully propagate while preventing the network from wandering into pathological regimes. These requirements of stability and flexibility are inherently at odds with one another. However, this work has demonstrated that they share a mechanistic link as both of these processes are actively maintained (at least partially) by the microRNA system.

microRNAs as maintainers of cell identity:

The work in chapter 2 lends support to the idea that microRNAs are necessary to maintain neuronal identity. We observed a decline in proprioceptor function, that began with the most specialized portion of the cell, its unique synaptic input structure, the annulospiral ending. These observations are similar to those made in other cell types. For example, loss Dgcr8 in photoreceptors, triggers atrophy in the outersegment, while mutation of motor neuron enriched mir-218 generates aberrant NMJ morphology (Amin et al., 2015; Busskamp et al., 2014; Thiebes et al., 2015). One hypothesis for how this may occur would be through the de-repression of

transcripts normally found in other cell types. Aberrant expression of genes normally found in other cell-types could interfere with cell-identity by disrupting the transcriptional machinery that normally maintains identity. However, this explanation for microRNA mediated regulation of cell-identity is hobbled by a number of other plausible explanations for the phenotypes observed in chapter 2.

Considering that Dicer has functions unrelated to microRNA biogenesis (Yang and Lai, 2011), identifying and then manipulating a specific microRNA(s) to see if any of the KO's phenotypes are recapitulated would potentially shed light on the mechanisms governing the maintenance of proprioceptor function. Given the large number of microRNAs expressed in any given cell-type, determining which sequence(s) to manipulate is difficult. However, the most important microRNA(s) is(are) likely the most highly expressed. For example, in photoreceptors, loss of Dgcr8, the enzyme upstream of Dicer that processes primary microRNA transcripts (Bartel, 2009), can be rescued by expression of mir-182/183 (Busskamp et al., 2014), which is the most abundant microRNA in these cells. In motor neurons, mir-218 (Amin et al., 2015) is the dominant microRNA, and is specific to motor neurons as well as critical to their development (Thiebes et al., 2015) and maintenance (Amin et al., 2015). We profiled the microRNA population within the Dicer KO proprioceptive sensory neurons and found only modest effects from the knockout (data not shown). This data was not published due to the small samples size (n=2). However, in this data the most abundant microRNA family member was let-7 (124,000 RPM) followed by mir-182 (33,700 RPM), although the most down-regulated microRNA, was mir-218 (wt = 4575 RPM, KO = 742 RPM, FC = 6.1). It should be noted, however, that although mir-218 did not appear to be the most abundant microRNA in these libraries, its actual concentration relative to other microRNAs is difficult to determine. Since mir-218 has low GC

content, the efficiency with which it can be isolated is lower than that of most other microRNAs (Kim et al., 2012). Hence our estimates of mir-218 abundance may not be accurate, especially given the small amount of starting material we used (each library was generated from ~150 neurons). Mir-218 is an intriguing candidate since Piezo2 and Tmem150C, both crucial to mechanotransduction in proprioceptors, (Hong et al., 2016; Woo et al., 2015), each contain highly conserved 8-mer binding sites for mir-218 (Agarwal et al., 2015). Conditional knockout of mir-218 in proprioceptive sensory neurons or more accurate quantification of this microRNA could support or reject this hypothesis. Regardless, to better probe the mechanisms of microRNA mediated control of cell-identity in the proprioceptors, a candidate microRNA would need to be identified.

Something else that would need to be resolved is the role of apoptosis. Considering that the decline of proprioceptor-enriched genes occurred just prior to cell-death, the causality of events is difficult to parse. It is entirely feasible that loss of cell-type specific expression is a secondary effect of deregulating apoptotic factors that alter the neuron's transcriptional priorities. In support of this notion, loss of cone-specific gene expression in photoreceptors during conditional loss of DGCR8 is mirrored by an increase in apoptotic gene expression (Busskamp et al., 2014). Examining the mRNA expression changes during ablation of Dicer in proprioceptive sensory neurons (or other cell-types) in animals where the pro-apoptotic gene Bax has been mutated would shed light on this question. It has been shown that Bax mutants block the proprioceptor cell death normally triggered by loss of Neurotrophin-3 (Patel et al., 2003). Although, the interpretation of this experiment would ultimately depend on how extensively the apoptotic response is blocked.

This brings me to another potential explanation for microRNA-mediated control of proprioceptor identity. Proprioceptive sensory neurons depend heavily on neurotrophic support from the intrafusal fibers within the muscle. It is possible that loss of Dicer directly destabilized the connection between the sensory neurons and the muscle. This broken connection would prevent neurotrophin signaling from the muscle to the sensory neurons and could lead to a loss of cell identity or possibly directly trigger apoptosis. So, as it stands, although there is support for microRNA-mediated control of neuronal identity, the mechanistic details necessary to fully embrace this claim are missing.

Cell-specific regulation of global plasticity through microRNAs:

As opposed to evidence for microRNAs controlling cell identity, there is stronger support for microRNA-mediated control of plasticity in response to network wide changes in activity. Mir-124 has been shown to be involved in synaptic scaling (Hou et al., 2015), while mir-132 helps mediate ocular dominance plasticity (Hou et al., 2015). The work in chapter three has added to this literature. We've shown that mir-7 controls FS cell excitability during activity deprivation in culture and sensory deprivation *in vivo*. In addition to this role for mir-7, we also demonstrated that, at least at long time scales, excitatory and inhibitory neurons respond to activity deprivation through altering the expression of differing microRNAs (mir-129 being the exception). This is the first demonstration that there is some degree of activity dependent cell-type specific microRNA expression changes in the neocortex. However, simply knowing which microRNAs are differentially regulated may not fully capture all cell-type specific microRNA-mediated responses to activity. Even if identical microRNAs were altered by activity, or if no microRNAs changed expression, the impact of activity on post-transcriptional regulation can still differ across cell types. This is because the 3'UTR landscape is not identical between excitatory

and inhibitory neurons, and how this landscape changes with activity is also likely to be different. For example, if one cell-type expresses an isoform of a gene with a UTR different than that expressed in another cell, the compliment of microRNAs that regulate each isoform may also be different. The end result could be differing magnitudes of up-regulation between these two cell-types. Understanding how the full complement of microRNAs interacts with and regulates the expression of mRNAs across cell-types might help us understand how different classes of neurons respond to activity.

Closing:

This thesis provides reasonable support for the idea that microRNAs contribute to the maintenance of neuronal identity. Additionally, they help the neuron modulate its properties in response to global changes in network activity. However, what remains unanswered is the relationship between these two roles. One possibility is that there is no connection. microRNAs are just regulatory building blocks employed by the cell and used for a number of unrelated functions. However, a more meaningful explanation is that microRNAs help to maintain the boundaries of expression. They help to encase a wandering expression state that the cell traverses through as a result of external perturbation and internal stochastic processes. So, any alteration of microRNA expression would change the shape of these boundaries. If these boundaries are apart of what we define as the cell's identity, then any form of global plasticity is really just a slight re-definition of that identity. To put it plainly, microRNA mediated control of a cellular property is equivalent to a slight redefinition of the cell's identity.

References:

Agarwal, V., Bell, G.W., Nam, J.W., and Bartel, D.P. (2015). Predicting effective microRNA target sites in mammalian mRNAs. Elife *4*.
Amin, N.D., Bai, G., Klug, J.R., Bonanomi, D., Pankratz, M.T., Gifford, W.D., Hinckley, C.A., Sternfeld, M.J., Driscoll, S.P., Dominguez, B.*, et al.* (2015). Loss of motoneuron-specific microRNA-218 causes systemic neuromuscular failure. Science *350*, 1525-1529.
Bartel, D.P. (2009). MicroRNAs: target recognition and regulatory functions. Cell *136*, 215-233.
Busskamp, V., Krol, J., Nelidova, D., Daum, J., Szikra, T., Tsuda, B., Juttner, J., Farrow, K., Scherf, B.G., Alvarez, C.P.*, et al.* (2014). miRNAs 182 and 183 are necessary to maintain adult cone photoreceptor outer segments and visual function. Neuron *83*, 586-600.
Hong, G.S., Lee, B., Wee, J., Chun, H., Kim, H., Jung, J., Cha, J.Y., Riew, T.R., Kim, G.H., Kim, I.B.*, et al.* (2016). Tentonin 3/TMEM150c Confers Distinct Mechanosensitive Currents in Dorsal-Root Ganglion Neurons with Proprioceptive Function. Neuron *91*, 708-710.
Hou, Q., Ruan, H., Gilbert, J., Wang, G., Ma, Q., Yao, W.D., and Man, H.Y. (2015). MicroRNA miR124 is required for the expression of homeostatic synaptic plasticity. Nature communications *6*, 10045.
Kim, Y.K., Yeo, J., Kim, B., Ha, M., and Kim, V.N. (2012). Short structured RNAs with low GC content are selectively lost during extraction from a small number of cells. Molecular cell *46*, 893-895.
Patel, T.D., Kramer, I., Kucera, J., Niederkofler, V., Jessell, T.M., Arber, S., and Snider, W.D. (2003). Peripheral NT3 signaling is required for ETS protein expression and central patterning of proprioceptive sensory afferents. Neuron *38*, 403-416.
Thiebes, K.P., Nam, H., Cambronne, X.A., Shen, R., Glasgow, S.M., Cho, H.H., Kwon, J.S., Goodman, R.H., Lee, J.W., Lee, S.*, et al.* (2015). miR-218 is essential to establish motor neuron fate as a downstream effector of Isl1-Lhx3. Nature communications *6*, 7718.
Woo, S.H., Lukacs, V., de Nooij, J.C., Zaytseva, D., Criddle, C.R., Francisco, A., Jessell, T.M., Wilkinson, K.A., and Patapoutian, A. (2015). Piezo2 is the principal mechanotransduction channel for proprioception. Nat Neurosci *18*, 1756-1762.
Yang, J.S., and Lai, E.C. (2011). Alternative miRNA biogenesis pathways and the interpretation of core miRNA pathway mutants. Mol Cell *43*, 892-903.